Facultat de Ciències Biològiques
Departament de Bioquímica i Biologia Molecular
Universitat de València

RECOMBINANT PRODUCTION AND CHARACTERIZATION OF SURFACTANT PROTEIN C (SP-C)

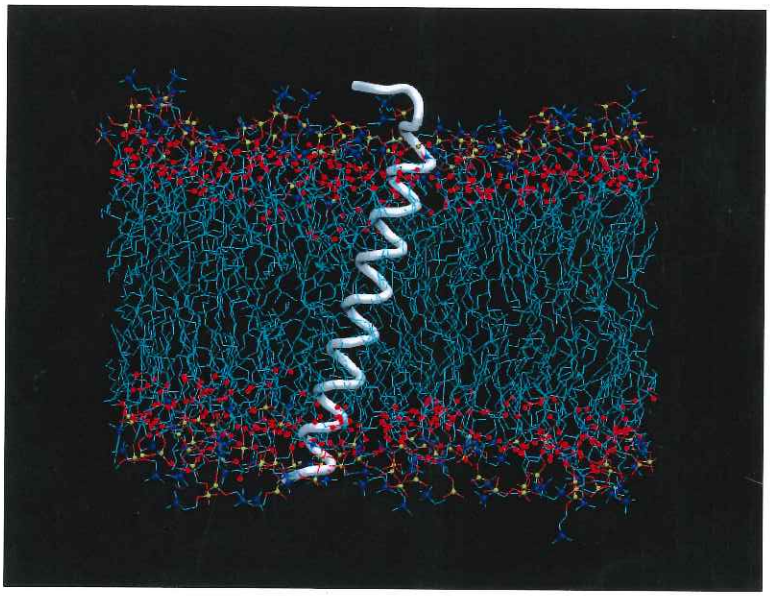

Doctoral Thesis

Dunja Lukovic

Valencia, 2007

Ismael
S.
23/03/07

Universitat de València

Facultat de Biologia

Departament de Bioquímica i Biologia Molecular

RECOMBINANT PRODUCTION AND CHARACTERIZATION OF SURFACTANT PROTEIN C (SP-C)

Doctoral thesis

Dunja Lukovic

Advisor: Dr. Ismael Mingarro
Co-advisor: Dr. Jesús Pérez Gil

Valencia, 2007

INDEX

1 INTRODUCTION

1.1 LUNGS AND PULMONARY SURFACTANT

Pulmonary surfactant is a lipid-protein complex that coats the internal side of the alveoli and enables the proper functioning of the lungs (Perez Gil, 2002). Alveolar sacs, the terminal portions of the bronchiolar tree, are tiny (250–300 μm^2), thin walled balloon-like structures which represent the main site for oxygen and carbon dioxide exchange between air and blood. The epithelium of alveoli is settled on the basal membrane, which lies on the capillary endothelium. Alveolar epithelium is composed of type I pneumocytes, very thin cells that make up to 97% of alveolar surface, while the rest consists of type II pneumocytes. The main role of type I cells is to provide a barrier of minimal thickness that is readily permeable to gases. Type II cells are cubical and very active metabolically whose main function is the production of surfactant. Upon its synthesis lung surfactant adsorbs at the interface between the air and hypophase, a capillar aqueous layer that covers the internal side of alveoli (figure 1). By lowering and modulating surface tension during breathing, lung surfactant reduces respiratory work of expansion and stabilizes alveoli against collapse during expiration.

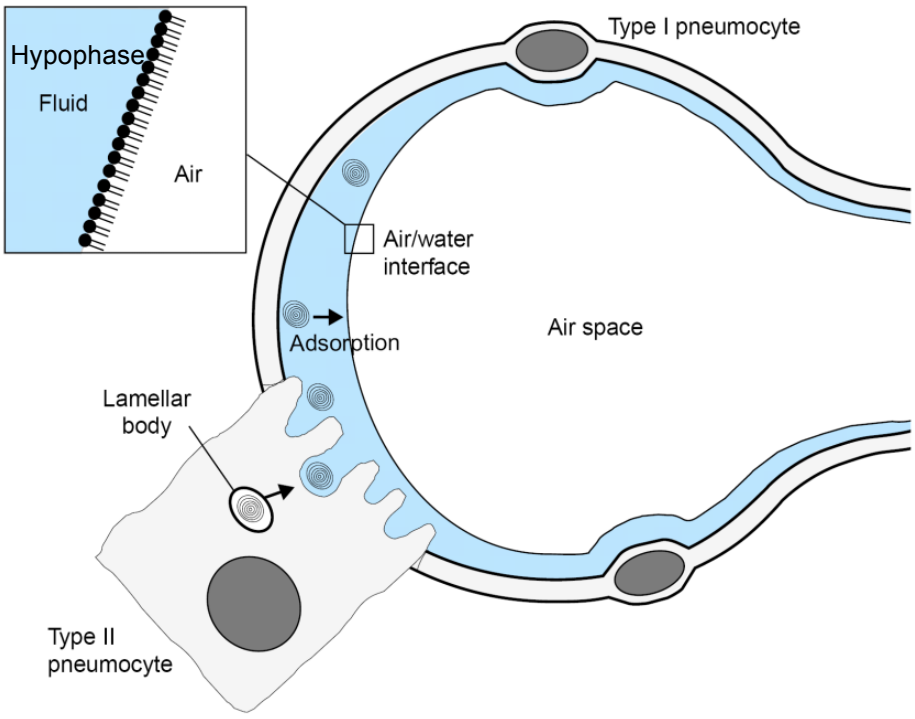

Figure 1. Schematic illustration of pulmonary surfactant location at an alveolus of the lung. Type II pneumocytes synthesise surfactant constituents and pack them into concentric bilayers of lamellar bodies. After secretion, bilayers unravel and adsorb into the air/water interface. Taken from Piknova et al., 2002.

1.1.1 Surface tension

At the air-liquid boundary, such as the one present inside the alveoli, the interfacial molecular layer generates a force named surface tension. Molecules inside the liquid are attracted equally in all directions by their neighbouring molecules, which is not the case with the interfacial molecular layer that

is in contact with gas phase. Being more dilute than the liquid, gas molecules exert a negligible attraction on interfacial molecules. This leads to an unbalanced attractive force on interfacial molecules toward the inside of the liquid that causes the surface to shrink its area resulting in the force called surface tension. Thermodynamically, surface tension is the work needed to expand the surface area. In the lung, a major part of static work of breathing results from expanding alveolar sacs.

Changes in surface tension in a surfactant film are often described in terms of surface pressure (π). Surface pressure is the amount by which surface tension is lowered by the presence of the surfactant film. Surface pressure is therefore defined as:

$$\pi = \gamma^0 - \gamma$$

where γ^0 is the surface tension of the pure liquid without any surfactant and γ is the surface tension in the presence of a surfactant film. Therefore, surface tension and surface pressure are measured in the same units (mN/m or dynes/cm) and they vary in opposite directions. When surface tension is high the surface pression is low and vice versa. Surface tension for pure water is 72mN/m at 37 ^{0}C (i.e. surface pressure is 0mN/m). The presence of a surfactant film on the water surface therefore generates values of π between 0 and 72 mN/m. When π=0 it indicates that no reduction of surface tension occurs while $\pi=\gamma^0$ indicates that the surface tension has been lowered all the way to 0 by the surfactant film.

1.1.2 Laplace' s law

The surface tension forces have significant effect on the stability and mechanics of the alveoli, which can be viewed as small air bubbles surrounded by liquid (hypophase). The Laplace's law equation states that pressure difference (ΔP) between the inside and outside of the bubble is directly proportional to the surface tension and inversely proportional to the radius of the sphere (r):

$$\Delta P = 2\gamma/r$$

In other words, the smaller the sphere the higher the pressure. This equation predicts that at equilibrium, a smaller alveolus requires a higher pressure to inflate compared to larger alveolus (figure 2). If two spherical alveoli of different sizes but equal surface tension are connected, the smaller will tend to collapse into the larger one. Hence, if air is introduced into such system, the larger alveolus will expand preferentially over the smaller one. In normal lungs this does not occur, smaller alveoli are stable during expiration and are recruited effectively during inspiration due to the action of lung surfactant. This implies that the alveolar surface tension is not constant but is lowered and varied as a function of alveolar radius during breathing.

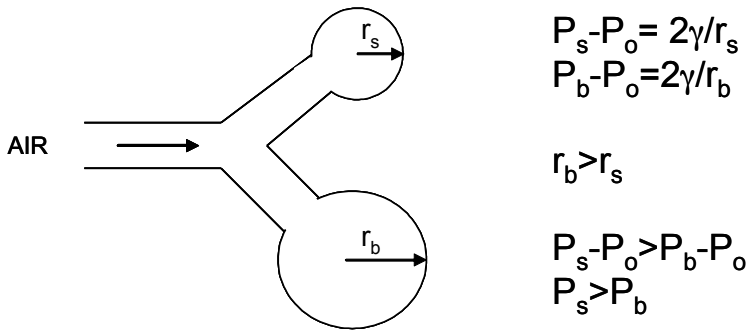

Figure 2. **Laplace's law**. Laplace's equation states that different sized alveoli with same surface tension cannot coexist at equilibrium at uniform pressure. The smaller alveolus requires a higher internal pressure to maintain its size and tends to collapse into the larger one. Conversely, the larger will tend to overexpand at the expense of the smaller one under a uniformly applied pressure. This can be avoided if surface tension is varied as a function of alveolar size. P_o:outside pressure, P_s:pressure inside a small alveolus, P_b :pressure inside a big alveolus. Taken form Notter, 2000.

Surface active agents, or surfactants, are molecules with the energetic preference for interfaces due the presence of polar (hydrophilic) and nonpolar (hydrophobic) regions. Examples for these types of molecules are detergents or phospholipids (PL). The presence of surfactant molecules at any interface reduces surface tension. Surfactant molecules arrange themselves at the interface in a thin surface film, which is the structure responsible for reducing surface tension. The surface film is typically composed of a single layer of surfactant molecules and is thus called a monolayer. The liquid phase supporting the surfactant film is referred to as subphase. A surfactant film always lowers surface tension below values found in the absence of surfactant. Surfactant molecules at the interface reduce unequal attractive forces that act on the liquid monolayer, since the attractive forces between surfactant molecules and liquid molecules are lower than attractive forces of liquid molecules for each other. Increasing the density of surfactant molecules (i.e. PL molecules) at the interface results in surface tension lowering until an equilibrium tension is reached, around 25mN/m in the case of PL interfacial films. Further adding of PL molecules does not affect the surface tension because they cannot insert into the monolayer. Only upon lateral compression, when surfactant molecules are packed beyond the equilibrium density can the tension be lowered below the equilibrium. The amount of surface tension lowering generated by a surfactant film depends on concentration (surface density), type of molecules, temperature and other environmental factors.

1.2 THE COMPOSITION OF THE LUNG SURFACTANT

1.2.1 Surfactant lipids

The composition of lung surfactant varies slightly between species and with age but certain compositional features are consistent. It is composed mainly of lipids (90% by weight) of which most abundant are phospholipids (85%) while neutral lipids, mainly cholesterol, are represented by around

5% in mass (Goerke, 1998). The remaining is composed of proteins. The most abundant component of every lung surfactant is phosphatydilcholine (PC) which constitutes around 80% of total surfactant pool. About half of PC is dipalmitoyl phosphatydilcholine (DPPC) which constitutes more than one third of all surfactant phospholipid mass (figure 3). Besides DPPC, lung surfactant contains a spectrum of saturated and unsaturated phospholipids. The second most abundant phospholipid is phosphatidyl glycerol (PG) which constitutes about 10% of lung surfactant. Another anionic lipid, phosphatidyl inositol (PI), is present in lower proportion. Total proportion of negatively charged species in surfactant, including PG and PI is around 15% of surfactant mass, with PI being the main acidic PL in some animal species. Other phospholipids present are phosphatidyl serine (PS) and phosphatydiletanolamine (PE) and sphyngomielin (SM).

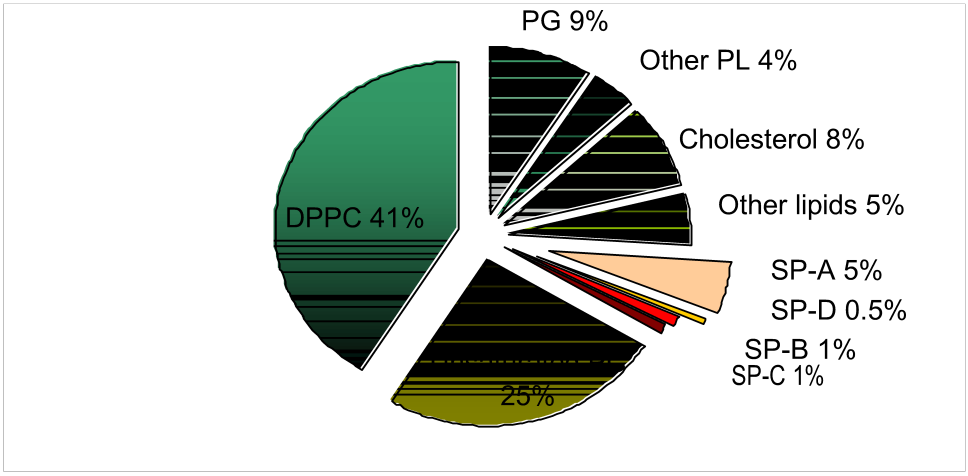

Figure 3. Typical composition of the lung surfactant isolated form brochoalveolar lavage from mammals (Hawgood, 1997; Johansson and Curstedt , 1997).

The composition of lung surfactant is remarkably different from other cellular membranes. The high DPPC content is unique to the surfactant as is the low level of PE, PS and SM. PG is atypical for animal membranes and common in bacteria and plants. Besides specificity related to phospholipidic classes, the presence of disaturated species differentiates surfactant phospholipids from cellular membranes. This unique lipid composition reflects the specific biophysical functions of the surfactant in the lung.

The active surfactant film needs to perform at least three functions. First, it needs to adsorb rapidly to the air-liquid interface, producing surface tension of around 25mN/m (π~45mN/m) within seconds. Second, once adsorbed to the interface, surface tension has to be reduced to 0mN/m (π~70mN/m) upon compression. Finally it has to provide effective replenishment of the surface film during expansion by reincorporation of surfactant material. None of the above mentioned surfactant components can accomplish all the tasks by itself. It is rather a combination of different components that has been evolutionarily optimised to provide stable breathing cycles. Undoubtedly, the main surface active components are PLs. However, lung surfactant is composed of two classes of PL, with

different surface properties. To achieve minimal surface tension (i.e. maximal surface pressure) effectively during cycling, the surface film at the alveolar interface must have significant content of rigid saturated phospholipids, particularly DPPC. DPPC monolayers with their saturated acyl chains in *trans* configuration can be highly packed and compressed to surface tension lower than 20mN/m at temperatures below their gel to fluid melting point. The temperature of gel to fluid phase transition of DPPC is 41^0C, meaning that at body temperature (37^0C) DPPC monolayers are rigid enough to sustain low tensions without collapse upon compression. DPPC films reduce surface tension to extremely low values (0mN/m) during dynamic compression, however they exhibit poor respreading on successive cycles of compression and expansion and large hysteresis (loss of material ejected after first compression). In contrast, films of unsaturated phospholipids do not reduce surface tension as effectively during compression (increase the pressure only up to 50mN/m), but show good respreading and lower hysteresis. Unsaturated lipids have melting points bellow 37^0C and are present in the fluid state in the body, exhibiting therefore collapse at lower surface pressures.

Squeeze-out and reservoir theory

These mutually exclusive properties required for functional lung surfactant lead initially to the "squeeze-out" theory. This theory states that DPPC must be selectively adsorbed from subphase while non –DPPC (fluidizing) PL squeezed out during the compression (e.i. exhalation). This theory assumes an idealized immiscible interaction between surfactant components, where lipids retain pure component phase behaviour within mixtures. Despite its widespread acceptance the experimental evidences for squeeze-out theory have not been found. Instead, Taneva and Keough (Taneva and Keough, 1994a) found that the material removed upon compression remains associated with the monolayer and readily reinserts upon decompression without a substantial loss of the material. In 1995 Schurch and collaborators (Schurch et al., 1995) provided electron microscopy evidence for surface associated material in Langmuir Blodgetts films of natural surfactant and in sections of rabbit lungs. Further studies confirmed that expulsed lipids and proteins upon compression (exhalation) act as a surface associated "reservoir" near the interface. Upon expansion of the film (inhalation) lipids readily respread from the reservoir again into the air-water interface. Interestingly, hydrophobic proteins were found to be crucial in the formation and dynamics of multilayer reservoirs. Films containing Surfactant Protein B (SP-B) were found to induce disc-like protrusions whereas Surfactant Protein C (SP-C) tends to promote the formation of extended plateaus of stacked bilayers (Krol et al., 2000; von Nahmen et al., 1997)

1.2.2 Surfactant proteins

The protein moiety present in 6-8% of total surfactant mass is represented by four surfactant proteins (SP) named A, B, C and D. The first three of these proteins remain associated with the lipids during centrifugation of the lung lavage and are important for lung surfactant functioning. The most abundant one is SP-A (constitutes around 5% of lung surfactant mass), while SP-B and SP-C make up around 1% each of lung surfactant mass. SP-D, the least abundant (accounts for only 0.5 %) is structurally very similar to SP-A and both belong to the family of proteins involved in innate immune

response named collectins. The SP-D is dispensable for LS surface active functioning. SP-A and SP-D primarily mediate the host–defence functions of lung surfactant. SP-A and SP-D knockout mice do not exhibit any respiratory dysfunction but manifest higher susceptibility to infections (LeVine et al., 1997; Botas et al., 1998)

Despite their low abundance (~1.5% mass) SP-B ad SP-C play critical roles in surfactant film functioning. SP-B and SP-C are small highly hydrophobic proteins that co-isolate with lipids during the organic extraction of the lung lavage. They are active components of the surfactant film in preventing alveolar collapse. SP-C is the only protein uniquely expressed by type II pneumocytes. SP-A, SP-B and SP-D are produced in other airway cells including Clara and submucosal cells. Since there is no lipid production in these later cells, they probably do not exert the surface tension reducing function in them.

SP-A and SP-D

SP-A and SP-D are water soluble and belong to the collectin family of proteins (figure 4). The common structural feature of these proteins is the presence of an elongated collagen-like N-terminal region with the repeating Gly-X-Y sequence, where X denotes any amino acid and Y a hidroxyproline residue. The collagen domains vary in length depending on the number of triplet repeats, with MBL (mannose binding lectin) having 19 repeats and SP-D 59. This collagen-like domain is preceded by a cysteine-rich N-terminal domain and followed by a coiled-coil neck domain. The carboxy-terminal end of collectins is a C-type (Ca^{2+} dependent) lectin globular head that contains a carbohydrate–recognition domain (CRD). CRD domains form trimeric clusters with high affinity for clustered oligosaccharides. Collectins are assembled as trimers that multimerize to larger oligomers.

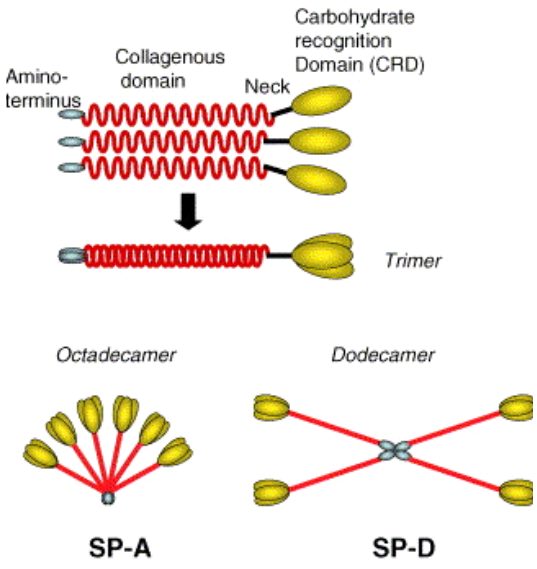

Figure 4. Structural organization of the lung collectins. Surfactant proteins A (SP-A) and D (SP-D) contain a collagenous domain and C-terminal carbohydrate recognition domain (CRD). SP-A forms a “flower bouquet” octadecamer, while SP-D assembles into a cruciform dodecamer. Taken form Sano and Kuroki, 2005.

The affinity for binding specific sugars is different for SP-A and SP-D even though they can bind

to some common sugars. SP-A binds preferentially to mannose and L-fucose, while SP-D binds to inositol, maltose and glucose. Consequently they have different affinities toward specific pathogens. While both SP-A and SP-D can bind to *Pneumocystis carinii*, only SP-D binds to *Saccharomices cerevisiae* (Crouch and Wright, 2001).

Members of the collectin family participate in pulmonary host defence by several mechanisms. Opsonization of pathogens by CRD binding to the pathogen surface results in enhanced phagocytosis of collectin –associated pathogen by the immune cells. Collectins can simply aggregate the pathogen which enhances its interaction with the immune cells without the interaction of collectins themselves with the immune cell. Collectins also act as activation ligands on immune cells independently of microbial binding. Finally, collectins can contribute to pathogen clearance by up-regulating expression of cell surface receptors involved in microbial recognition. For example, SP-A increases the expression of scavenger receptor A and therefore promotes the uptake of *Streptococcus pneumoniae* (Kuronuma et al., 2004). SP-A up-regulates the activity of the mannose receptor on phagocytic cells (Beharka et al., 2002). Collectins also participate in pathogen elimination by regulating the production of inflammatory mediators. SP-A interferes with lipopolysaccharide (LPS)-induced pro-inflammatory responses by competing with LPS for CD14 receptor (Sano et al., 1999). Finally, collectins also bind to apoptotic cells and enhance their clearance by macrophages.

SP-A

SP-A monomer is a 28-35 kDa (depending on the level of posttranslational modification) peptide that oligomerizes to an active bouquet-like octadecamer (630 kDa) of six trimers generated by the interaction of collagen-like regions (23 repeats long) of three SP-A monomers into a triple helix (figure 4). CRD bears 4 cysteine residues that form intrachain disulfide bonds essential for binding carbohydrates. Each CRD contains one carbohydrate-binding site and two high affinity Ca^{2+} binding sites.

Besides its pathogen clearing function, SP-A plays a role in regulation of surfactant metabolism. It binds to type II specific receptors which are involved in capturing and recycling of PL (Stevens et al., 1995). SP-A also has a protective role against plasma proteins. In certain pathologic conditions alveolar spaces are invaded by plasma proteins which inactivate surfactant (Cockshutt et al., 1990), and SP-A is able to at least partially reverse that effect.

SP-A has important effects on PL organization. It can increase aggregation and order of phospholipids in a Ca^{2+} and pH dependent fashion. SP-A enhances phospholipid interfacial adsorption in the presence of SP-B and SP-C in a synergistic manner (Schurch et al., 1992; Possmayer et al., 2001). SP-A can bind phospholipid vesicles and promote phospholipid exchange between them (Cajal et al., 1998). It can also promote phospholipid aggregation and reorganization into large aggregates in water, such as tubular myelin, which promotes surfactant adsorption. SP-A is essential for the formation of tubular myelin in the presence of SP-B and calcium and locates at the bilayer intersections (McCormack and Whitsett, 2002), although the presence of tubular myelin was found not be essential for the biophysical activity of surfactant. In SP-A knock out mice, tubular myelin is not formed but surfactant still reaches the interface and stabilizes the lung (LeVine and Whitsett, 2001).

SP-D

SP-D is not a functional constituent of pulmonary surfactant and does not co-isolate with surfactant lipids. It is also a member of the collectin protein family, of about 40 kDa size (depending on the processing and level of posttranslational modification) that oligomerizes into a dodecamer (figure 4). Similarly to SP-A, it has a collagen like N-terminal region which is longer than the one in SP-A, and a globular CRD that bears four cysteine residues that form intramolecular disulfide bonds. SP-D binds carbohydrates but does not interact with phospholipids and therefore does not exert any activity on phospholipids. It has been attributed exclusively a pathogen clearance function. Surprisingly, genetically manipulated SP-D deficient animals apart from being more susceptible to infections, exhibited accumulation of LS in alveoli and lamellar bodies suggesting that SP-D has a role in maintaining surfactant homeostasis (Wert et al., 2000; McCormack et al., 2002).

SP-B and SP-C

These two proteins are functionally active components of pulmonary surfactant. Despite their common hydrophobicity and small size, SP-B and SP-C differ markedly in their amino acid sequence and secondary structure. Both proteins undergo posttranslational processing from larger precursors to generate small active peptides. SP-C is smaller than SP-B and does not belong to any known protein family. It is synthesised only in type II pneumocytes. The mature protein is 3.7kDa big or 4.2kDa including two palmitoyl chains and has a mostly helical structure when embedded in the phospholipid bilayer. Both of these proteins interact extensively with phospholipids. Although both proteins enhance the adsorption of phospholipids, a variety of studies indicate that SP-B is apparently more effective than SP-C in performing this function.

SP-B

SP-B monomer has a molecular weight of 8.7 kDa and forms dimers through disulfide linking on cysteine 48. Three additional intramolecular disulfide bridges are formed within each monomer. SP-B is synthesized as a 381 amino acid long precursor and the processing is completed between *trans*-Golgi and lamellar bodies (figure 5).The sequence homology and the presence of three intramolecular disulfide bridges classifies SP-B as saposin-like polypeptide, which besides saposins (lisosomal lipid hydrolases), include Nk-lysin and amoebapores (pore-forming peptides from *Entroamoeba histolitica*). SP-B however, differs from other members of that family by being highly hydrophobic and dimeric. Based on sequence homology and similar helical content, Andersson and colleagues proposed a four helix topology for all saposins (Andersson et al., 1995). According to this model the amphipatic helices bounded by residues 8-22, 27-38, 42-50, 67-74 are aligned in an antiparallel left hand hairpin like motif. NK-lysin structure determined latter by NMR confirmed the predicted helices (Liepinsh et al., 1997).

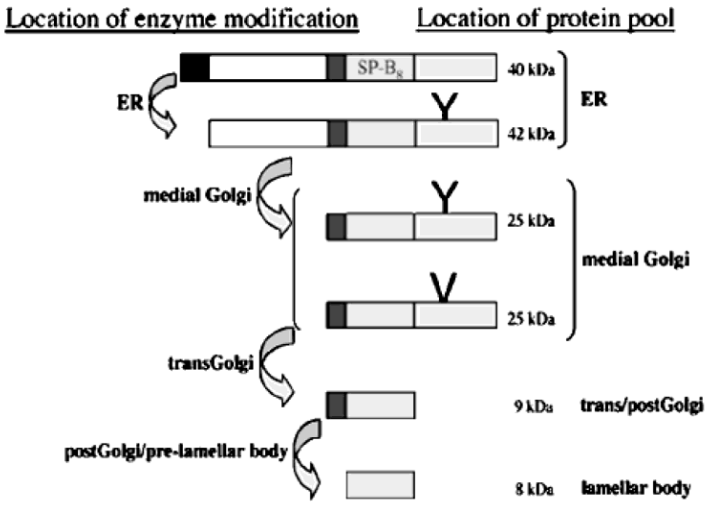

Figure 5. Model of intracellular localization of SP-B Processing. Black box denotes a signal peptide, Y denotes glycosylation and a grey box denotes a final N-terminally cleaved fragment. Taken from Korimilli A et al., 2000.

The structure of SP-B was studied in organic solvents in micelles and lipid bilayers by circular dichroism, fluorescent spectroscopy and infrared spectroscopy and it was found that the α helical content of SP-B was 27-45% (figure 6) (Perez Gil et al., 1993). Attenuated total reflection spectroscopy in DPPC:PG (7:3) bilayers (Vandenbussche et al., 1992a) showed that SP-B interacts through its polar residues with polar heads of the lipid bilayer, associated more or less parallel to the bilayer plane without spanning it. The interaction is thought to occur between 9 positively charged residues in SP-B and anionic phospholipids i.e. PG.

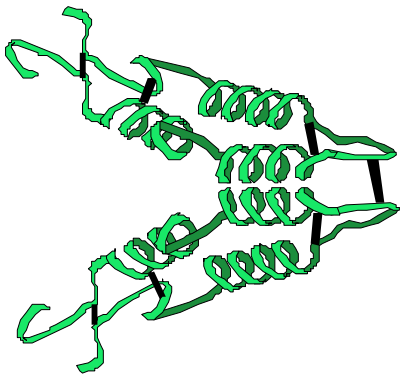

Figure 6. Model for the secondary structure of SP-B dimer, including the position of disulphide bonds. An intermolecular disulfide bond is established between cysteines at position 48, while each of the molecules presents 3 intramolecular disulfide bonds.

SP-B was demonstrated to induce phospholipid mixing between vesicles and loss of aqueous

content (Poulain et al., 1992, Poulain et al., 1996). SP-B also promotes PL adsorption to the interface from aqueous subphase (Oosterlaken-Dijksterhuis et al., 1992). Recent studies aimed at elucidating the mechanism of surfactant compression-expansion cycling, point to the role of SP-B as a promoter of surfactant associated reservoir associated to the interface, which facilitates the reincorporation upon expansion of material excluded during compression (Taneva and Keough, 1994a; Cruz et al., 2000).

SP-B is essential for several steps in surfactant metabolic cycle. It is crucial for surfactant assembly in LB as well as tubular myelin formation and its transfer to the interphase (Veldhuizen and Haagsman, 2000). SP-B promotes PL re-uptake in pneumocytes (Sane and Young, 1994) and reduces the inhibitory effect of plasma proteins (Amirkhanian et al., 1993). SP-B is also able to modulate inflammatory response by inhibiting nitrogen oxide formation (Miles et al., 1999).

The importance of SP-B is obvious from studies in SP-B knock out mice, which results in irreversible respiratory failure. Moreover, genetic deficiency of SP-B in humans has lethal outcome. The hereditary SP-B deficiency was found to be caused by a variety of mutations that cause either reduced or absent SP-B levels (Nogee et al., 2000). The absence of SP-B is accompanied by deficient processing of SP-C leading to the accumulation of a 8-12kDa precursor instead of 4kDa mature protein (Clark et al., 1995; Vorbroker et al., 1995). For this reason, the specific role of SP-B can not be unequivocally established.

A correctly folded SP-B analogue has not been produced so far in heterologous systems, due to the high hydrophobicity and high cysteine content. Therefore, a number of studies were performed using synthetic peptides that correspond to distinct SP-B segments in order to find a minimal region that retains surface activity. A peptide corresponding to amino acids 1-25 in the mature protein has been the most intensively studied one since it conferred full surface activity in the presence of PL. This peptide was shown to promote PL adsorption and reuptake during expansion (Veldhuizen et al., 2000). The peptide was active only as a dimer suggesting that it may act as a bridge between bilayers with the hydrophobic side in contact with the membrane (Whitsett et al., 1995; Zaltash et al., 2000). This peptide has been assayed in animal model of respiratory distress syndrome (RDS) where, combined with lipids, it demonstrated the activity equivalent to the natural surfactant (Walther et al., 2002). Recent experiments have confirmed that the N-terminal half of SP-B sequence contains most of the functional determinants of the protein (Ryan et al., 2005; Serrano et al, 2006).

SP-C

SP-C, the smaller of the two amphipatic peptides present only in the lung surfactant, constitutes ~1% of surfactant by mass. It is a 35 amino acid long peptide with a polar N terminal and C-terminal stretch of aliphatic residues, with predominating valine residues, from residue 13 to 35. Two palmitoyl groups are linked by tioester bonds to cysteines at positions 5 and 6, increasing further peptide`s hidrophobicity. SP-C is synthesised as a 21kDa propeptide with only one transmembrane region that adopts a type II orientation (N-terminus in the cytoplasm) in the membrane (figure 7). Mature SP-C is generated by several proteolytic steps at both N- and C-terminal ends of its precursor proSP-C. Palmitoyl chains are attached early during its maturation, distant to the trans-Golgi network. The protein is synthesised in the ER and routed through Golgi, multivesicular body (MVB) and stored in lamellar bodies (LB). As

mentioned above, processing of SP-C is proSP-B dependent, since SP-B deficient animals show an accumulation of unprocessed SP-C (Clark et al., 1995; Vorbroker et al., 1995). The enzymes involved in proSP-C processing are largely unknown. Catepsin H is the only enzyme known to be involved in the first N-terminal processing step of the large precursor (Brasch et al., 2002).

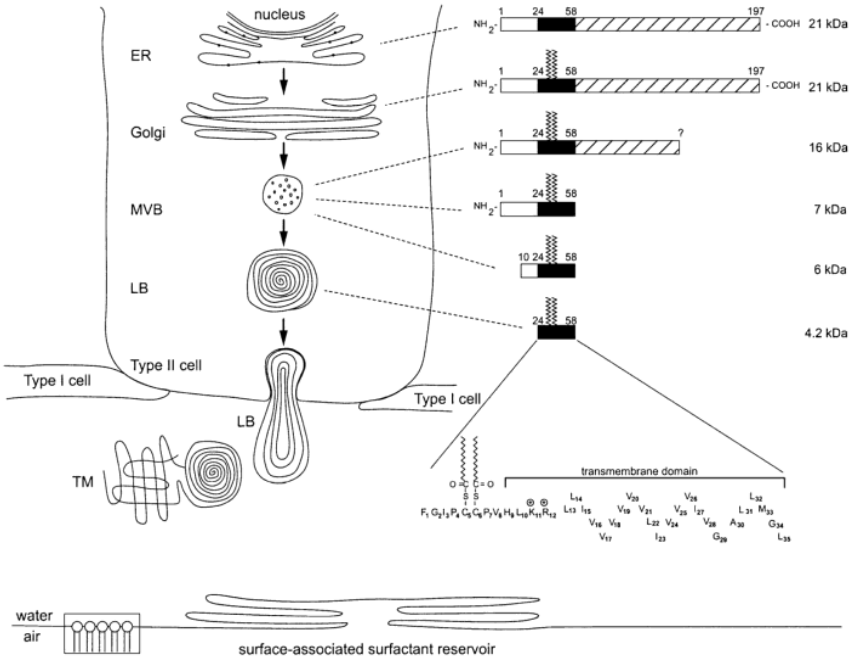

Figure 7. Processing and sorting of proSP-C. To the left of the figure processing of proSP-C and location of the different processing intermediates in different organelles of the type II cell is represented. ER intermediates are depicted, as well as the amino acid sequence of mature SP-C. ER: endoplasmic reticulum; MVB: multivesicular body; LB: lamellar body; TM: tubular myelin.

Comparative analysis between different species reveals highly conserved regions (figure 8): the poly–valine stretch (residues 13-28) which contains aliphatic residues with Val as the most abundant; a Lys-Arg dibasic pair at position 11 and 12; palmitoylated cysteines at positions 5 and 6 present in all species, except in mink and dog where Cys 6 is replaced by Phe . The C-terminal heptapeptide that follows the poly-Val stretch is highly conserved as well.

FGIPCCPVHLKRLLIVVVVVVLIVVVIVGALLMGL human

LRIPCCPVNLKRLLVVVVVVVLVVVVIVGALLMGL pig

FGIPCCPVHLKRLLIVVVVVVLVVVVIVGALLMGL rabbit

FGIPCCPVHLKRLLIVVVVVVLVVVVIVGALLMGL monkey

FRIPCCPVHLKRLLIVVVVVVLVVVVIVGALLMGL rat

FRIPCCPVHLKRLLIVVVVVVLVVVVIVGALLMGL mouse

LRIPCCPVNIKRLLIVVVVVVLVVVVIVGALLMGL sheep

LGIPCFPSSLKRLLIIVVVIVLVVVVIVGALLMGL dog

LGIPCFPSSLKRLLIIVVVIVLVVVVIVGALLMGL mink

Figure 8. Sequences of SP-C from different species. Cysteine or phenylalanine residues at positions 5 and 6 are highlighted in red. In the porcine sequence the helical region from NMR structure is underlined (Johansson et al., 1994).

The secondary structure of SP-C was determined initially in the bilayer of lipid vesicles using attenuated total reflection Fourier-transform infrared spectroscopy (ATR-FTIR) (Vandenbussche et al., 1992b). In that study it was found to have high α helical content with the helical axis oriented parallel to the lipid chains. The α helix was confirmed between residues 9 and 34, while residues 1-8 and 35 were found to be disordered, by NMR spectroscopy in organic solvents and in the presence of detergent micelles (Johansson et al., 1994; Johansson et al., 1995a). The helix is 37 Å long, which matches with the thickness of the fluid DPPC bilayer, consistent with the transmembrane position of SP-C in membranes (figure 9). Moreover, the poly-valyl stretch is 23 Å long which nicely matches the estimated 26 Å thickness of the acyl-chains length in a fluid DPPC bilayer. The length of the acyl chains in gel phase DPPC bilayer is 39 Å, less suited for insertion of the SP-C helix. In lipid monolayers, it was shown that SP-C helix has a tilt of 70^0 relative to the monolayer plane (Gericke et al., 1997; figure 9). Haagsman and colleagues suggested that the helix tilt in the monolayer depends on the surface pressure and is influenced by the presence of acyl chains (Crewels al., 1993). The α helix can change from being almost parallel to perpendicular to the interface with pressure increase.

The position of the palmitoylcysteines in surfactant multilayer is still uncertain, as they can be either embedded into the same phospholipid bilayer as their α helix or they could interact with the neighbouring bilayer. This latter possibility is consistent with the hypothesis that SP-C is responsible for the association of lipids that have been squeezed-out during compression in order to be reinserted into the interfacial film upon inhalation. In other words, acyl chains can remain inserted into the monolayer while the helix can switch from monolayer to bilayer with associated lipids during compression. With subsequent expansion the helix can flip back into the monolayer promoting the reincorporation of collapsed PLs.

Recent studies using synthetic peptides derived from the N-terminal segment of SP-C demonstrate that this region has a high affinity toward membrane interface even in the absence of

palmitoyl residues, and is able to produce perturbations in lipid packing and membrane permeability (Plasencia et al., 2004). It is proposed therefore that the N-terminal segment is responsible for SP-C ability to promote interfacial adsorption of PL.

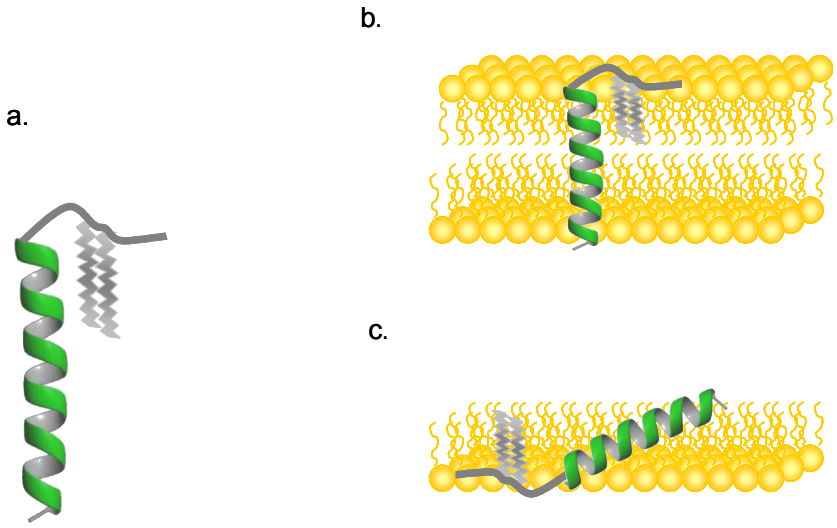

Figure 9. Structural model of SP-C with palmitoylated cysteins (Based on the study of Johansson et al., 1994). Proposed model for its insertion into lipid bilayers (b) and monolayers (c).

SP-C promotes PL monolayer formation from vesicles in the subphase to the air-water interface (Oosterlaken-Dijksterhuis et al., 1991). A study from Mendelssohn's lab (Gericke et al., 1997) provided an insight to the molecular mechanism of SP-C activity. By applying infrared reflection absorption spectroscopy (IRRAS), the orientation of SP-C was determined in DPPC monolayers and demonstrated that α helix changes the tilt during bilayer to monolayer transition keeping the maximum hydrophobic matching between the lipid acyl chains and the helix. In this study it was proposed that SP-C can act as a "hydrophobic lever" that carries the phospholipid molecules to the interphase. Taneva and collaborators demonstrated that SP-C (as well as SP-B) promotes respreading of DPPC molecules from collapsed phases during dynamic cyclic compression-expansion (Taneva and Keough, 1994a). It was shown that upon compression SP-C causes formation of 3-D surface associated structures, probably including squeezed-out PLs which remain associated with the monolayer film at high pressures (Von Nahmen et al., 1997). The reversibly squeezed out material during compression was seen by fluorescent light microscopy as layered protrusions rich in protein. The number of formed layers increased as the film was compressed (Amrein et al., 1997).

A particular role and dispensability of palmitoyl chains has not been clearly established. In general, any palmitoylation serves to anchor the protein to membrane bilayers implying that in SP-C the palmitoyl groups promote its interactions with PL monolayer or bilayer. Crewels and collaborators showed that the lack of palmitoylation affects PL insertion into the interface (Crewels et al., 1993). In accordance with this, Bi and co-workers (Bi et al., 2002) found that acyl chains were required to maintain the association of surfactant reservoirs with the interface at the highest compression stages. Under dynamic conditions it was observed that palmitates are required for reincorporation of collapse phase lipids but not for selective DPPC adsorption and PG exclusion (Possmayer et al., 2001).

However, *in vivo* data with recombinant proteins that lack acyl chains strongly suggest that their efficiency is comparable to the native protein (Davis et al., 1998).

On the other hand SP-C was shown to prevent surfactant inactivation by plasma proteins (Amirkhanian et al., 1993). SP-C also modulates the immune response toward pathogens by interacting with LPS and its receptor CD14 (Augusto et al., 2002; Augusto et al., 2003).

Unlike SP-B, targeted disruption of the SP-C gene is not lethal at birth but can develop severe progressive pulmonary disease associated with emphysema, epithelial cell dysplasia in conducting and peripheral airways and monocytic infiltrates later in adulthood (Glasser et al., 2001; Glasser et al., 2003).

In addition to its pronounced hydrophobicity, manipulation and studies of SP-C are further complicated by structural instability of SP-C under certain conditions. SP-C can transform irreversibly from monomeric α helix into aggregated β sheets (Szypersky et al., 1998) which visually resemble amyloid fibrils (Gustafsson et al., 1999). This behaviour is observed when SP-C is dissolved in organic or aqueous solution in the absence of lipids and does not occur when SP-C is embedded in lipid membranes. *In vivo* amyloid fibrils are observed in patients suffering form pulmonary alveolar proteinosis (PAP) where protein aggregates accumulate in the alveoli (Seymour and Presneill, 2002). Deacylation was found to be another factor that increases the instability of the SP-C α helix (Gustafsson et al., 2001). This conformational conversion probably stems from dual conformational propensity of helical amino acids in distinct environments. The SP-C transmembrane fragment is represented by 10-12 valines, depending on the species, the other residues being Ile or Leu. Valines and isoleucines have branched β–carbons which issues their propensity toward β strands and their underrepresentation in α helices. However, in lipid environment β-branched Val and Ile promote helix formation (Li and Deber, 1994). β-fibrilation is not unique to SP-C. In fact, similar conversion was observed for amyloid β peptide involved in Alzheimer disease and prion proteins involved in spongiform encefalopathies (Kelly et al., 1996; Aguzzi and Weissmann, 1997; Johansson et al., 2004). Surprisingly, none of these proteins share any similarities in their sequence. The specific mechanism by which amyloids form is not yet known.

1.3 LUNG SURFACTANT METABOLSM

Lipids and proteins of the pulmonary surfactant are synthesised, processed, packed, secreted and recycled in type II pneumocytes (figure 10). Both components are synthesised in the endoplasmatic reticulum. Surfactant phospholipids are synthesised from glycerol-3-phosphate which is double acylated to form phosphatydic acid. Phosphatydic acid is subsequently converted to diacyl-glycerol which is then subjected to specific transferases to generate PC, PG and PI. Phosphatidyl cholines are synthesised by a CDP-choline pathway. Around 45% of DPPC in lung surfactant is obtained in this way, while the remaining 55% is obtained through a specialised deacylation–reacylation mechanism that converts monoenoic PC to disaturated PC. Cholesterol, on the other side, is derived from circulating low-density lipoproteins (LDL) and high-density lipoproteins (HDL). A small portion is synthesised endogenously from acetate or glucose.

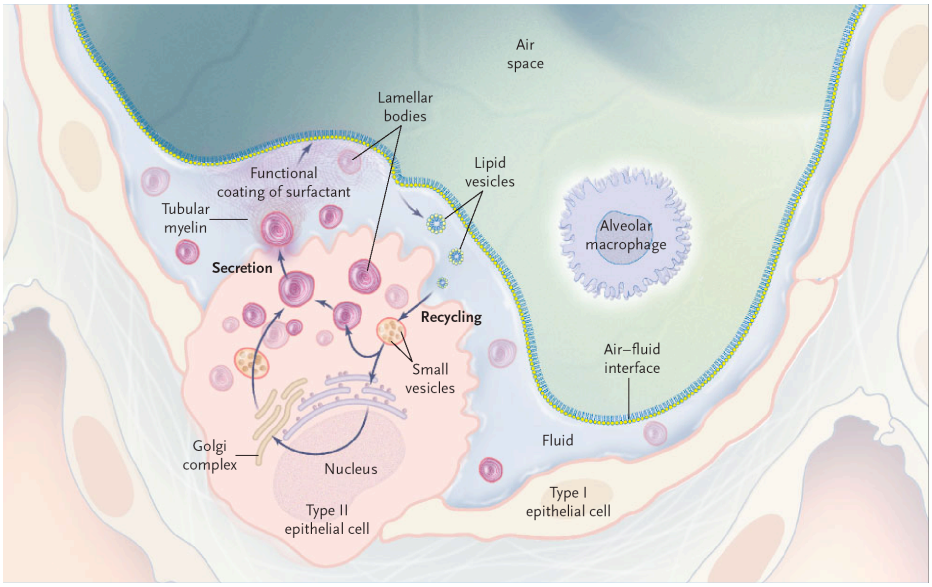

Figure 10. Surfactant production and recycling in the alveolus. Surfactant is synthesised and packed into lamellar bodies in the cell cytoplasm. These LB migrate to the cell membrane, with which they fuse and then are released in the air-fluid interface within the alveolus. They subsequently form tubular myelin, which participate in promoting the formation of the functional interfacial monolayer (taken form Baudouin, 2004)

After their synthesis in the endoplasmatic reticulum, lung surfactant lipids are transferred via Golgi to multivesicular bodies (MVB) and immature lamellar bodies (LB), type II pneumocyte-specific organelles that are characterized by multiple round concentric bilayers with approximately 1µm diameter. Type II cells can have between 100-150 lamellar bodies per cell. Surfactant proteins, on the other hand enter multivesicular bodies after leaving Golgi, which then fuse with lamellar bodies (figure 11). In addition to phospholipids, lamellar bodies contain transporter proteins that provide them with acidic pH (5.5) and high calcium concentration. Moreover, it was observed that MVBs and LBs contain enzymes that participate in the final processing of SP-B and SP-C. The presence of SP-A, SP-B ad SP-C was shown in lamellar bodies while SP-D is absent from these structures.

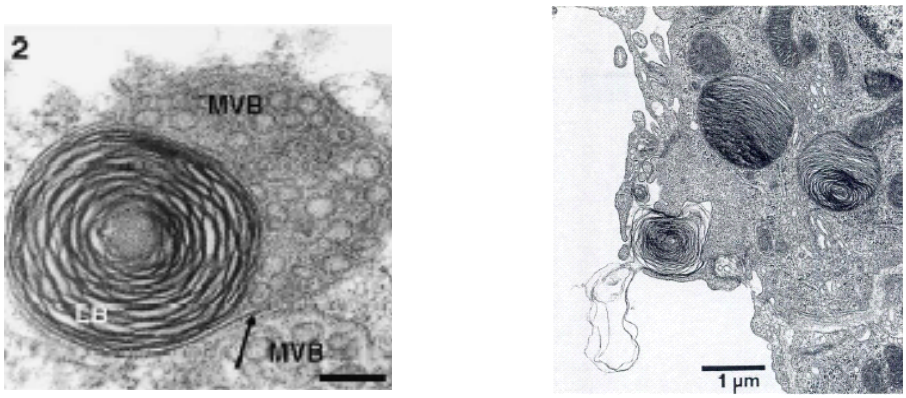

Figure 11. A. Fusion of a multivesicular body (MVB) with lamellar body (LB) in type II pneumocytes (Weaver et al., 2002). B. A lamellar body in the process of exocytosis (Rooney, 2001).

Upon specific stimuli the LB content is released into the aqueous hypophase that covers alveolar epithelium (figure 11b). Studies in swimming rats indicate that major inducers of exocytosis are hyperventilation and mechanical stretch (Nicholas et al., 1982). This finding was confirmed in cultured cells (Wirtz et al., 1990). Mechanical stretch was found to be accompanied by Ca^{2+} increase and ATP release (Rooney et al., 2001). LB secretion is also stimulated via receptors on type II cells, including β adrenergic, histamine, vasopressin, endothelin receptors, etc. The pathways involved in secretory signal transduction are mediated by cAMP activation, protein kinase C and Ca^{2+}-calmodulin dependent protein kinase (Dietl et al., 2001).

In the hypophase, lung surfactant is assembled into a unique new structure named tubular myelin. Different factors, such as increase in hydratation, change in Ca^{2+} concentration or increase in pH have been proposed as inducers of tubular myelin formation. Under the electron microscope this structure is seen as a regular network of crossing phospholipid bilayers (see figure 10 for a cartoon). Tubular myelin can be assembled *in vitro* from DPPC, PG, SP-A and SP-B, and Ca^{2+}. It is considered as a direct precursor and as a reservoir of the interface film although it must be not the only one as the absence of TM is compatible with interfacial film formation and lung stability (Korfhagen et al., 1998). Once at the interface, the surfactant film is compressed and expanded during breathing and performs its role of surface tension lowering and modulating.

After performing their function, surfactant molecules eventually leave the interface and are cleared from the alveolar space by endocytosis. After their reuptake into type II cell, the phospholipids are found directly into the lamellar bodies and proteins are first localized in MVB and latter on in LB. Hence LBs are composed of both newly synthesised and recycled material. Nevertheless, a minor portion of surfactant material is degraded by alveolar macrophages.

1.4 SURFACTANT DYSFUNCTION ASSOCIATED PATHOLOGIES

Lung surfactant dysfunctions occur when surface activity is compromised. Pulmonary surfactant deficiency or dysfunction contributes to several respiratory pathologies (Hallman et al., 2001). A primary lung surfactant deficiency disease is neonatal respiratory distress syndrome (RDS) in premature infants. The other important pathology associated with surfactant dysfunction as a secondary effect is acute lung injury (ALI) ending in acute respiratory distress syndrome (ARDS).

RDS is a disease of prematurity (Rodriguez, 2003). Lung surfactant is fully developed at around week 32 of gestation, which causes that infants born prematurely (before that threshold) have high probability to develop neonatal RDS, characterised by the abnormal transition from a fluid filled to an aerated lung at birth. In the absence of injury, type II cells mature rapidly upon birth due to mechanical stimuli or steroids released on birth. However, the course of RDS in many infants is prolonged by acute and chronic lung injury and other complications of prematurity. These infants require clinical treatment by exogenous surfactant.

Supplementation of the immature lungs of preterm babies with exogenous surfactant at birth has dramatically improved clinical prognosis. Surfactant therapy is used to reduce the risk of RDS in pre-term infants (prophylactic) or to treat already established RDS (rescue therapy). This encouraging

results in RDS led to the idea of using the exgenous surfactant for treatment of several other forms of lung pathology in children and adults. RDS is the only respiratory disease clinically treated with approved surfactants so far.

ARDS affects patients of all ages including infants and children (Lewis and Veldhuizen, 2003). It is characterized by multiple etiologies, such as sepsis in children, inhaled toxic gases or shock of any cause, uremia, most of them producing acute lung injury (ALI). The pathology of lung injury is complex and involves damage of alveocapillary membrane, edema, inflammation, oxidant injury and surfactant dysfunction. Multiple cell types are involved in this syndrome, as well as a huge number of inflammatory mediators. Surfactant therapy in ARDS is complicated by the sophisticated ethiology of this disease. Exogenous surfactant therapy is showing promising results mainly in the early phase of ARDS, when lung injury is less established.

1.4.1 LUNG SURFACTANT REPLACEMENT IN ANIMAL MODELS

Experiments in animals have provided a crucial link between *in vitro* surfactant studies and clinical application. Animal models of surfactant deficiency founded successful clinical trials with exogenous surfactant therapy applied today in the treatment of RDS and its potential in treatment of ARDS. Basically, animal studies showed that active surfactants can be instilled into the lungs to improve pulmonary function (Enhorning et al., 1973). Animal models of RDS use: i) premature animals that are naturally deficient in endogenous surfactant, or ii) adult animals where endogenous surfactant has been removed by bronchoalveolar lavage. An animal model of RDS that is widely used is surfactant deficient premature rabbit foetuses (for example Johansson et al., 2003;Takei et al., 1996a; Davis et al., 1998; Hawgood et al., 1996). At 27 days of gestation the animals are anesthetised and foetuses delivered by hysterectomy. The animal is weighted and trachea cannulated. Surfactant suspensions containing around 100mg/kg of body weight of PL are instilled into the cannula which is then connected to a syringe and a water manometer. Control littermates which have undergone the surgery but have not been treated are always matched to compare with the ones treated with the surfactant. Premature large animals used are premature lambs, baboons and monkeys that allow assessment of lung mechanics and other physiological parameters over longer periods of time. Excised lavaged lungs of adult rats are another common model (Hafner et al., 1998; Hafner et al., 1999). The removal of endogenous surfactant in excised lungs produces changes in lung compliance that can be reversed by the addition of exogenous surfactant.

Unlike RDS, which is accurately modelled in above mentioned animal models, ARDS is not easily modelled due to the complexity of this disease (Lewis and Veldhuizen, 2003). Various different models have been established, each with its own advantages and disadvantages. ARDS models that have been used are adult rat lungs treated with repetitive saline lung lavage, acid or meconium aspiration, smoke inhalation, endotoxin infusion etc.

All these models are used today to test the efficiency of exogenous surfactant preparations and also to compare new surfactant mixtures in their *in vivo* activity (Hafner et al., 1995; McLean et al., 1992).

1.4.2 Surfactant replacement therapy for neonatal RDS

Several factors contributed to the development of successful RDS therapy. In 1950's the surfactant deficiency was found to be a cause of RDS, which encouraged further studies of surfactant. The initial clinical trials in the early '60s, taking DPPC as the only agent, did not offer promising results. In 1980, inspired by the studies of Robertson and Enhorning on preterm rabbits (Robertson and Enhorning, 1972), Fujiwara made a landmark in the clinical surfactant therapy by applying chloroform/methanol extract of lavaged porcine lung surfactant in several preterms which resulted in significant respiratory improvements (Fujiwara et al., 1980). This and the following trials demonstrated that the exogenous surfactant replacement therapy is highly efficient in improving respiratory function, reducing pulmonary dysfunctions and reducing neonatal mortality in premature infants. Although generally exogenous surfactant therapy efficacy is well established, it is currently being improved in terms of exogenous surfactant preparation, delivery methods, timing of therapy, ventilation patterns, use with other agents etc. (Robertson and Halliday, 1998).

1.4.3 Surfactant therapy of ARDS

ARDS in adults and children is a severe respiratory failure with multiple etiologies. Endogenous surfactant dysfunction occurs in ARDS by several mechanisms and is known to contribute to its pathophysiology. The widespread incidence and clinical severity of ARDS have promoted the efforts to treat this complex disease. The specific changes in ARDS include a decrease in the levels of PC, PG and increase in other minor PL in the bronchoalveolar lavage (BAL). The mechanism responsible for these changes is altered synthetic and secretory pathways within type II cells and activation of lipases in the air spaces. Surfactant protein levels are also decreased. In addition, increased permeability of the lungs results in leakage of serum into air spaces whose proteins inhibit the activity of the surfactant. Exogenous surfactant therapy in this case addresses only one aspect of this disease and complementary treatment is required to target other aspects of the syndrome. Animal studies have demonstrated that administration of exogenous surfactant early in the injury results in improvement of lung function whereas only transient improvement is found with later treatment (Eijking et al., 1993; Ito et al., 1996). Treatment of rats with acute lung injury with surfactant containing 2% recombinant SP-C showed significant improvement of the injury (Hafner et al., 1999)

Clinical trials performed with natural surfactants showed promising results. Phase II clinical trials were performed with synthetic surfactant containing recombinant SP-C and showed improvement in gas exchange compared with nontreated patients (Spragg et al., 2003).

.

1.5 EXOGENOUS LUNG SURFACTANTS

1.5.1 Natural surfactants

Clinical exogenous surfactants currently in use are derived form animal lungs and are obtained by organic extraction of bovine or porcine lungs. Within these animal derived surfactants some are obtained by organic extraction of lavaged animal lung surfactant (bLES, Infasurf (CLSE)), and the others by organic extraction of processed animal tissue. Curosurf® is obtained by this later method, as well as Survanta® and Surfactant TA®, which bear additional synthetic derivatives. In summary, natural preparations vary in source and composition and do not have an absolutely defined composition. A summarized description of these formulations is included:

Alveofact® (Thomae GmBH, Bilberach, Germany) is a surfactant obtained by chloroform/methanol extraction of bovine lung lavage. It contains 99% lipids with 4% cholesterol and 1% hydrophobic proteins SP-B and SP-C.

bLES® (bLES biochemicals Inc, Ontario, Canada) is a chloroform/methanol extract of surfactant isolated by centrifugation from bronchoalveolar lavage of bovine lungs. bLES is acronym for "Bovine Lipid Extract Surfactant". An additional extraction with acetone is used to deplete cholesterol and other neutral lipids. In the final composition bLES contains 98-99% phospholipid (79% PC) and around 1% of surfactant proteins.

Curosurf® (Chiesi Farmaceutici, Parma, Italy) is a surfactant extract prepared from minced porcine lungs by washing, centrifugation, chloroform/methanol extraction and liquid gel affinity chromatography purification. Curosurf® undergoes an additional purification step that eliminates neutral lipids which make 11% in moles (with almost no cholesterol) comparing to 44% of Survanta®. Curosurf® contains 99% lipids and 1% protein. It contains a lower percentage of PC (65%) and higher percentage of PE and SM than found in lavaged lung surfactants.

Infasurf® (ONY, Inc, Amherst, NY, USA) is a chloroform/methanol extract of saline bronchoalveolar lavage of intact calf lungs. Infasurf contains 93% phospholipid, 5% cholesterol and neutral lipids, and 1.5% proteins (SP-B and SP-C). Within the phospholipids, 83% accounts for PC, 6% for PG, 3% for PE and 2% for SM. DPPC accounts for almost 50% of total phospholipids.

Surfactant TA® (Surfacten, Tokyo Tanabe, Tokyo, Japan) is the organic extract of minced lung tissue supplemented with synthetic DPPC, palmitic acid and tripalmitin. Surfactant TA® contains the higher level of saturated lipids comparing to Curosurf® (66% in moles comparing to 31% of Curosurf®).The final product contains 84% phospholipids, 7% tripalmin, 8% palmitic acid and 1% protein. Its protein content is lower than in the native surfactant due to the losses during extraction process.

Survanta® (Beractant, Abbott Laboratories, IL, USA, licensed form Surfacten, Japan) is organic extract of bovine lung tissue supplemented with the same additives as Surfactant TA.

1.5.2 Synthetic surfactants

Although very efficient, natural surfactants bear serious defects. They vary in composition between animals and source (tissue or lavage), which results in different surface activity in *in vitro* experiments as well as in animal models. Their production has huge costs and the sources are limited. Natural source limitations would would particularly affect treatment of possible adult patients where more material is required (the amount of surfactant is relative to the body weight). The incidence of preterm

infants is rising which requires higher availability of the sources. Additionally, the risk of transmission of animal infectious agents and the possibility of immunological reaction especially in immunocompromised patients with ARDS justify the necessity for a highly controlled synthetic material.

The efforts aimed at new surfactant development include modification of existing exogenous surfactants by adding molecules that can enhance its activity, or the development of completely new preparations. Completely synthetic surfactants are currently actively investigated. Controlled production, composition and quality control preparation are some of the advantages of synthetic over natural surfactants.

Experience form exogenous surfactant therapy in premature infants in the early 80's clearly indicated that an artificial surfactant must contain hydrophobic surfactant proteins B and C apart from lipids. This finding is supported by surface adsorption measurements which have shown that under equilibrium or dynamic conditions PL mixtures reconstituted with hydrophobic surfactant proteins mimic the surface activity of natural surfactants (Takahashi and Fujiwara, 1986; Mathialagan and Possmayer, 1990). However, the successful synthetic surfactant formula has not yet been found mainly due to technical problems associated with obtention of active SP-B and SP-C analogues. Each of the proteins was approached differently taking into account their fold, length and oligomerization status. SP-B is too big to be chemically synthesised, and its insolubility in aqueous solvents and correct folding including three intramolecular disulfide bonds precluded its expression in heterologous systems. Efforts are therefore focused on finding a minimal peptide analogue that could mimic the behaviour of SP-B. As a result of such efforts a peptide named KL4 was created (21 amino acid long peptide with repetitive lysine and leucine residues) to mimic SP-B (Cochrane and Revak, 1991) and is currently undergoing clinical trials. Another successful peptide based on the residues 1-25 of SP-B in dimeric form was shown to enhance surface activity and *in vitro* and *in vivo* data show that its addition at 2% to lipid mixture improves surface activity, oxygenation and lung volume (Veldhuizen et al., 2000)

On the other hand, SP-C is less challenging in terms of its size and fold, however, its tendency to aggregate poses problems for its chemical synthesis. Recombinant expression was succeeded in bacteria as host and such recombinant SP-C is currently tested clinically as a component of single protein surfactant preparation, since there is accumulating evidence that SP-C may be used as the only protein component in therapeutic preparations. SP-C based synthetic surfactant was tested successfully in rabbit and lamb preterm models (Hawgood et al., 1996; Davis et al., 1998). In ARDS models surfactant containing only SP-C was shown to be comparable to bovine derived preparation which contains both hydrophobic proteins (Hafner et al., 1994). A recombinant surfactant protein C based surfactant has been found beneficial in preclinical studies (Hafner et al., 1998) and phase I-II clinical trials (Spragg et al., 2003). However in phase III clinical trial failed to improve survival (Spragg et al., 2004).

The selection of lipid components for synthetic surfactant is also important since the activity of particular peptide varies depending on the lipid environment (for example Johansson et al., 2003). Natural surfactants are composed by more than 50 different lipid types and our incomplete knowledge of their function together with limited commercial availability of many PLs results in the use of simplified PL mixtures in synthetic surfactant preparations. Most of the synthetic preparations tested today contain DPPC and PG in different proportions. With improved understanding of particular lipid function the

selection of lipids in synthetic preparations will probably be revised.

In the category of synthetic surfactants ALEC® and Exosurf® bear only lipid components while KL4 bears a synthetic peptide and Recombinant SPC Surfactant a recombinant SP-C in addition to lipids.

*ALE*C® (Britannia Pharmaceuticals, UK), the first entirely synthetic surfactant is a protein free surfactant composed of DPPC and egg derived PG in 7:3 molar ratio. Alec was withdrawn from the market following clinical trials comparing it to the natural Curosurf®, since higher mortality was observed in infants treated with ALEC.

Exosurf® (Glaxo Wellcome, NC, USA) is a mixture of synthetic DPPC and the spreading agents hexadecanol and tyloxapol in 1:0.111:0.075 weight ratio. DPPC is the primary surface tension lowering component, while non-ionic detergent tyloxapol and hexadecanol enhance adsorption and spreading. This preparation failed to show efficacy in phase II clinical trial for ARDS.

KL4® (Surfaxin, Discovery Laboratories, San Diego, California) is a synthetic surfactant composed of DPPC, POPG, palmitic acid and 21 amino acid long peptide containing repeating units of one lysine and four leucine residues. 82% by weight accounts for lipids DPPC:POPG in 7:3 weight ratio, palmitic acid accounts for 15% by weight and KL4 peptide is present in 3% by weight relative to phospholipids. KL4 peptide was designed to approximate the balance of hydrophobic and hydrophilic residues in SP-B. KL4 surfactant is undergoing phase III clinical trials for RDS in premature infants. The initial studies in prematures with RDS show improvement similar to natural surfactants (Cochrane et al., 1996).

Recombinant SPC surfactant® (Venticute, Altana Pharma, Konstanz, Germany), Recombinant SP-C with glycine as the first amino acid, cysteines at position 5 and 6 mutated into phenylalanines and Met 32 mutated into isoleucine, is mixed at 2% weight with DPPC:DPPG (7:3) with addition to 5% palmitic acid. This surfactant has been shown highly effective in animal models (Davis et al., 1998) and is currently under evaluation for clinical use.

1.6 OVERVIEW OF SP-C ANALOGUES

As mentioned earlier, SP-C is a critical component of synthetic surfactant preparations. Mixtures with SP-C as a single protein component have been found to be successful in treating animal models of surfactant deficiency. Since the early 90´s various attempts to obtain synthetic SP-C have been performed.

One of the earliest efforts to obtain SP-C by organic synthesis was made by Johansson and collaborators (Johansson et al., 1995a). The study using chemically synthesized protein focused on structure-function correlation in addition to questioning the contribution and function of palmitoyl residues. In this study a purified native protein, its depalmitoylated form and synthetic peptides with varied amino acids at position 5 and 6 demonstrated a correlation between helical content and biophysical activity (Johansson at al., 1995a). Synthetic peptides, which in this case showed lower helical content, displayed also lower ability to accelerate lipid spreading at the air water interface. This lead to the idea that analogues mimicking the secondary conformation rather than exact amino acid

sequence could serve as active substitutes in synthetic preparations. Even the substitution of the helical segment by another transmembrane segment from bacteriodopsin mimicked the surface properties of the SP-C wild type sequence.

Since poly-Val sequence does not favour helix formation, analogues with substitutions in this region have been designed. SP-C (Leu) is an analogue with a poly-Leu stretch instead of poly-Valine one which folds efficiently into α helix. Airway instillation of this molecule together with lipids to the prematurely born rabbits improves lung function by about 30% (Takei et al., 1996b)

Synthetic lipids with synthetic SP-C analogues with natural poly-Val sequence and its truncated forms have been shown to be effective surfactants *in vitro* and in rabbit preterm RDS model (Takei et al., 1996a). The peptide comprising amino acids 6-32 was demonstrated to be sufficient to provide good activity in a Langmuir balance as well as in rabbit premature model. However no data on their secondary structure has been reported.

SP-C 33, a chemically synthesised analogue containing leucines instead of valines and serines at position 5 and 6, was created as a result of efforts to circumvent technical problems with synthetic SP-C analogue bearing leucines that formed higher order oligomers (Nilsson et al., 1998). This poly-Leu derived peptide could not be suspended at concentrations higher than 20mg/ml which is four times lower that the dose of natural surfactants given in therapy. SP-C33 is based on the human sequence and starts with the isoleucine at position three in human sequence (Johansson et al., 2003). This peptide is highly soluble and does not oligomerize. The surfactant preparations based on this molecule increase lung compliance in preterm rabbit foetuses to levels similar to surfactant preparations currently in clinical use (Curosurf®). It was observed that the activity of this peptide depends on lipid composition.

Non-natural analogues of SP-B and SP-C that capture amino acid sequence patterning and 3-D fold of natural proteins SP-B and SP-C have been tested in synthetic mixtures (Seurynck et al., 2005; Wu et al., 2003). These molecules are based on N-substituted glycines with mimetic sequence of side chains that adopts stable helical secondary structure in aqueous and organic solvents. When added at 10% (w/w) ratio to lipid mixtures of DPPC:POPG:PA (68:22:9,w:w:w) they improve the kinetics of lipid adsorption to the interface and reduce the degree of film compression necessary to reach the minimum surface tension during cycling in pulsating bubble surfactometer. No data on their *in vivo* performance has been published yet.

As mentioned above, SP-C has been also produced in recombinant form. Veldhuzein and co-workers tried to overcome the lack of palmitoyl chains by expressing the mature protein in insect cells, which are able to perform proper posttranslational modifications (Veldhuizen et al., 1999). However, only 15 % of the protein was palmitoylated. *In vivo* palmitoylation occurs very early after the synthesis of the preproprotein and a proteolysed sequence may contain palmitoylation signals. Imperfect protein purity and lower activity in captive bubble surfactometer pointed to the necessity for a different approach.

The only recombinant form that has reached clinical trials is a recombinant form of SP-C from Altana Pharma. This protein, based on human sequence bearing two non-palmitoylated cysteines at position 5 and 6 is made as a fusion protein, from which it is chemically cleaved and extracted organically, followed by a reverse phase HPLC purification. This protein was first tested in rabbit model

of RDS, where it was shown to restore lung function in surfactant deficient animals similarly to the autologous surfactant (Hawgood et al., 1996). Posterior chemical palmitoylation did not show to improve its activity. The protein was later modified at positions 5 and 6, where phenylalanines were introduced in place of cysteines in order to be closer to the natural variant that has one palmitoylated cysteine changed into phenylalanine and to prevent aggregation. This molecule was tested in rabbit and lamb preterm models of surfactant deficiency as well as in animal model of acute lung injury which showed that rSP-C can be formulated into an effective surfactant (Davis et al., 1998; Hafner et al., 1998).

2 OBJECTIVES

OBJECTIVES

The great interest in SP-C stems from the finding that it is essential for optimal biophysical and physiological activity of exogenous surfactants applied in clinical therapy of RDS in infants. Surfactant replacement therapy in premature infant with respiratory distress has now become accepted as a standard therapy. Currently the therapy is based on lipid and protein components extracted from animal lung tissue and has proven efficient in reducing mortality and morbidity from RDS. Although very efficient, native surfactant preparations need to be revised for several reasons. Native surfactant preparations vary significantly in their composition depending on the tissue source and extraction procedure which can generate variations in treatment outcome. In addition, their production is expensive and bears a risk of animal pathogen transmission. Synthetic surfactants overcome these problems by providing a more controlled production and composition. Despite big efforts a successful synthetic formula has not been designed yet. The lipid portion of the artificial surfactant is readily available by chemical synthesis which is not the case for the two essential surfactant proteins SP-B and SP-C. The main restriction for organic synthesis or expression in heterologous systems is imposed by their extreme hydrophobicity and the tendency of SP-C to aggregate in the absence of lipids.

On the other hand, the recombinant proteins are also useful in a wide variety of experimental conditions in which the wild type sequence can not be handled. The possibility to generate targeted amino acid changes or other manipulations in its sequence will improve our insights into the structure, dynamics of interaction with phospholipids and the molecular mechanisms of this protein.

The main objective of this thesis is to set up a new approach for recombinant large scale production of SP-C which could serve as a base for new synthetic surfactant preparation as well as a tool for structure-function studies.

This general objective was approached in several successive specific steps:

1. The design and optimisation of heterologous recombinant SP-C production.
    I. Optimisation of expression conditions in bacterial host
    II. Optimisation of purification steps
    III. Confirmation of the recombinant peptide identity and secondary structure

2. Study of recombinant protein surface activity compared with the native protein isolated from animal lungs.
    I. Study of surface spreading activity of recombinant versus native proteins
    II. Characterization of protein and lipid/protein interfacial films subjected to compression.

3. Study of the effect of the presence of aromatic amino acids on recombinant protein activity.

    I. Expression and purification of recombinant variants bearing tryptophans and cysteines at positions 5 and 6.
    II. Study of surface activity *in vitro* of new variants compared with the one bearing

phenylalanines.

4. Test the capacity of recombinant forms of SP-C as a single protein component of surfactant preparations to restore lung function in a rabbit model of RDS.

3 MATERIALS AND METHODS

3.1 Protein expression and purification

Construction of plasmids encoding the His-tagged chimerical protein (SN/GpA) has been described previously (Mingarro et al., 1996). The glycophorin A (GpA) sequence in the original plasmid was replaced by a PCR-amplified sequence of human SP-C (generous gift from Dr. Joanna Floros, University of Pennsylvania at Hershey), using *ApaI*/*BamHI* restriction sites. The N-terminal His-tag, the optimised thrombin digestion site, and all point mutations in the wild type sequence of SP-C were introduced by site-directed mutagenesis using the QuikChange kit from Stratagene (La Jolla, California) and verified by DNA sequencing.

The expression of the fusion protein was performed as described earlier (Orzaez et al., 2000). Briefly, a 10 mL overnight culture of BL21 (DE3) pLys (Novagen, Madison, WI) cells transformed with the corresponding vector was inoculated into 1 L of LB medium and grown at 37 ºC until the OD_{600} reached 0.6. IPTG (1 mM) was added for induction and the culture was grown for additional 3 hours. The cells were harvested by centrifugation at 3800 g for 10 min in a Sorval centrifuge and resuspended in resuspension buffer (10 mM Tris HCl pH 7.9, 1 mM EDTA, 0.01 M PMSF). Pellets were frozen until use. In order to break the cellular membranes, the pellets were freeze-thawed three times, sonicated and added to the same volume of TBS 1% lauroyl sarcosine detergent. This mixture was centrifuged at 18000 g for 10 minutes. The fusion protein was purified from the supernatant via immobilized metal affinity chromatography. An ÄKTA purifier liquid chromatography system (Amersham Bioscience) was used with a His-Trap column filled with nickel containing resin. The buffers for chimerical protein purifications were the following: equilibration buffer, TBS 0.5% lauroyl sarcosine; wash buffer, TBS 0.2% lauroyl sarcosine 10mM imidazol; and elution buffer, TBS 0.2% lauroyl sarcosine 500 mM imidazol. The eluted protein was dialysed to remove imidazol and finally concentrated by using an Amicon concentrator with YM10 ultra-filtration membrane (Milipore, Bedford MA) 5-6 times. Generally, 4 mg of the fusion protein were obtained per 1 litre of LB medium.

3.1.1 Thrombin digestion

A thrombin cleavage site (LVPR↓GP), introduced between SN and SP-C allowed the proteolysis of the fusion protein. A glycine-rich 'kinker' next to the thrombin cleavage site was introduced to improve the cleavage efficiency (Hakes and Dixon, 1992). Thrombin (Novagen) digestion trials were performed before each large-scale digestion. Usually, 10 U of thrombin were required for digestion of 1 mg rSP-C and 1 U of thrombin was needed for 1 mg of rGP/SP-C. Thrombin digestions were performed at 21^0C in the buffer recommended by the supplier, with shaking at 550rpm in an eppendorf thermomixer. The reactions were concentrated again using a cell concentrator with membranes of 1 kDa molecular cut off. Aliquots taken from the digestion reaction mixture were applied to tris-tricine gels in order to monitor the appearance of the bands corresponding to the *Staphylococca*l *nuclease* (18.5 kDa) and rSP-C (3.9kDa) (figure 20).

3.1.2 Organic extraction

An organic extraction of the cleaved protein solution was performed according to the protocol of Bligh and Dyer (Bligh and Dyer, 1959) for lipid extraction. Shortly, two volumes of methanol and one volume of chloroform were added to the protein mixture, which was vortexed and incubated at 37^0C. After addition of one more volume of chloroform and one of water, the mixture was vortexed and centrifuged at 550g/5min. The lower, organic, phase was collected and two volumes of chloroform were added two more times to the aqueous phase in order to increase protein recovery. All organic phases were stored in glass bottles at -20^0C. The organic extract was concentrated to approximately 2 mL prior to application to the lipophilic chromatographic column. Protein concentration was performed in the presence of egg yolk PC (Avanti Polar Lipids, Alabaster, AL) at 1:5 (w:w) ratio in a rota-vaporizer apparatus.

3.1.3 Sephadex LH-20 lipophilic size exclusion chromatography

In order to eliminate components other than SP-C that could have co-extracted in the organic phase, the organic extract was applied to a Sephadex LH-20 column (Amersham Biosciences). This column is used for lipid separation and is adapted to the use with organic solvents. Proteins and lipids are eluted from the column by a chlorofom:methanol (2:1, v:v) eluting system. Fractions were collected and absorbance at 240 and 280 nm were recorded on a spectrophotometer. Absorbance peaks were pooled and loaded on SDS-PAGE and subsequently analysed for their amino acid content and by mass spectrometry.

3.1.4 Mass spectrometry

For determination of the molecular masses, 0.85 μL of the of peptide dissolved in chloroform:methanol (2:1, v:v) were spotted onto a MALDI-TOF sample holder and allowed to dry at room temperature. An equal volume of a saturated solution of sinapinic acid (3,5-dimethoxy-4-hydroxycinnamic acid) (Sigma) saturated in 70% acetonitrile containing 0.1% TFA was added, let dry, and analyzed with an Applied Biosystems Voyager-DE Pro MALDI-TOF mass spectrometer, operated in delayed extraction and linear or reflector modes. The mass calibration standard in linear mode consisted of a mixture of the following proteins, whose calculated isotope-averaged molecular masses in Daltons are given between parentheses: bovine insulin (5734.6), *E. coli* thioredoxin (11674.5), horse apomyoglobin (16952.6). For reflector calibration, a tryptic peptide mixture of *Cratylia floribunda* seed lectin (SwissProt accession code P81517) prepared and previously characterised in Dr. Juanjo Calvete (IBV, CSIC) laboratory was used.

3.1.5 Circular dichroism

To prepare the samples for CD measurements, the purified protein (50 μg) in chloroform:methanol solutions was mixed with lysophosphatidylcholine (LPC) or DPPC:POPG (7:3) at a protein: lipid ratio of 1:5 (w:w), dried under a stream of N_2 and then under vacuum for 2h. The resulting dried films were hydrated by addition of 0.5 mL of 5mM Tris buffer (pH 7) containing 150 mM NaCl with intermittent vortexing at room temperature for LPC micelles formation, or at 55^0C for DPPC:POPG vesicles. The suspensions were then sonicated during 1 min. CD spectra were obtained on a Jasco J-810 CD spectropolarimeter. Quartz cells of 1 mm optical path were used to record spectra at a scanning speed of 50 nm/min. Generally, 15 scans were accumulated and averaged, subjected to noise reduction and corresponding blanks subtracted. Data analysis was performed with the help of the CDPro software package, which contains three commonly used programs: SELCON3, CONTIN/LL and CDSST (Sreerama et al., 2000; Sreerama et al., 2004). This software allows the use of different reference sets of proteins, including 13 membrane proteins (SMP50), to increase the reliability of the analysis.

3.1.6 SDS-PAGE

Fusion proteins and protein samples obtained after organic extraction or eluted from the Sephadex column were analyzed onto 16% SDS-PAGE. The SP-C peptide samples were first evaporated under Nitrogen stream, resuspended in the loading buffer, boiled 5 min at 95^0C and applied to the gel. After running, gels were fixed, stained with Comassie blue stain and distained. In order to resolve small molecular mass peptides generated after thrombin digestion, the samples were loaded on tricine 15% acrylamide gel. Tricine gels were processed identically as SDS-PAGE gels.

3.2 Lung surfactant organic extraction/ native SP-C separation

Pig lungs were lavaged with a solution of 0.15M NaCl, pH 7, filtered through the cheesecloth and centrifuged at 2000rpm/5min/4^0C in Sorvall centrifuge. Lung surfactant was isolated according to Casals et al., 1989. Briefly, lung lavage was first centrifuged at 105000g for 2h at 4^0C. The pellet obtained, which contains lipid and protein components of lung surfactant was then resuspended in 16% NaBr in NaCl 0.15M. Over this layer another solution was deposited 16% NaBr in NaCl 0.15M and centrifuged at 116000g during 2h 4^0C in Beckman L5. The purified surfactant was collected at the interface between NaCl (0.15M) NaBr (13 %) and freezed to -80 ^{0}C. Alternatively, surfactant lipid/protein complexes used to purify SP-C, were obtained from minced porcine lungs as previously described (Perez Gil et al., 1993). In this case, minced lungs were exhaustively washed with a solution of 150mM NaCl, Tris 5mM pH=7, and the solution was subjected to two consecutive centrifugation steps. A first centrifugation at 650Xg /4^0C/5min

removes tissue and cell debris and second centrifugation at 3300xg/4^{0}C/2h produces a pellet containing a mayor fraction of pulmonary surfactant complexes. Purified surfactant or surfactant pellets were then subjected to organic extraction (as described above) and loaded onto Sephadex LH-20 column. The column is equilibrated by chloroform/methanol (2:1 v/v) and fractions were collected. The absorbance of the fractions was measured at 240 and 280 nm in a Beckman DU-640 spectrofotometer. Figure 12 represents the elution profile of the organic extracted surfactant. The first peak corresponds to hydrophobic proteins and the rest are surfactant lipids. Fractions corresponding to hydrophobic proteins were pooled and applied on a Sephadex LH-60 resin equilibrated with chloroform methanol (1:1, v/v) containing 0.5% volume HCl 0.1N. The elution chromatogram is represented on figure 13. The first peak corresponds to SP-B and the second to SP-C. The peak corresponding to SP-C does not absorb at 280 due to the absence of aromatic residues. Fractions corresponding to each protein were collected and stored at -20^{0}C. Protein concentration was determined by quantitative amino acid analysis.

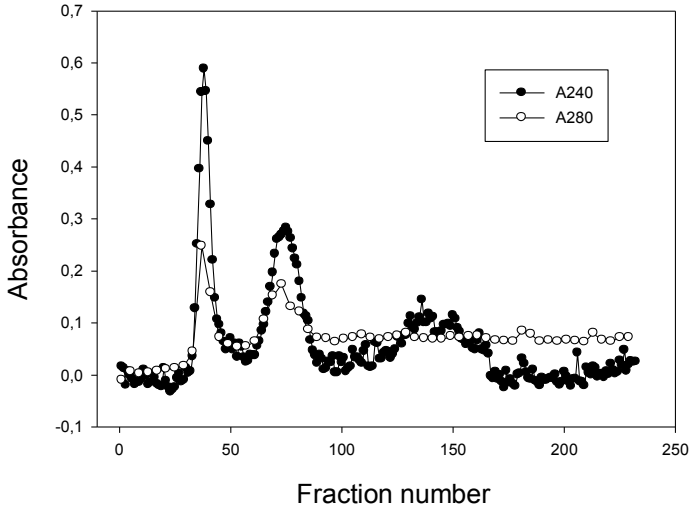

Figure 12. **LH 20 elution profile of organically extracted surfactant.** The first peak corresponds to proteins (SP-B and SP-C) and the remaining (marked by brackets) correspond to lipids.

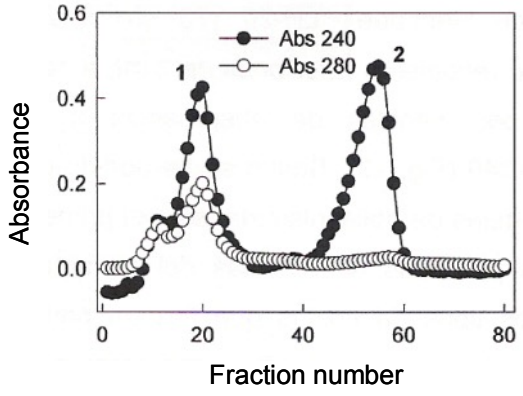

Figure 13. Elution profile of protein fractions collected from Sephadex LH-20 on Sephadex LH-60. Peak 1 corresponds to SP-B while peak 2 corresponds to SP-C.

3.3 Quantitative amino acid analysis

Usually 100μl of native or recombinant SP-C was dried under a stream of nitrogen and 100μl of HCl 6N with 0.1%(w/v) of phenol was added and a known amount of nor-leucine as a internal control was added. The tubes were closed under vacuum and maintained for 24h at 110 ^{0}C in order to allow for extensive hydrolysis of the peptide bonds. Next, the tubes were opened and allowed to dry in order to evaporate HCl. The samples were washed twice with 100μl of water and dried in a speed vac. Finally, 50μl of amino acid analysis buffer was added and samples were analysed in automatic analyzer Beckman System 6300 High Performance.

3.4 Phospholipid quantification

The amount of phospholipid present in different samples was determined by measuring phosphorus content according to Rouser et al., 1966. After evaporating organic solvents from the samples, 0.13ml of perchloric acid (70%) was added and incubated in sand bath for 25 minutes at 250^{0}C. Control samples with known phospholipid content were analysed in parallel. By this method the phosphorus present in phospholipids is mineralized. Such mineralized phosphorus is then quantified by a colorimetric method by adding 0.15ml of ammonium molibdate (2.5%) and 0.15 ml of ascorbic acid (10%). The samples were boiled for 7 min in water bath and the reaction was stopped by introducing the tubes on an ice water bath. Absorbance was measured at 820nm in a Beckman DU 640 spectrophotometer and the concentration of phosphorus determined by interpolating the data in calibration curve prepared using samples with known phosphorus content.

3.5 Behaviour of surfactant films at the air-water interface

3.5.1 Surface balance

The Wilhemy surface balance is the most widely used technique to study the interfacial behaviour of surfactant molecules. It is composed of a teflon trough where a certain volume of aqueous subphase is deposited. Surface pressure is measured by a flag consisting in a filter paper plate that is submerged into the aqueous subfase and connected to the surface pressure sensor. The surface pressure (the difference between the surface tension of clear water and that of the sample) is measured as a function of time or the area occupied by the molecules deposited at the interface.

3.5.2 Surface spreading

Surface spreading kinetics was monitored by a Wilhemy balance (Nima, Coventry, UK)

equipped with a minitrough (15 cm^2 of surface, 5 mL volume of sub-phase) and using a Whatman Nº 1 paper dipping plate attached to the pressure transducer. Material in the form of large multilamelar suspensions was deposited on the surface of the aqueous buffer and the change of surface pressure was monitored with time.

Reconstitution of recombinant proteins or native SP-C obtained by organic extraction of porcine material into synthetic phospholipids leads to the formation of lipid protein complexes that have been used extensively to characterize protein structure and lipid protein interactions. Protein-lipid mixtures dissolved in organic solvent were evaporated under nitrogen and 2h in speed vac and the resulting film rehydrated in Tris buffer. Specifically, 1 mg of a mixture of DPPC:POPG (7:3, w:w) containing 0, 2, 5 or 10% protein (w/w) was dried and reconstituted in 100 μL of 5 mM Tris buffer pH 7.0 containing 150 mM NaCl in a termomixer during 1.5 h/ 50^0C with cycles (2 min vortex 1400 rpm every 10 min). Adsorption π-t kinetics following the formation of phospholipid films from vesicles as promoted by native and recombinant forms of SP-C was monitored. To start acquisition of the π-t adsorption isotherms, 10 μL of this suspension was deposited directly on top of the buffer and allowed to spread on the surface of the balance. When the interface is saturated with molecules the equilibrium pressure is reached. Further addition of molecules without changing the area does not increase the pressure. Experiments were performed at 25 °C and repeated at least three times with two different samples from each protein.

3.5.3 Surface pressure-area isotherms

The organization of surfactant molecules at the air-water interface can be described as two-dimensional surface states: gas, expanded (also called liquid expanded) and condensed (figure 14). In the gas state the molecules are diluted in the surface film with the hydrophobic portions of the molecules making significant contacts with the water surface but little contact with each other. A gas monolayer has therefore little effect on the surface pressure and hence the surface pressure is nearly zero. Compression induces the formation of the liquid –expanded (LE) phase from the gas phase.

In the expanded state the film molecules are closer to each other and interact through their tail or head regions. The hydrophobic portions of the molecules lift from the water surface but remain largely disordered and fluid. Further compression leads to transition to liquid-condensed (LC) phase, which in certain films is indicated by a plateau in the isotherm corresponding to LE and LC coexistence. LC phase is characterized by higher molecular order. Further compression of condensed films produces solid-like states with tight molecular packing. The fatty acyl chains of condensed films can have various degrees of tilt with the most condensed films having vertical tilt and extended chains. Eventually, when there is no more space to accommodate all the molecules in the available surface the film collapses, ejecting the molecules from the monolayer and forming subsurface and/or suprasurface structures. Pressure-area (π-A) isotherms describe the state of the monolayer at any compression extent, provided that a known amount of surface active material is deposited on a known area.

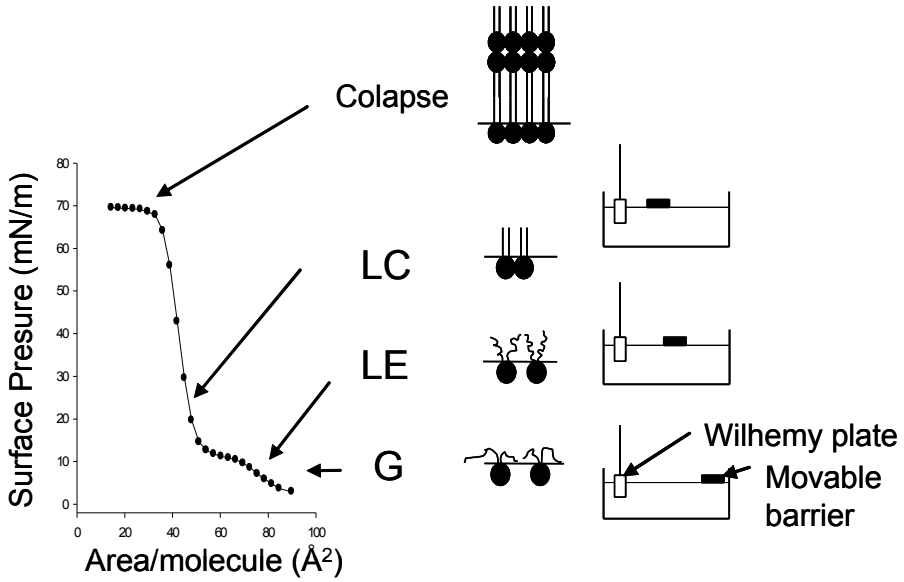

Figure 14. Schematic representation of a Wilhemy balance and the different states reached by a phospholipid interfacial film during compression. On the left is represented the pressure-area isotherm recorded from the Wilhemy balance, indicating the segments where the different states are reached. G, gas phase, LE, liquid expanded phase; LC, liquid condensed phase.

Pressure-area isotherm defines quantitatively the surface behaviour of surfactant films subjected to compression/expansion dynamics. The surface pressure-area isotherm is obtained in a surface balance which allows compression and expansion of the surface film while surface pressure is measured. Surface pressure rises as the film is compressed to smaller areas. The area is usually expressed in $Å^2$ per molecule, provided that the amount of material deposited in the surface is accurately known.

Pressure-area isotherms were monitored here by Wilhemy balance specially designed by Nima Technologies (Coventry, UK) equipped with a trough of 200 cm^2 of surface and 300 mL volume of subphase and with a deformable ribbon barrier to minimize film leakage during compression.

3.5.4 π-A compression isotherms

Monolayers of lipid (DPPC:DPPG, 7:3, w/w) or lipid/peptide binary systems were made by spreading a small volume of a concentrated lipid or lipid/peptide solution in chloroform:methanol (3:1, v/v) at the surface of a 5 mM Tris buffered sub-phase, pH 7, containing 150 mM NaCl. These monolayers were prepared as previously described (Serrano et al., 2005) in a thermostatic (25°C) Langmuir-Blodgett trough (NIMA Technologies, Coventry, United Kingdom) equipped with a ribbon barrier to minimize film leakage during compression. Sub-phases were prepared with double distilled water (the second distillation performed in the presence of potassium permanganate).

After spreading the sample on top of the sub-phase, the organic solvent was allowed to evaporate for 10 minutes before starting compression. The total area of the interface was 200 cm^2 and the monolayer was compressed at 65 cm^2/min, while changes in surface pressure were recorded and plotted against the area occupied per phospholipid molecule.

To analyse the effect of native and recombinant SP-Cs on successive compression-expansion cycles, monolayers prepared as described above were compressed and expanded at 65 cm^2/min five times while surface pressure-area data were collected.

3.5.5 Microscopy

Fluorescence microscopy has been used to follow structural transitions in surfactant lipids during compression of the air –liquid interface. To observe monolayers with epifluorescence microscope the films were formed as for compression isotherms, by depositing the protein/lipid mixture dissolved in chloroform/methanol on the top of the supbhase (Tris-HCl 5mM, NaCl 150mM, pH =7). To observe the interface, a trace (typically 0.5-1% molar to phospholipids) of a fluorescent lipid probe such as 1-palmitoyl-2-{12-[(7-nitro-2,1,3-benzoxadiazol-4-yl)amino]dodecanoyl} phosphatidyl choline (NBD-PC) is included into the lipid mixture used to form the monoalyer. The probe partitions into the lipid in the liquid expanded phase, whereas the gel-like liquid condensed regions are observed as dark regions due to the exclusion of the bulky probe. In the epifluorescence microscopy experiments, the monolayers were compressed (at 20mm^2/s) along the pressure-area isotherms while simultaneously transferred onto glass slides. The slides were dried on air and stored until being analysed under the fluorescent microscope. The acquired fluorescence images were analyzed digitally using the program SigmaScan Pro 5 (©SPSS Inc).

For AFM microscopy, pure protein films were compressed until a surface pressure of 30mN/m was reached, and subsequently transfered to freshly cleaved mica supports while maintaining constant pressure. AFM images of monolayers transferred to mica supports were obtained with a Nanoscope III scanning probe microscope (Digital Instruments, Santa Barbara, CA) operated in contact mode, using silicon nitride tips with a force constant of 0.05N/m. Both topography and friction images were recorded from each sample. Digitally recovered images from both AFM and epifluorescence microscopy were quantitatively analyzed using the program Scion Image (Scion Corporation, Frederick, MD).

3.5.6. Stability of compressed lipid and lipid/peptide monolayers

The effect of proteins on the stability of monolayers compressed to very high pressures was analyzed by compressing DPPC or DPPC:DPPG (7:3) monolayers with or without different protein proportions, up to 60 mN/m, under the same conditions explained above. Once this pressure was reached, compression was stopped and the spontaneous decay of surface pressure was monitored over time.

3.6 Captive bubble surfactometer

Interfacial adsorption was studied in captive bubble surfactometer, an apparatus that allows measurements of surface tension in a bubble captured against agar gel support and inside a surfactant suspension. The bubble can be compressed and expanded by pressure changes from an exterior reservoir mimicking alveolar compression and expansion. Surface tension is computer calculated from diameter and height of the bubble from recorded video images and used in theoretical equations relating surface tension and bubble shape. Interfacial adsorption was measured in a bubble captured in solution (10%sucrose, NaCl 9mg/ml) and injection of 2 μl of surfactant suspension at 10mg/ml prepared as described below. After completed adsorption the bubble was sealed and quasi–static and dynamic compression-expansion of the bubble was performed as described in Rodriguez-Capote et al., 2001.

3.6.1 Preparation of synthetic surfactants for captive bubble and *in vivo* experiments

Recombinant variants rGP/SP-Cff, rGP/SP-Cww and rGP/SP-Ccc and lipids (DPPC:POPG, 68:31) in weight proportion peptide/lipid = 0.02 were mixed in chloroform/methanol (1:1, v:v), the solvents were evaporated and the resulting peptide/lipid films were subsequently hydrated in NaCl 0.9 mg/ml at a lipid concentration 80mg/ml. Surfactant samples used for analyses in captive bubble surfactometer were diluted with the same solution to 10mg/ml. Curosurf® (Chiesi Farmaceutici, Parma, Italy) was resuspended at 80 mg/ml. Both recombinant protein surfactants and Curosurf® were given at a dose of 200 mg/kg body weight.

3.7 *In vivo* experiments

The surfactant mixtures were tested in 29 preterm newborn rabbits, obtained by hysterectomy at a gestational age of 27 days (term, 31 days) (Sun et al., 1991). The animals were tracheotomized at birth, kept in pletysmograph boxes at 37°C, and ventilated in parallel with 100% oxygen, a frequency of 40 breaths/min, and 50% inspiration time. Before the onset of ventilation, experimental animals received, via the tracheal cannula, 2.5 or 4 ml/kg of the surfactant preparations indicated above. Littermates receiving no material into the airways served as controls. After surfactant instillation, peak pressure was first raised to 35 cmH_2O for 1 min, to facilitate distribution of surfactant in the lungs, and then lowered to 20 cmH_2O. The animals were then ventilated with a peak pressure of 15 cmH_2O for 15 min, after which pressure was lowered to 10 cmH_2O for 5 min, and further to 7 cmH_2O for 5 min, and then raised again to 15 cmH_2O for 5 min. Positive end-expiratory pressure (PEEP) applied was 3 cmH_2O. Tidal volumes (VT) were recorded at 5-min intervals by means of a pneumotachograph connected to the plethysmograph box.

At the end of the scheduled period of ventilation, animals were killed by intracerebral

injection of lidocaine. Their abdomen was opened, and the position of the diaphragm was inspected for evidence of pneumothorax.

3.7.1 Determination of lung gas volumes

After the scheduled 30-min period of ventilation with 100% O_2, with or without PEEP, the animals were ventilated for an additional 5 min with 100% N_2 at a peak inspiration pressure of 25 cmH_2O. The tracheal cannula was then clamped at end expiration. The trachea was ligated, and the lungs were carefully excised and weighed. Lung volume was determined by water displacement technique as described by Scherle (Scherle, 1970). Lung gas volume was calculated from the difference between lung volume (in ml) and lung weight (in g), based on the assumption that the density of lung tissue is the same as that of water.

Statistical evaluation. The values for VT, compliance and gas volumes are given as mean ± SD, and differences between groups were calculated for the last VT recording and gas volumes with ANOVA, followed by Newman-Keuls test.

4 RESULTS

4.1 EXPRESSION AND PURIFICATION OF RECOMBINANT SURFACTANT PROTEIN C (SP-C)

As described in the general introduction, SP-C is one of the most hydrophobic proteins in the proteome. It is a 35 amino acid polypeptide composed of a short N-terminal region, palmitoylated at residues Cys-5 and Cys-6, followed by an α-helical hydrophobic transmembrane (TM) C-terminal stretch made of aliphatic residues. Apart from the extreme hydrophobicity, the difficulty for obtaining artificial SP-C analogues derives from its strong tendency to misfold and aggregate in the absence of phospholipids (Gustafsson et al., 1999; Beers et al., 2005). The highly conserved TM sequence represented by 10-12 valines with intermittent isoleucines and leucine residues is capable of converting irreversibly into a fibrilar β-structure aggregate. The reason for such behaviour is probably that in aqueous solutions β-branched valines and isoleucines display a preference toward β-strands and are usually underrepresented in α helices while in lipid environments valine and isoleucine residues promote helix formation (Li and Deber, 1994). In agreement with this general tendency, the α helical polyVal-rich region of SP-C was found to convert spontaneously into β sheets *in vitro*, with an enhanced rate of α→β transition in the presence of polar solvents and deacylation (Gustafsson et al., 2001). Moreover, SP-C amyloid fibrils are found in patients with pulmonary alveolar proteinosis (Gustafsson et al., 1999). The fact that the loss of helical structure directly correlates with loss of activity was demonstrated by Johansson and colleagues (Johansson et al., 1995a).

Therefore the following critical issues had to be considered when designing the expression and purification strategy of this protein: the hydrophobicity conferred by the TM segment, the palmitoylation at Cys-5 and Cys-6, which represents an insuperable challenge for the bacterial expression machinery, and the protection from aqueous environment which induces protein aggregation.

The high hydrophobicity was overcome by making a fusion with the hydrophilic nuclease A (SN) from *Staphylococcus aureus* (SN/SP-C, see Materials and Methods). The use of the nuclease A (SN) as a fusion partner provides several advantages (reviewed in Laage and Langosch, 2001) for high-level heterologous expression of integral membrane proteins at full-length. For instance, the three-dimensional structure of SN shows numerous basic residues exposed to the solvent (Hynes and Fox., 1991), therefore precluding aggregation of fusion proteins and becoming a versatile system for membrane protein over-expression. This protein has been proved to be highly effective in the expression of the TM domain of Glycophorin A, a model system for studying helix-helix interactions in membrane proteins (Mackenzie, 2006). The fusion chimera is later proteolized in order to liberate the SP-C.

In order to prevent possible dimer formation via disulphide bonds in the absence of palmitoyl chains we introduced a double $C_5C_6 \rightarrow F_5F_6$ mutation. Phenylalanine residues were chosen because: i) they represent a native surrogate to the missing Cys-6 in the native SP-C of some animals (figure 8), ii) they have high propensity to partition into the membrane interface (Wimley and White, 1996), and iii) the Cys→Phe substitutions were shown not to affect the activity of the recombinant SP-C with phenylalanines in place of cysteines in animal models of RDS (Davis et al., 1998).

Finally, in order to protect the protein form aqueous environment the initial purification steps were performed in the presence of detergent while the later ones in the presence of lipids. During both,

the initial purification step, when protein chimera was enriched by membrane sedimentation, and the subsequent enzymatic cleavage of the nuclease moiety, the presence of detergents is essential in order to dissolve the cellular membrane, where a large part of the fusion protein is localised and, most importantly, to prevent aggregation of the cleaved recombinant SP-C. We optimised thrombin digestion in the presence of various detergents (SDS, Triton X, CHAPS and Lauroylsarcosine) of which lauroylsarcosine showed as most permissive for thrombin digestion. The protein was then separated form the rest of the digestion products into organic phase and concentrated in the presence of lipids.

4.1.1 OVER-EXPRESSION AND DIGESTION OF CHIMERIC PROTEINS

Vector design

Recombinant SP-C produced in the present work is based on the primary sequence of human SP-C (figure15a). The SP-C sequence was introduced in a pET11 vector bearing SN which was previously used for overexpression of GpA TM fragment in *E.coli*. The fusion sequence is preceded by a His-tag to enable its purification through nickel-agarose affinity chromatography. The thrombin cleavage site is preceded by a Gly kinker which facilitates thrombin digestion (Hakes and Dixon, 1992). A thrombin cleavage site was introduced between the SN and the SP-C sequence to allow removal of the nuclease moiety. The first four (out of six) conserved thrombin recognition amino acids (LeuValProArg) were introduced in the expression vector in front of the restriction site *(Apa I)* that was used to insert SP-C sequence (figure 15b). *ApaI* sequence (*GGGCCC*) codes for GlyPro, resulting in LVPR↓GP sequence which fulfils the consensus sequence for thrombin recognition. Thrombin digestion, therefore, leaves GP at the N-terminus of the SP-C sequence. We deleted GP in a second construct (figure 15c). Both constructs were subjected to site directed mutagenesis in order to introduce $C_5C_6 \rightarrow F_5F_6$ double mutation.

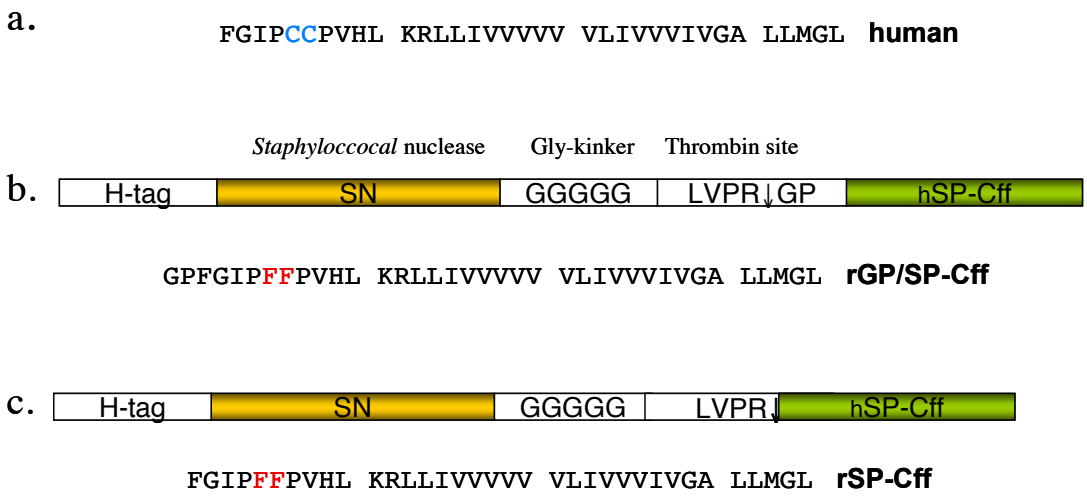

Figure 15. Vector design for expression of recombinant SP-C variants. (a) Human SP-C sequence highlighting the Cys residues in blue. (b) Schematic organisation of the chimerical protein bearing a LVPR↓GP thrombin recognition motif and the sequence of the resulting recombinant protein after thrombin digestion (rGP/SP-Cff). (c) Schematic organisation of the chimerical protein lacking GP in the thrombin recognition motif and the sequence of the resulting recombinant protein after thrombin digestion (rSP-Cff). Mutated residues $C_5C_6 \rightarrow F_5F_6$ are shown in red.

Over-expression and purification

Experimental parameters optimized for protein expression were: growth media, concentration of inducer (IPTG), size of culture batch, number of freeze-thaw cycles and sonication, time and temperature. The best results in pilot experiments were obtained in BL21(DE3)pLys cells growing in Luria Bertani medium up to O.D=0.6, protein expression induction by IPTG. After 3 hours the cells were pelleted subjected to three freeze-thaw cycles followed by sonication and subsequent addition of the same volume of a buffered (TBS) solution containing 1% lauroylsarcosine detergent (figure 16). This mixture was centrifuged separating the undisolved membranes from fusion protein-containing supernatants. Fusion protein content was enriched by washing the pellet with the same buffer several times and subsequently purified via immobilized-metal affinity chromatography (figure 17a). The remaining inclusion bodies were extracted with TBS buffer containing 3% TritonX detergent, and washed in urea 8M. Importantly, less than 10% of the total SN/SP-C fusion is expressed as inclusion bodies, as estimated by Coomassie-stained gels (figure 17b).

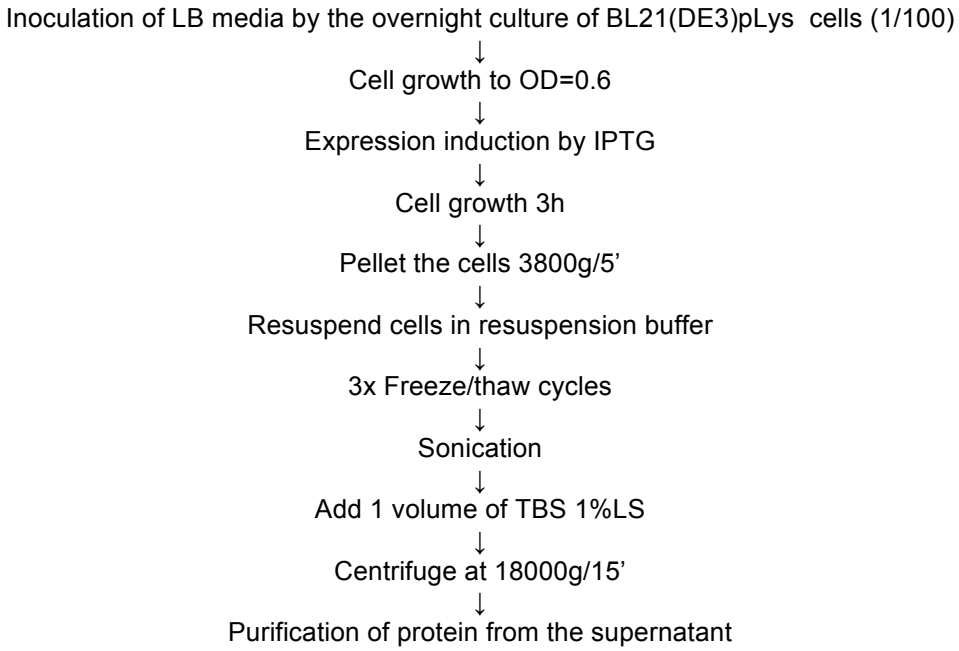

Figure16. Scheme of recombinant SP-C expression.

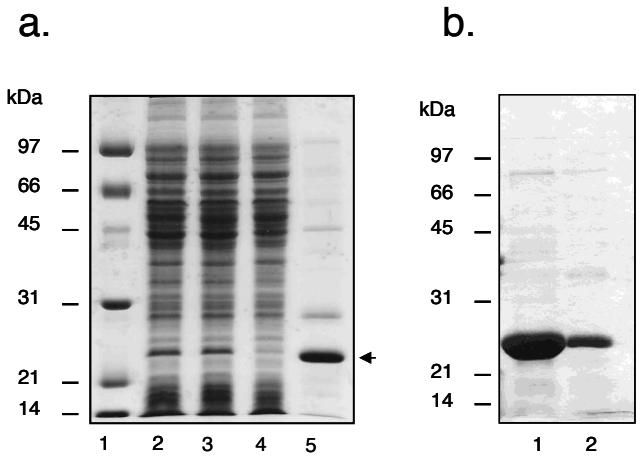

Figure17. SDS-PAGE analyses of over-expressed chimeric proteins through out the purification procedure. (A) Representative Coomassie blue-stained 12% SDS-PAGE of aliquots taken during the purification of chimeric protein. Lane 1, molecular markers; lane 2, whole cell extract; lane 3, supernatant of bacterial lysate; lane 4, nickel column flow through; lane 5, eluate form nickel column. The SN/SP-C chimera is marked with an arrowhead to the right. (B) SDS-PAGE loaded with equal aliquots of eluted protein from the supernatant of bacterial lysate (lane 1) and extraction from inclusion bodies using 3%TritonX-100and urea 8M in TBS (lane 2).

The gels in figure 17 show that the nuclease fusion proteins can be expressed to high levels and partially purified on a Ni-agarose resin (Fig. 17a). For high yield overexpression 1l cultures were processed as previously mentioned and the supernatant was loaded onto a Ni^{2+} charged resin by means of ÄKTA (GE Healthcare), automated purifier with high data reproducibility. The purifier was programmed to perform three steps: 1) equilibration of the Ni^{2+} charged column with TBS buffer, 2) wash unspecifically or loosely bound proteins with TBS containing 10mM imidazol and finally 3) to elute bound proteins with TBS containing 500mM imidazol. All the solutions contained lauroylsarcosine detergent (see Materials and Methods). A representative elution profile is shown in figure 18. Samples form each step were loaded on the SDS-PAGE gel in order to assure the protein location. Finally the elution fractions were pooled together, dialyzed against imidazol and concentrated to smaller volume.

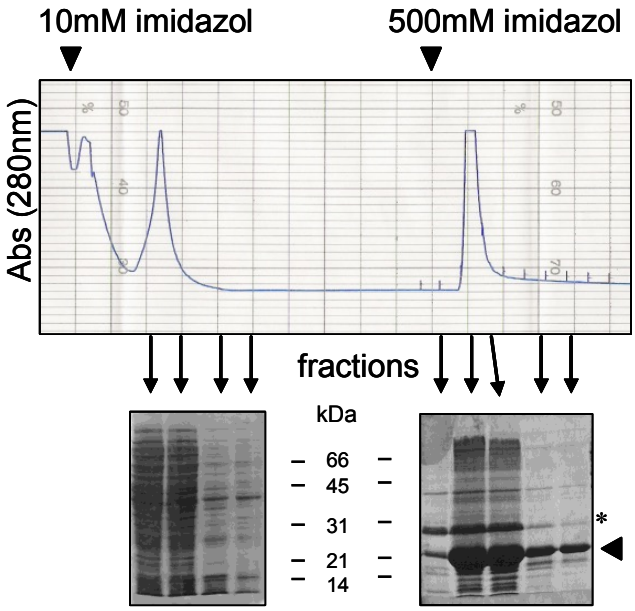

Figure 18. ÄKTA purification profile. A representative absorbance profile during the wash and elution of Ni^{2+} charged resin loaded with the fraction containing the chimeric protein. Arrowheads indicate the buffer switch. The first peak corresponds to the elution of loosely bound protein after addition of 10mM imidazol and the second one corresponds primarily to the designed fusion chimera (SN/SP-C) indicated by an arrowhead. An unspecific band of ~ 30 kDa (*) is usually copurified.

Thrombin digestion

The nuclease moiety was removed from the fusion by specific digestion with thrombin. The digestion of the fusion variant with the 6 amino acid thrombin recognition site (LVPR↓GP) results in a recombinant variant with two additional amino acids at the N-terminus, glycine and proline and this variant was named rGP/SP-Cff (figure 15b). After deletion of these two residues the fusion protein was still susceptible to thrombin digestion, although with a significantly decreased efficiency (figure 19). The resulting recombinant protein without additional amino acids was named rSP-Cff (figure 15c). Figure 20 shows a tricine gel loaded with undigested (lane 3) and digested (lane 2) fusion protein (SN/rSP-Cff). The two major protein bands emerging after cleavage correspond to the nuclease (SN) and the rSP-Cff moieties, respectively. The lower intensity of the rSP-Cff (lane 2, bottom band) compared to the nuclease moiety (top band) results from the six times lower molecular weight of the former. Both recombinant SP-Cs produced were analysed in parallel in the rest of the work. As mentioned above during both, the initial purification step and the enzymatic cleavage of the nuclease moiety, the presence of detergents was essential.

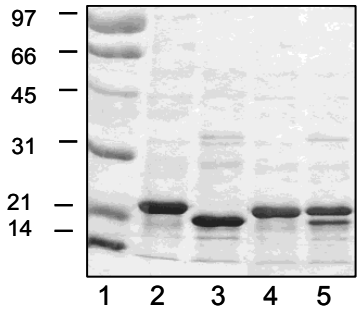

Figure 19. Different susceptibility to thrombin digestion. SDS PAGE loaded with molecular weight marker (1), rGP/SP-Cff (2), rGP/SP-Cff digested with thrombin (3), rSP-Cff(4), rSP-Cff digested with the same amount of thrombin as in lane 3 (5).

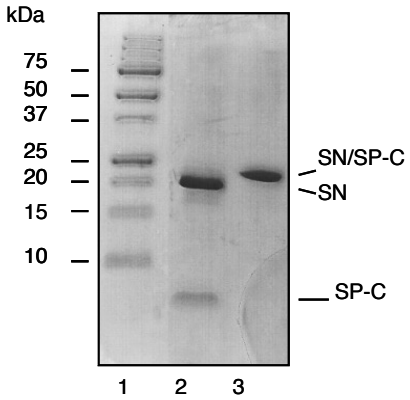

Figure 20. Thrombin digestion of the fusion protein. Coomassie blue-stained 15% acrylamide tricine gel loaded with an aliquot of the SN/SP-C chimera after (lane 2) and before thrombin digestion (lane 3). Molecular weight marker is loaded in lane 1.

4.1.2 EXTRACTION AND PURIFICATION

Organic extraction

The highly hydrophobic nature of SP-C was used to separate recombinant proteins from the rest of the thrombin reaction mixture. The thrombin digestion mixture was added to the equal volume of chloroform/methanol, mixed and the two phases were separated by short centrifugation (see Materials and Methods). Recombinant SP-Cs are expected to partition into the organic phase, whereas the hydrophilic nuclease moiety and the thrombin itself would remain in the water-soluble phase. In this way, passing from a detergent-rich environment to an organic solution, the recombinant protein is likely to maintain its helicity, a crucial feature for its activity. In order to study the electrophoretic mobility of the recombinant polypeptides and roughly estimate the amount of protein, an SDS-PAGE analysis was performed (Figure 21).

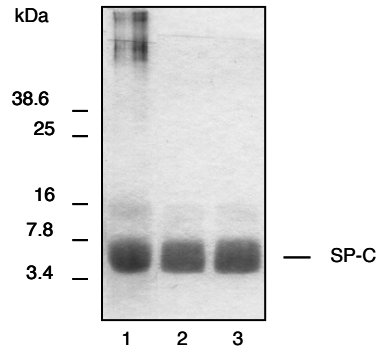

Figure 21. Organic extraction of recombinant proteins. SDS-PAGE loaded with 15 μg of organically extracted native SP-C (lane 1) and recombinant SP-Cs (rGP/SP-Cff, lane 2 and rSP-Cff, lane 3) stained with Coomassie blue.

Figure 21 shows aliquots of the organic phase bearing rSP-Cff (lane 2) and rGP/SP-Cff (lane 3) applied to the SDS-PAGE and compared with a known amount of the native protein, isolated from porcine lungs (lane 1). In agreement with previous SDS-PAGE analysis of native SP-C (Palmblad et al., 1999; Perez-Gil et al., 1993), SP-C runs as a smeared band while recombinant peptides display identical electrophoretic mobility, corresponding to an apparent molecular weight of ~6 kDa.

Size exclusion chromatography

The final purification step involves separation of recombinant protein from components that could have been co-isolated in the organic phase, by using a lipophilic Sephadex LH-20 resin (GE Healthcare). This size exclusion chromatography resin is resistant to organic solvents and has been widely used for lipid-lipid and protein–lipid separations (Perez Gil et al., 1993; Curstedt et al., 1987). Organic extracts of the natural lung surfactants are subjected to this chromatographic procedure in order to separate the lipid fraction from surfactant proteins (SP-B and SP-C). Large-scale extractions of thrombin reaction yielded large volumes of extract, therefore a concentration step was necessary to minimise the sample volume loaded onto the chromatography column. In order to prevent protein self-aggregation and precipitation, the recombinant SP-C-bearing organic-extracted solution was concentrated in the presence of egg yolk phosphatidylcholine (PC) added at 1:5 protein:lipid ratio (w:w), in a rota-vaporizer. The concentrated extract was loaded onto a chloroform:methanol (2:1, v:v)-equilibrated LH-20 column and eluted using the same solvent system. The eluted fractions were measured for their absorbance at 240 and 280 nm (figure 22a). The protein peak was identified by SDS-PAGE. The presence of the band at expected migration position identified the proximal peak as the one corresponding to proteins (figure 22b).

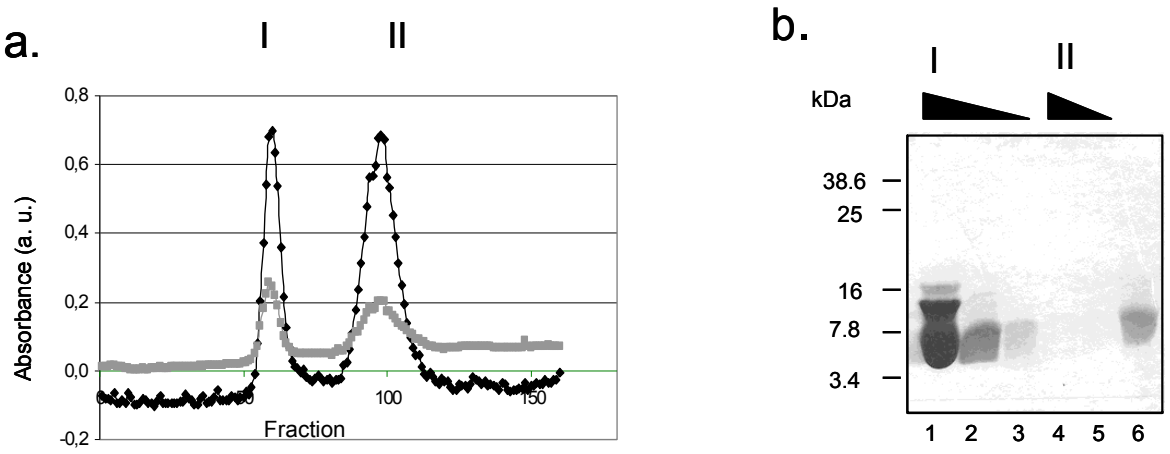

Figure 22. Purification of rSP-Cffs by Sephadex LH20. (a) LH 20 chromatographic analysis of organic extracts. Absorbance at 240 (black line) and 280 (grey line) nm was monitored. (b) Comassie blue stained SDS-PAGE analysis of increasing aliquots of the proximal peak (lanes 1-3) and two aliquots of the distal peak (lanes 4 and 5). Lane 6 was loaded with 15 μg of native SP-C. Size markers are indicated on the left.

Mass spectrometry

In order to test recombinant proteins' identity and integrity, the organic solutions bearing recombinant molecules were analysed by mass spectrometry. The mass spectra of the purified peptides were in agreement with the expected molecular masses of 3783 and 3938 Daltons, for rSP-Cff and rGP/SP-Cff, respectively (figure 23).

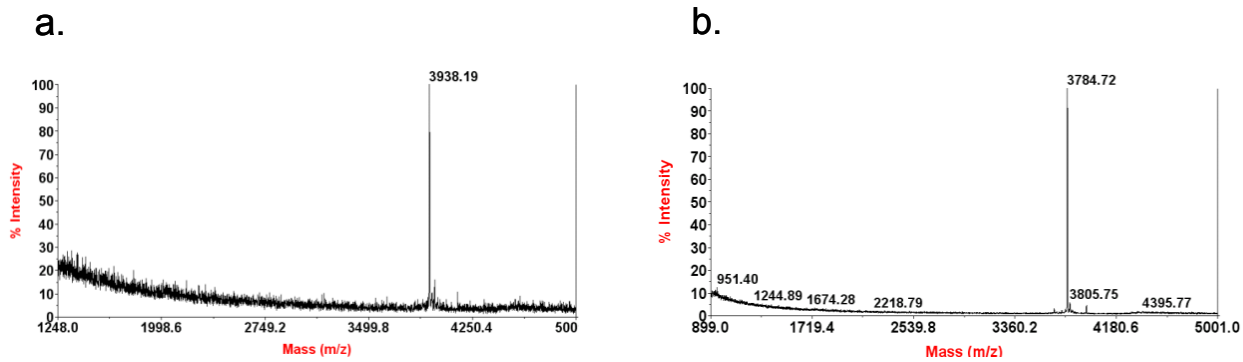

Figure 23. Mass spectra of recombinant SP-Cs purified on Sephadex LH20. The content of the first peak in the chromatograms of figure 22 were analysed by MALDI-TOF-MS as described in Materials and Methods. rGP/SP-Cff and rSP-Cff spectra are shown in panels a and b, respectively.

The identity of these recombinant surfactant peptides was further confirmed by amino acid sequencing (data not shown) and their precise concentration was established by quantitative amino acid analysis (see Materials and Methods). The final yield obtained for purified recombinant SP-C was up to 0.5 mg per litre of bacterial culture.

4.1.3 SECONDARY STRUCTURE DETERMINATION

In order to test whether the recombinant proteins retained their helical conformation after the purification process, necessary in order to avoid fibrilar aggregates, their secondary structure was evaluated by circular dichroism (CD) spectroscopy (figure 24).

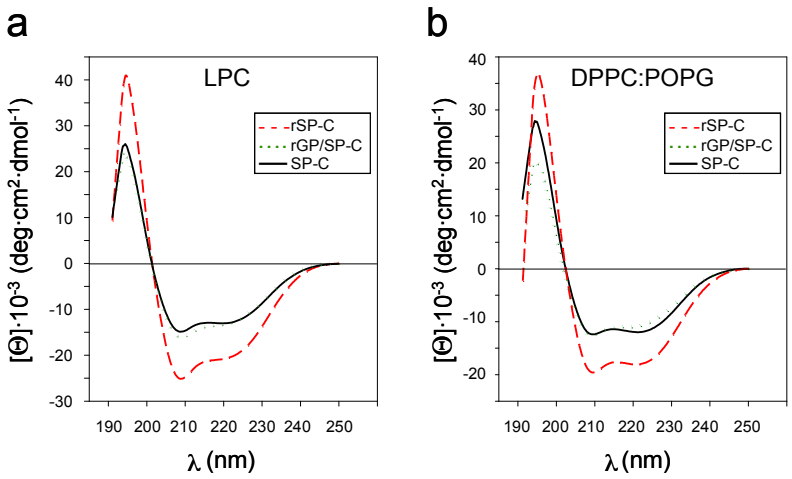

Figure 24. Circular dichroism spectra of native and recombinant SP-Cs reconstituted in surfactant-mimetic media. Native SP-C (solid line), rGP/SP-Cff (dotted line) and rSP-Cff (dashed line) spectra were recorded in the presence of LPC micelles (panel a) and DPPC:POPG (7:3) vesicles (panel b). In all samples 25 μM of proteins were analysed (see Materials and Methods).

CD spectra in the far UV region, between 250 and 190nm, are commonly used to estimate the contributions of different secondary structures to the conformation of proteins. We studied the structure of recombinant and native SP-Cs in LPC micelles (figure 24a) and lipid (DPPC:POPG, 7:3 w/w) vesicles (figure 24b), to mimic the natural environment of SP-C. As seen in figure 24, all proteins exhibited CD spectral features consistent with a predominantly α-helical conformation, as judged by the presence of two peaks at 208 and 222 nm. The spectra of rGP/SP-Cff and the native SP-C were quantitatively comparable and similar to those reported in the literature (Perez Gil et al., 1993; Cruz et al., 1995), while rSP-Cff exhibited a somewhat higher content of α-helix. To obtain a more detailed structural description, the CD spectra were analyzed by using the CDPro suite of programs (SELCON3, CONTIN/LL and CDSSTR) (Sreerama et al., 2000; Sreerama et al., 2004). Similar results were obtained with the three programs using a reference set of proteins that includes several membrane proteins, which supports the reliability of the structure estimation for recombinant SP-C variants. Table 1 summarizes the relative proportions of different types of secondary structure obtained, although the values should be taken with caution because small proteins flexibility may reduce the dichroic properties of the C=O bond.

Table 1: Secondary structure (%) of the native and recombinant SP-C proteins after analysis of the CD spectra using the CDPro package (Sreerama et al., 2004; Sreerama et al., 2000).

	LPC				DPPC:POPG			
	H [a]	S [b]	t [c]	r [d]	H [a]	S [b]	t [c]	r [d]
SP-C	**50**	**7**	**21**	**22**	**49**	**10**	**19**	**22**
rGP/SP-Cff	**52**	**7**	**22**	**19**	**47**	**8**	**22**	**23**
rSP-Cff	**75**	**7**	**9**	**9**	**72**	**8**	**8**	**12**

[a] H: accumulated value for regular and distorted α-helix

[b] S: accumulated value for regular and distorted β-strand

[c] t: turn

[d] r: random

The increased α-helical content of rSP-Cff relative to the native SP-C is consistent with an N-terminal extension of the helical region of the protein, as observed in recent NMR structures of a recombinant SP-C mutant and a synthetic SP-C analogue, both bearing phenylalanine instead of cysteine residues at position 5 and 6 (Luy et al., 2004, Li et al., 2006). Thus, NOE-data supported an extension of the α-helical region from residues 11 and 34 in the native protein (Johansson et al., 1995a), to residues 5 and 34 in the recombinant variant (Luy et al., 2004), or starting at residue 7 in the synthetic SP-C analogue (Li et al., 2006). In the same line, recombinant SP-C has been observed previously to have significantly higher helical content than canine SP-C by Shiffer and colleagues under several conditions (Shiffer et al., 1993).

4.1.4 DISCUSSION

Membrane proteins are generally difficult to over-express and purify (Kiefer, 2003) mainly due to their extreme hydrophobicity. They are usually produced in heterologous systems, as fusions with soluble portions of bacterial proteins. The presence of detergents during the purification is often required in order to prevent formation of aggregates, especially at the point where the TM portion is cleaved from its fusion. Following enzymatic cleavage the TM proteins are generally purified by reverse phase chromatography (RP-HPLC) (Therien et al., 2002). Membrane proteins that do not have fibril forming propensities can, once unfolded and precipitated, be recovered in the presence of detergents or lipids. However, this three-step method is not readily applicable to SP-C, since purifying the protein by RP-HPLC bears the risk of its denaturation leading to irreversible aggregation and complete inactivation.

The production of a recombinant SP-C has been a challenging task since the revealing of its importance in the late 80s. The extreme hydrophobicity and its tendency to aggregate make this protein very difficult to manipulate and many different approaches have been taken in order to circumvent these

features. Synthetic peptides (Johansson et al., 1995b; Palmblad et al., 1999; Nilsson et al., 1998) and peptoids (Wu et al., 2003) mimicking the essential structural features of SP-C have been tested to enhance the surface-active properties of surfactant formulations composed of synthetic phospholipids. Protein expression in recombinant form was also published, in eukaryotic baculovirus expression system (Veldhuizen et al., 1999) and using bacterial cultures (Hawgood et al., 1996; Stults et al., 1991). We decided to employ a prokaryotic system in order to obtain SP-C in large quantities, since bacteria are to date the best large-scale protein-producing organism. We have employed SN as a fusion protein which proved to be efficient for expression of other TM fragment (Glycophorin A) previously in our laboratory as opposed to N-terminal portion of chloramphenicol acetyl transferase (CAT) employed previously (Hawgood et al., 1996). SN fusion is soluble when treated with small amounts of detergent (lauroylsarcosine), while CAT fusion accumulates in inclusion bodies which require additional resolubilization steps. The CAT fusion is cleaved chemically during 48 hours comparing to 16 hours of cleavage by thrombin. Finally, the authors employed exposure to polar solvents during RP-HPLC while our procedure maintains the cleaved SP-C in an apolar environment. Details about the yield, efficiency and biophysical activity of this protein *in vitro* have not been reported (Hawgood et al., 1996). In general, our strategy is highly reproducible, time sparing and more protective of the α-helical conformation necessary for optimal surface activity.

Here we describe a novel approach for expression and purification of human SP-C, based on the combination of a successful TM protein expression strategy in bacteria with the established organic extraction protocol typically used for separation of native SP-C from lung surfactant lipids. This new procedure is very effective for preserving the native helical structure of SP-C throughout the purification process and for protein production in reasonable amounts. We have modified the SP-C sequence by double Cys5Phe and Cys6Phe substitutions. The rationale behind these changes is that the naturally occurring palmitoylation of the two Cys residues cannot be achieved through bacterial protein expression. The modified protein remains very close to the native sequence present in some animal surfactants (figure 8). Moreover, the same Cys→Phe replacements are present in the recombinant SP-C produced by Davis and colleagues that was shown to be efficient component of single-protein-containing synthetic surfactant preparation (Davis et al., 1998). The role of palmitoyl chains in SP-C is still under debate. It is evident that SP-C maintains its function in the presence of one phenylalanine in place of palmitoylated cysteine, as in the case of dog and mink SP-Cs, and the possibility remains that this particular amino acid (phenylalanine) can mimic, at least partially, the role of acylated cysteines. The fact that SP-C variant harbouring this Cys→Phe replacements has been successfully used both *in vitro* and in animal experiments supports the idea that it could be a functional equivalent to the natural SP-C (Davis et al., 1998).

The protocol presented in this work is a combination of a common strategy for over-expression of integral membrane proteins and the organic extraction used for native SP-C isolation from animal pulmonary lavages. This purification scheme may also be used for obtaining other highly hydrophobic proteins. The flexibility for creating mutants of the SP-C, aimed for specific structural or functional studies, will greatly improve our understanding of the role of this protein in the lung surfactant, as well as optimizing current replacement preparations for respiratory diseases. Further biophysical studies are presented in the following chapters in order to explore the full potential of these and new SP-C variants for surfactant therapy.

4.2 INTERFACIAL BEHAVIOUR OF RECOMBINANT FORMS OF SURFACTANT PROTEIN C

4.2.1 INTERFACIAL SPREADING π-t ISOTHERMS

Early studies of SP-C activity demonstrated that, when present in phospholipid vesicles, SP-C leads to an enhanced adsorption of PL to the air-water interface (Oosterlaken-Dijksterhuis et al., 1992). In the present study we have compared the ability of recombinant variants to the native protein to induce the formation of interfacial phospholipid films from suspensions of multilamellar vesicles (MLV) containing phospholipids and an increasing amount of protein. Three different lipid mixtures were assayed. First, a mixture of DPPC:POPG (7:3 w/w) was tested. This combination of phospholipids is commonly used to study the effect of surfactant proteins on phospholipid organization since it represents surfactant composition in its simplest form. Although not equivalent to the *in vivo* situation simple mixtures help to elucidate particular effects exerted by a protein on specific lipids. DPPC is taken as the most abundant surface active lipid species and POPG as representative of unsaturated species required for fluidizing the material. PG, the main anionic phospholipid in surfactant, is likely to establish an electrostatic interaction with cationic SP-C. The MLV suspension was deposited on the surface of the Wilhemy balance and the changes in surface pressure were monitored as a function of time. The increase in surface pressure (i.e.surface tension reduction) can be observed only if the interfacial film is formed. The maximum surface pressure that could be reached by any lipid/protein combination is the equilibrium surface pressure that corresponds to the particular mixture. As shown in figure 25 DPPC:POPG bilayers adsorb very poorly by themselves over long periods of time upon deposition of the MLV in the absence of proteins. However, both native and recombinant variants of SP-C facilitate monolayer formation even at 100:2 lipid-protein (w/w) ratio. The protein levels in this last case were too low to reach equilibrium surface pressure during the time assayed. The monolayer formed almost instantaneously by depositing MLV with the lipid to protein ratio in the vesicles of 100:5 (w/w). Further increase in protein proportion in the membranes did not affect the maximal pressure but reduced the time required to reach the equilibrium pressure. Proportions of around 1% of SP-C in native surfactant are sufficient to induce PL adsorption and respreading during the respiratory cycle. The lower surface pressures produced by this low protein content in the present assays are probably due to various reasons: the more simple lipid context, the temperature (25^0C), which is lower than the physiological one, slowing lipid film formation and/or the absence of the other hydrophobic protein that has equivalent or superior ability to induce film formation (SP-B). The same assay was performed with vesicles prepared with the mixture of DPPC:POPC:POPG:Cholesterol (50:25:15:10, w:w:w:w). This lipid mixture resembles better the native surfactant composition regarding the ratio of disaturated to unsaturated lipids, the proportion of charged species, and the presence of cholesterol. As can be observed from the middle panels this mixture has a potentiating effect comparing to the two-component system. Lipids alone again do not form interfacial film but the film is formed more rapidly in presence of low amount of protein (2%). This indicates that the lipid mix which is closer in composition to native surfactant is optimized for rapid film formation in the presence of proteins. Finally, as a reference the proteins have been tested as incorporated into the total lipid fraction obtained from native porcine lung surfactant was assayed (figure 25, bottom panels). The complete set of surfactant lipids has by itself the ability to

induce monolayer formation, although at a slower rate than in the presence of proteins. The lipid fraction was tested for the presence of native protein by quantitave amino acid analysis in order to discard the possibility of native protein contamination that could contribute to the minor monolayer formation activity detected. Native protein traces were not detected meaning that a particular combination of surfactant lipids is responsible for surface pressure increase. The presence of 2%(w/w) protein in this mixture is sufficient to reach rapidly surface pressures close to equilibrium. In all these assays the activity of both recombinant variants of SP-C was similar to the native protein. This means that the recombinant forms produced in bacteria have similar activity to promote interfacial phospholipid adsorption as the protein isolated from natural sources.

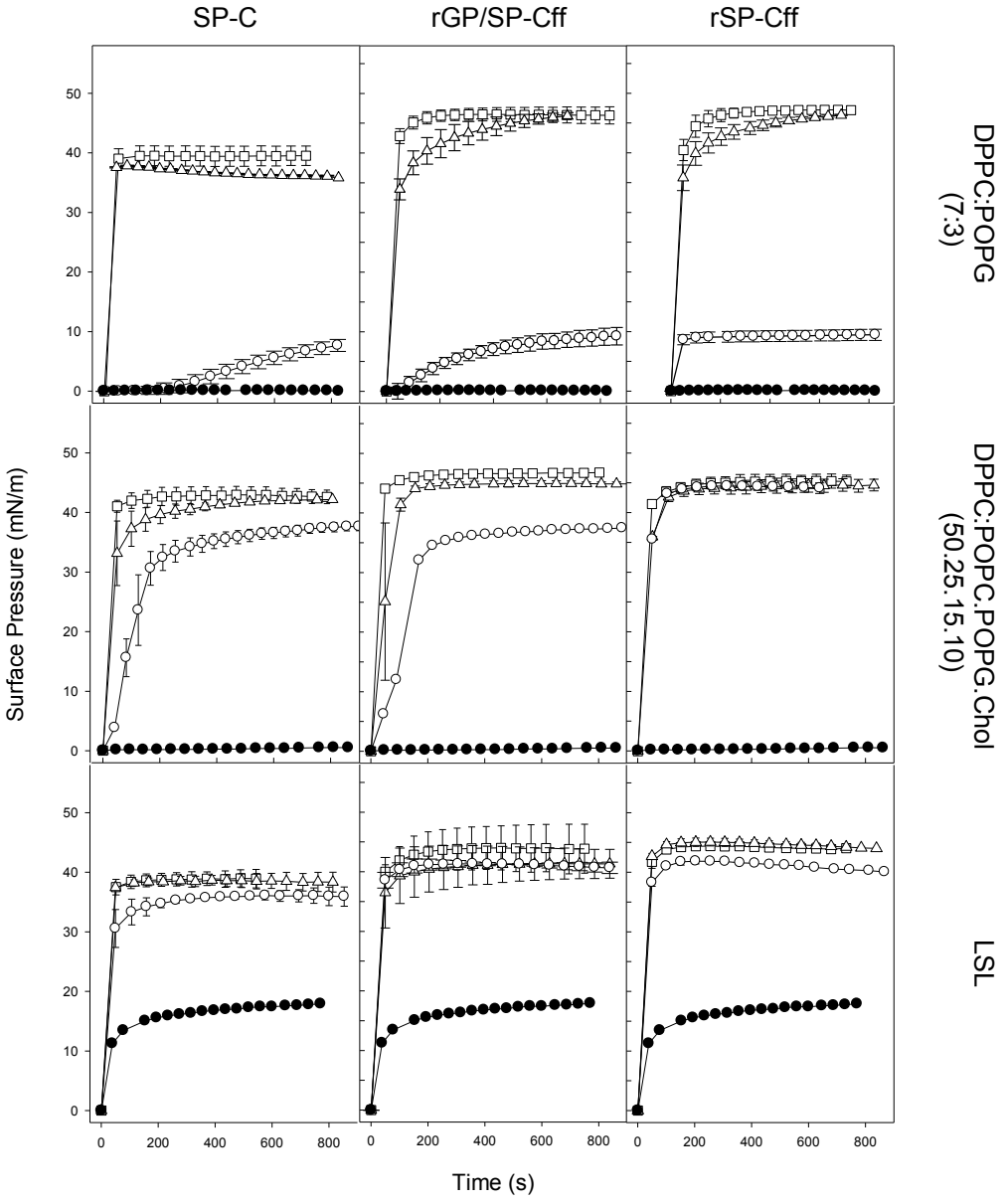

Figure 25. Interfacial adsorption activity. The panels show π-t adsorption isotherms for interfacial film formation after deposition of 10µl of 10mg /ml of lipid suspension in the absence (dark circles) or presence of 2 (open circles), 5 (triangles) or 10 (squares) % protein (w/w). The left panels depict adsorption kinetics of lipid suspensions with native SP-C, middle panels, rGP/SP-Cff, and right panels, the activity of rSP-Cff. LSL: lung surfactant lipids.

However, recombinant variants assayed exhibited slightly, but consistently better activity, reaching the equilibrium pressures of 48mN/m in few seconds with the highest amount of protein assayed. Native protein produced slightly lower maximal pressures, what should be interpreted as a consequence of differences in composition of the formed film. The palmitoylated region of native SP-C could insert into the monolayer conferring different equilibrium pressure. Other possibility is that there are structural differences between the native and recombinant proteins generated during the purification process that cause partial inactivation of the native protein. The purification methods of native and recombinant variants are similar in their final steps; however there is a difference in the last purification step. The native protein is obtained from lung lavage organic extract, which is loaded onto Sephadex LH 20 in order to separate hydrophobic proteins from surfactant lipids. This step is similar to the last purification step of the recombinant protein when it is mixed with egg derived PC and loaded onto Sephadex resin. In the case of recombinant proteins this is the final purification step. In contrast, the native protein is subjected to an additional purification step on higher resolution LH-60 resin in order to separate SP-C from the other hydrophobic peptide (SP-B). LH-60 resin is equilibrated with chloroform/ methanol (1:1) bearing 0.5% HCl 0.1N and this acidic methanol solution may induce structural changes such as methylation of C-terminal groups (Taneva et al., 1998). Methyl-ester formation changes the overall peptide charge leading to possible functional alterations. An isoform of native protein has been previously found which contains additional palmitoyl group linked to Lys-11 constituting about 4% of all native forms (Gustafsson et al., 1997). This modification leads to charge neutralization with possible functional consequences (Crewels et al., 1995). In addition to these covalent variations suffered by the native protein, distinct purification process can induce partial loss of helicity, undetectable by circular dicroism, or partial helical aggregation which could provoque different surface behaviour of native versus recombinant forms. Finally, the possibility that batches of native protein purified from animal lungs could contain certain amounts of unidentified inhibitors can not be discarded.

4.2.2 Compression isotherms

In vitro studies of the interfacial behaviour of SP-C provide insight into its potential role at the alveolar interface during respiration. Besides promoting PL adsorption, it has been proposed that SP-C plays a role in modulating structural reorganizations of the surfactant layers upon compression to high surface pressures. This structural reorganization involves material exclusion and formation of 3-D associated structures that serve as a reservoir for lipids that are reinserted during alveolar expansion. The molecular mechanism by which SP-C exerts this role is not completely understood but most of its effects stem from its ability to closely interact with and mobilize lipids. The evidences for this interaction are various, for example Taneva and co-workers found that SP-C facilitates the exclusion of lipids from the interface upon compression (Taneva et al., 1994b) and it has also been reported that SP-C induces reorganization of compressed films into surface associated 3-D structures as observed by microscopic techniques (Kruger et al., 1999). To get a deeper insight into the surface activity of recombinant forms of SP-C, we analysed pressure-area (π-A) compression isotherms of interfacial films composed of proteins in the absence or in the presence of different lipid mixtures. By comparing the interfacial behaviour of the created recombinant variants to that of the native protein we expected to learn more

about their potential as equivalent substitutes to the native protein.

4.2.3 Protein monolayers

Earlier studies showed that native SP-C is able to form by itself insoluble monolayers at the air–water interface (Taneva et al., 1994c). To determine the area available per molecule at any defined surface pressure, an exact quantity of protein was deposited on the surface of the hypophase (5mM Tris, 150mM NaCl, pH=7) and compressed with constant speed until collapse pressure was reached. These pressure-area curves are characteristic for each protein. The representative isotherms for the native, rGP/SP-Cff and rSP-Cff variants are presented in figure 26. The curves shown are representative of three different isolates of native and three batches of each recombinant variant.

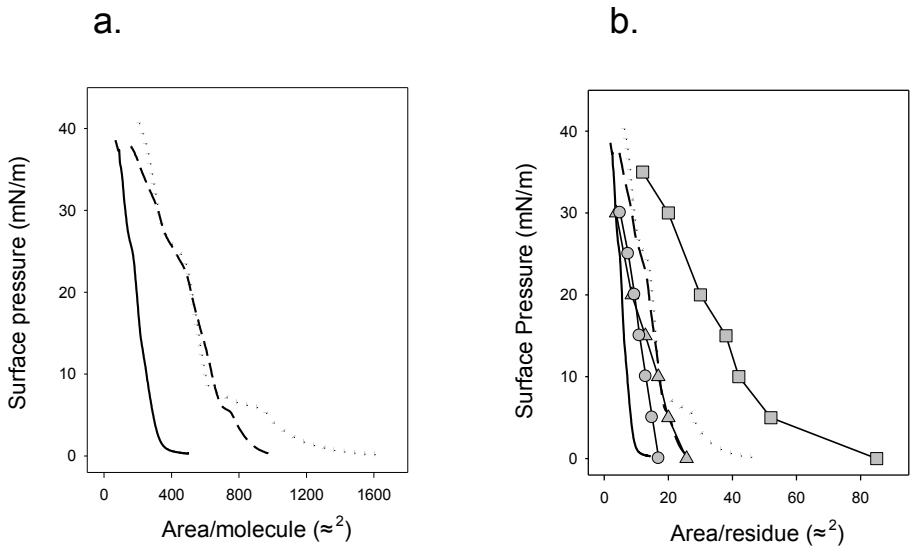

Figure 26. Compression isotherms of pure SP-C films. a. Pressure-area/molecule isotherms of SP-C (full line), rGP/SP-Cff (dashed line) and rSP-Cff (doted line). b. Pressure-area/residue isotherms of the same proteins and schematized isotherms of native SP-C from other authors: Taneva et al., 1994b (circles), Perez Gil et al., 1992 (triangles) and Oosterlaken-Dijksterhuis et al., 1991 (squares).

Table 2.Characteristics of pressure-area curves of native and recombinant SP-Cs

	Extrapolated area in the isotherm ($Å^2$)*	Area at lift-off at π= 0mN/m ($Å^2$)
SP-C	200	350
rGP/SP-Cff	780	980
rSP-Cff	680	1600

* Determined by extrapolation of linear parts of the surface pressure-area curves to π=0

It is worth mentioning that π-A isotherms of SP-C isolated form natural sources differ

significantly throughout literature (figure 26b, Oosterlaken-Dijksterhuis et al., 1991; Perez-Gil et al., 1992, Taneva et al., 1994c). Other published isotherms are more expanded comparing to the ones obtained in the present work. The isotherms are influenced by temperature, compression rate, subphase composition and balance features that could all contribute to the observed differences. We have repeated π-A measurements with three separate preparations of native SP-C and repeatedly obtained curves such as the one shown on figure 26.

The secondary structure of SP-C present in the pure protein monolayers at different surface pressures, as determined by circular dicroism showed that SP-C had a high content of α helical structure (Oosterlaken-Dijksterhuis et al., 1991; Creuwels et al., 1993), which is consistent with its solved structure in organic solvents and lipid vesicles. Films consisting of purely α helical proteins are calculated to have around 12.8 $Å^2$ area per amino acid of limiting surface, which is above the obtained areas for the native SP-C protein in the monolayer (10.8 $Å^2$, figure 26b). This could indicate that native SP-C, although maintaining the α helical structure (see figure 24 in chapter 4) could be partly aggregated. Still the fraction of amino acids that resides in the plane of the interface agrees with their distribution as α helical residues. The amino acid areas obtained for SP-B are higher than the ones predicted in the helical monolayer confirming the presence of non helical domains and potentially less perpendicular orientation (Taneva et al., 1994b).

However, recombinant protein isotherms were shifted to significantly higher areas. The native protein exhibited the lowest area per molecule. The lift–off area for the native protein was 350 $Å^2$ per molecule, while the ones for the recombinant variants were around 980 $Å^2$ and 1600 $Å^2$ for rGP/SP-Cff and rSP-Cff molecules, respectively (Table 2). The basic difference between the native and recombinant variants is the absence of palmitoyl chains coupled to cysteines. Differences in the maximal expansion of protein isotherms therefore suggest that palmitoyl groups might induce a more perpendicular position of the helix than achieved in their absence, being possibly themselves positioned parallel to the helix. The contribution of the N-terminal segment to the area per molecule of the native protein could then be relatively small. The non-palmitoylated N-terminal segment of the recombinant peptides seem to confer larger area per protein molecule at maximal extension, indicating that this motif could have a significant contribution in modulating the conformation/disposition of the proteins at the air-water interface.

A possibility that had to be discarded is that the shift of the isotherm to larger areas could be due to the presence of different contaminants such as lipids. The presence of lipids as a consequence of an incomplete delipidation on Sephadex LH-20 resin was always tested after protein purification (see Materials and Methods). Low levels of phosphorus were usually found in recombinant protein samples corresponding to between 0.3 and 0.5 mol of phospholipids per mol of recombinant protein. The values for native protein were 0.05-0.1mol of lipid/ mol of protein, while the values reported in the literature go up to 1.5mol lipid/mol protein (Oosterlaken-Dijksterhuis et al., 1991; Wiliams et al., 1991). The variation in phosphorus of our samples did not apparently influence the π-A isotherms. TLC assay however, did not confirm the presence of lipids (PC, PS, PE, PI, PG) in the protein sample. Another potential contaminant could be bacterial LPS, which has been reported to bind specifically to SP-C (Augusto et al., 2002; Augusto et al., 2003). We therefore tested the possibility that the recombinant protein is contaminated by this molecule liberated during the disruption of bacterial cell wall, which is the natural source of LPS. However no LPS was detected in the recombinant batches analysed. The other

possibility is that part of the traces of detergent used during the purification procedure remain associated with recombinant peptides. To check for this possibility we monitored the compression curve of native or recombinant protein in the presence of 1/10 molar ratio of lauroylsarcosine, and no curve expansion was observed. On the other hand, lauroylsarcosine did not form stable monolayers by itself (not shown). So far, we have not been able to detect the possible presence of trace amounts of this detergent by analytical means.

A distinct feature of the isotherms obtained from recombinant proteins compared with that of native SP-C is the presence of plateaus at low pressures regimes. rGP/SP-Cff variant batches exhibited a small plateau of variable length at around 6 mN/m while rSP-Cff has an additional one at 9mN/m. The presence of these plateaus, where compression induces very little pressure increase, is usually interpreted as compression-promoted structural transitions occurring in the plane of the interface. In the particular case of SP-C variants such transition could reflect a coordinated change in helical tilt from a parallel-like to a rather perpendicular disposition with respect to the interface. In the case of the native protein the palmitoyl chains anchored to the N-terminal of the protein could induce a perpendicular orientation of the protein already from the lowest pressure. Further compression could then allow only small helical reorientation toward the interface normal. The proximity of palmitoyl chains to the helix may also restrain the molecule's flexibility due to their mutual hydrophobic interactions, creating thus a more rigid molecule compared to the recombinant one. Recombinant proteins on the other hand, with the N terminus freely interacting with the interface, may occupy larger area possibly including a much more extended conformation. Furthermore, the presence of introduced aromatic residues (absent in the native SP-C) with potentially high affinity toward the membrane interface (Wimley and White, 1996; Serrano et al., 2006) may further stabilize an extended interfacial disposition. Aromatic rings could additionally facilitate protein-protein interactions and thus stabilize extended conformations absent in native SP-C. Monolayer compression during the observed plateau could induce a progressive helical lift-off, while maintaining the position of the N-terminal segment associated with the interface. Further compression would lead to the reorientation/expulsion of the N-terminal segment from the interface, finishing at the end of the plateaus.

We wanted also to discard the possibility that the plateau could reflect the presence of non proteinaceous contaminants which persist on the interface together with the protein only below certain compression level (in this case π~6mN/m). To explore this hypothesis we compressed films of recombinant SP-Cs to pressures above the plateau, then we relaxed the film by expansion and repeated the compression. We expected that expulsion of possible contaminants at pressures above the plateau would be irreversible. Figure 27 shows that the plateau was maintained during the second compression, suggesting that the plateaus are due to defined protein features, and probably not to non-protein interfacial molecules.

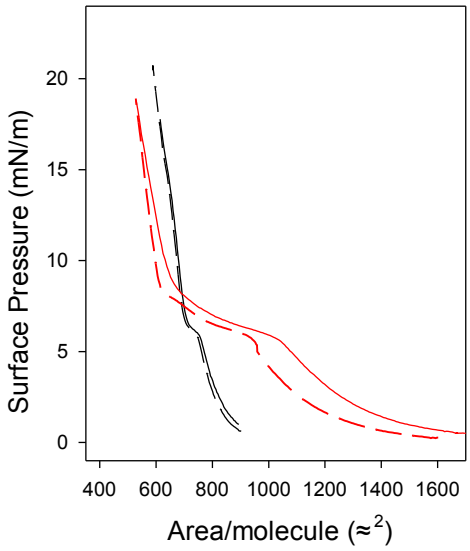

Figure 27. Reversibility of the plateau in protein film isotherms after compression. Full line reflects π-A isotherms upon compression of rGP/SP-Cff (black) and rSP-Cff (red) monolayers to pressures above the plateau. The monolayer was then relaxed and compressed again (dashed lines). The plateau persists in the second compression.

The collapse pressures of native and recombinant proteins are similar, around 36-38mN/m, consistent with earlier reports (Taneva et al., 1994c). The smallest area to which the monolayer can be compressed is larger for recombinant than native protein reflecting possibly the inability of non-acylated forms to achieve a fully perpendicular orientation or the incomplete expulsion of the N-terminal segment from the interface. Another common characteristic is the presence of a shoulder at 25mN/m, which is more pronounced in the recombinant SP-C forms (figure 26). Similar plateaus were observed with recombinant proteins earlier (Crewels et al., 1993).

Lipid/ protein monolayers

The effect of SP-C on the surface behaviour of PL monolayers was studied by monitoring compression isotherms of protein/lipid films (figure 28). DPPC monolayer exhibits a well-characterized typical isotherm which at 25^0C presents a lift-off area around 100 $Å^2$ per molecule, a LE-LC phase transition plateau at 12mN/m, and collapse at pressures higher than 70mN/m. Figure 28 shows that in the low pressure regimes, increasing protein amounts added to DPPC induce an increasing expansion of the isotherm to larger areas as a consequence of space taken by the protein molecules. Recombinant forms produce larger area expansion than the native palmitoylated protein as expected from pure protein isotherms. However, the resulting expansion can not be attributed to the protein incorporation solely, since the resulting protein/lipid isotherm is shifted to areas that are larger than the sum of pure lipid and protein areas suggesting that the presence of proteins induces perturbation of lipid configurations. The expansion of the isotherm from the lift-off pressures may be interpreted in terms of hydrophobic interactions between lipids and protein. At pressures of around 50mN/m the lipid/protein

isotherms converge with the pure lipid isotherm. This feature is indicative of protein squeeze-out induced at pressures above 50mN/m. Earlier studies performed with native protein concluded that this compression-driven protein exclusion is accompanied by expulsion of some lipids (Taneva et al., 1994c). The recombinant proteins produced larger shifts than the native protein at pressures above those producing protein squeeze-out, indicating that the expulsion of each recombinant SP-C molecule is accompanied by more lipid molecules than native SP-C. The collapse plateau of 71mN/m corresponds to the collapse pressure of a practically pure DPPC film and remains in the presence of the lowest amounts of protein assayed (2%).

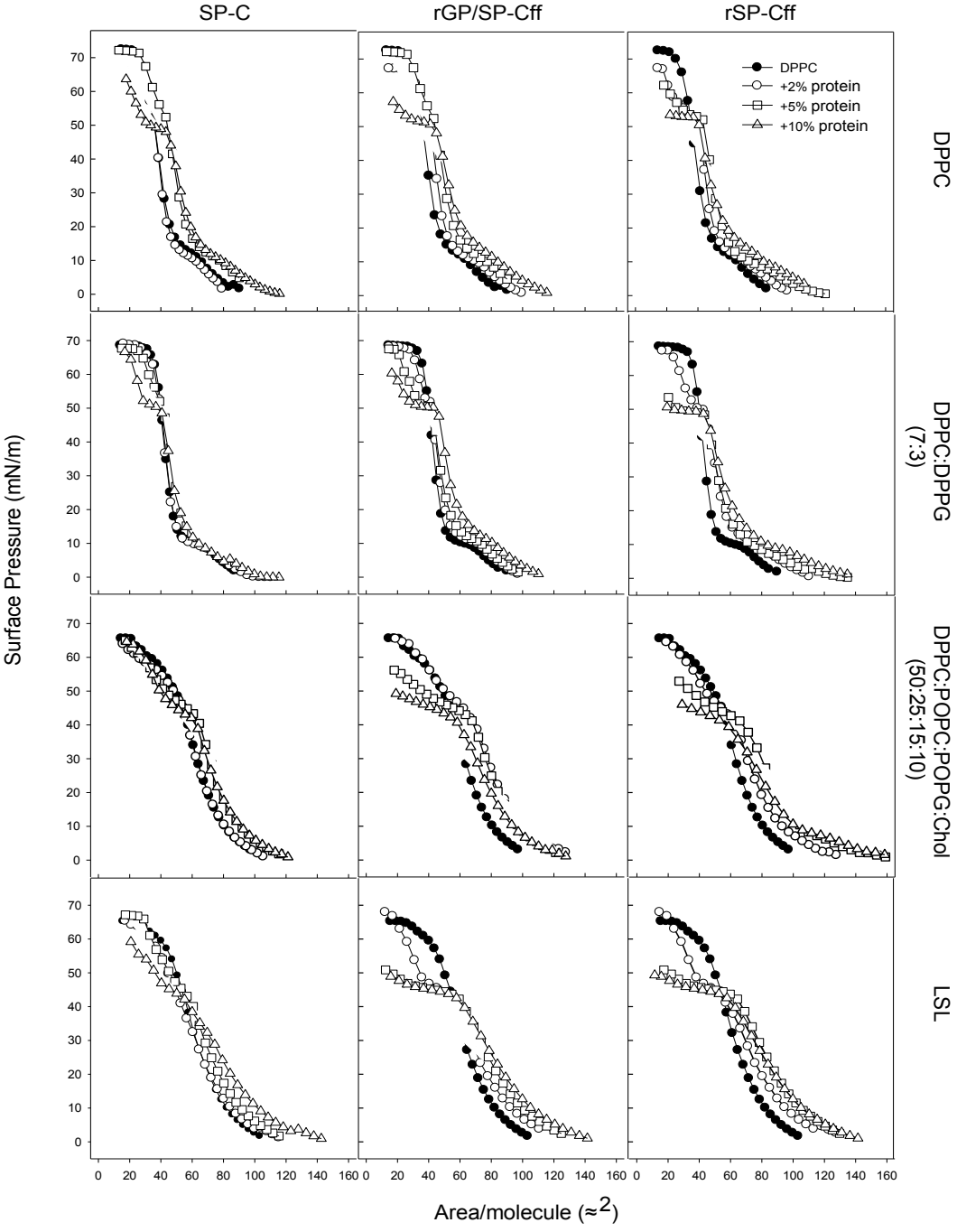

Figure 28. Compression π-A isotherms of lipid and lipid/protein films. Lipid films in the absence of protein (black circles) or in the presence of 2% (open circles) 5% (squares) and 10% (triangles) of native SP-C (left panels), rGP/ SP-ff (middle) or rSP-Cff (right) were spread onto the aqueous hypophase and compressed at 65cm^2/min at 25 ^{0}C. Lipid composition in each row is shown on the right. LSL, lung surfactant lipids.

A qualitatively similar behaviour was observed in ternary monolayers of DPPC:DPPG (7:3) containing native or recombinant SP-C, although in this case, the progressive incorporation of protein induced isotherm expansion of lower magnitude than observed in DPPC films, probably due to the condensation effects produced by the electrostatic interaction between positively charged protein and anionic lipids (figure 29). It was previously reported that SP-C, as a positively charged molecule, interacts more strongly with anionic than zwitterionic PL (Perez-Gil et al., 1995). The recombinant forms again exhibited a more pronounced expansion at lower pressures and larger squeeze out at high pressures. Compression isotherms of films of the lipid mixture used in spreading experiments (DPPC:POPC:POPG: Cholesterol) or the whole surfactant lipid fraction (two bottom panels in figure 28) showed similar qualitative behaviour in the presence of the proteins. These films did not show the LE-LC plateaus typical of simple monolayers, and showed indications of protein squeeze-out at lower pressures. In these complex mixtures recombinant proteins also showed larger expansion at low pressures than native SP-C and produced expulsion of more lipids upon compression above 40mN/m.

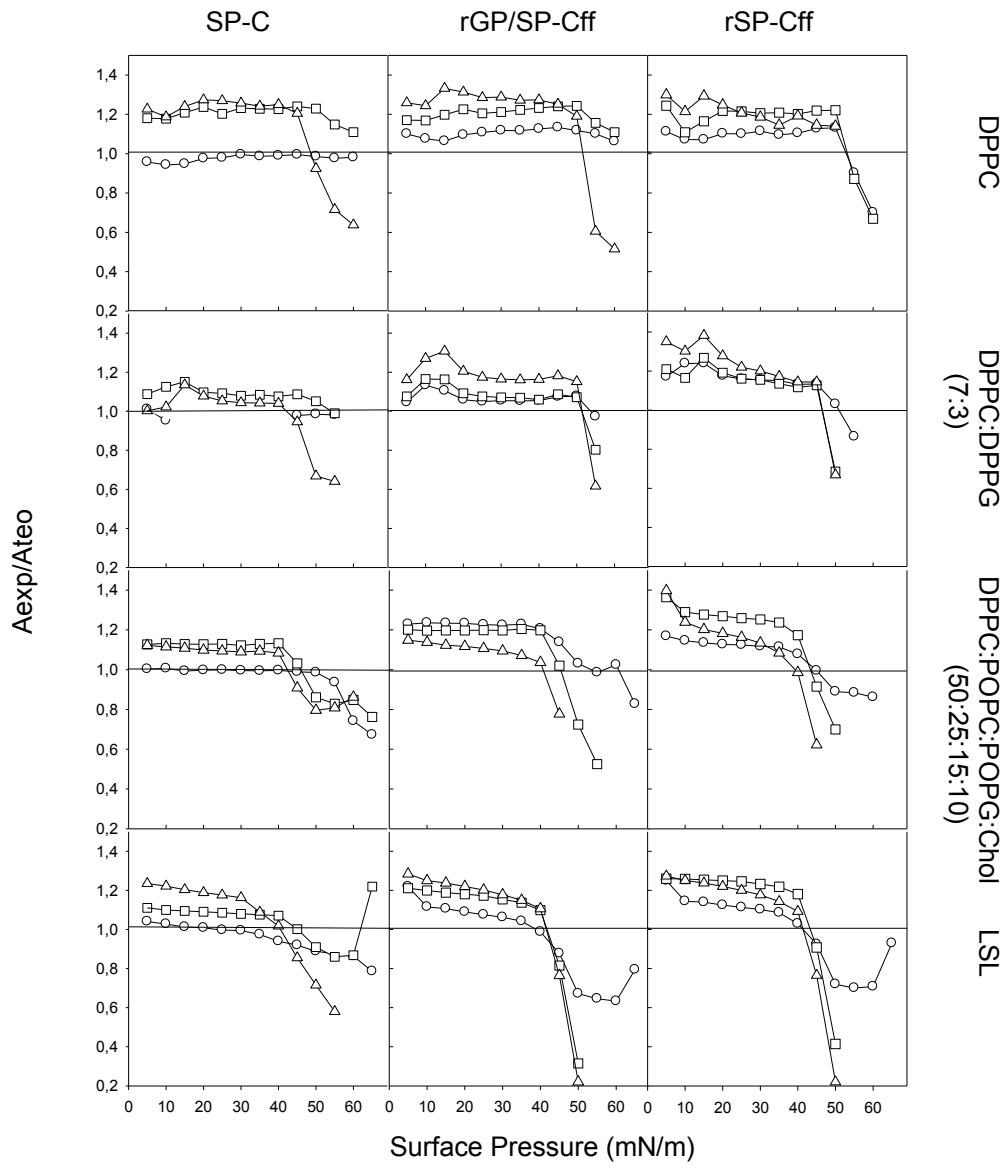

Figure 29. Expansion and expulsion effect of protein/lipid monolayers. Experimental (Aexp) to theoretical (Ateo: calculated as the fractional sum of area/molecule calculated from pure lipid or protein films) area ratio at different surface pressures during monolayer compression.

Figure 29 analyses the effect of pressure on the interaction of native and recombinant forms of SP-C with the different PL assayed. The different plots represent the ratio between the experimental area per molecule measured in the π-A isotherm (Aexp) and the theoretical area (Ateo) calculated as the algebraic addition of the fractional areas occupied by the lipid and protein moieties obtained from their pure isotherms. Ratios around 1.0 indicate no interaction while values different than 1.0 are indicative of perturbations due to lipid-protein interactions. Figure 29 illustrates how increasing amounts of the three SP-C forms produce a progressively higher value of the ratio Aexp/Ateo at pressures below 40mN/m. The ratio higher than 1.0 can be interpreted as a consequence of lipid packing perturbation resulting from protein/lipid interaction. Lipid and protein molecules occupy therefore larger surface at the interface than the sum of their areas in pure films. The largest effect is observed in DPPC films, made exclusively of zwitterionic molecules. Lower protein-induced expansion observed in negatively

charged films is probably a consequence of two opposite effects: perturbation of packing by lipid/protein interaction and condensation due to electrostatic lipid/protein interaction. At pressures higher than 40mN/m, all lipid/protein films exhibit Aexp/Ateo <1. This is interpreted as a consequence of enhanced compression-driven squeeze-out of lipid and protein molecules due to lipid/protein interaction. Such film exclusion is clearly favoured by recombinant SP-C forms compared with native protein.

Figure 30 represents quantitative analysis of protein effect on the pressure-induced exclusion of lipid from monolayers assessed as the amount of area removed from the interface at 55mN/m compared to the pure lipid isotherms. Assuming that all the protein molecules were squeezed-out at 55mN/m, the slope of the plots in figure 30 reflects molar lipid/protein ratio excluded. In the case of DPPC:DPPG films native SP-C is calculated to be squeezed-out accompanied by 17±2 lipid molecules, while rGP/SP-Cff apparently expel 25±2 and rSP-Cff 53±3 PL per protein molecule. Although the numbers obtained from our isotherms may not be entirely correct without considering the protein segments that could still maintain insertion into the films at high pressures, the differences observed clearly indicate that the recombinant proteins bearing phenylalanines remove more lipid molecules per mol of protein than the native acylated protein. This feature can be correlated with a potentially higher affinity of the N-terminal segment of the recombinant proteins to maintain association with phospholipid films, compared with the natural SP-C, which could be also responsible for the observed higher ability to promote interfacial adsorption of phospholipids.

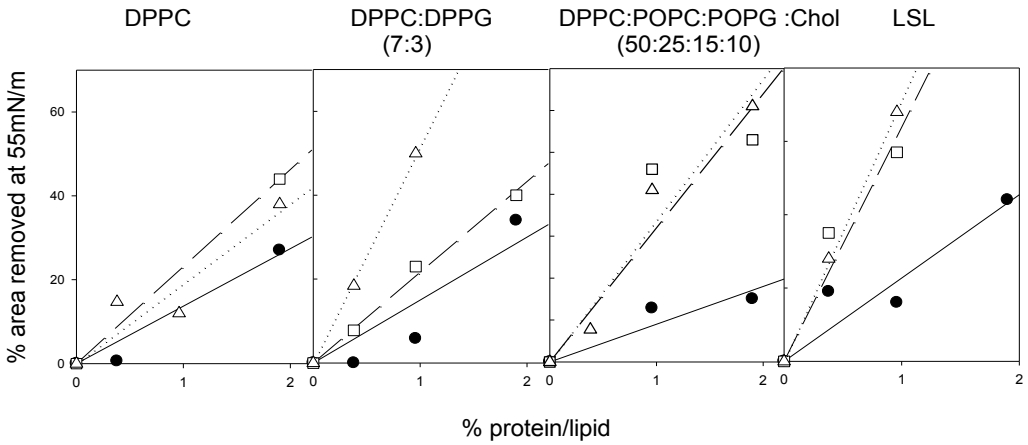

Figure 30. Effect of native and recombinant SP-Cs on the removal of lipid/protein material from highly compressed interfacial film. Percent of lipid film area at 55mN/m reduced by the presence of native porcine SP-C (full line, closed circles), rGP/SP-Cff (dashed line, squares) and rSP-Cff (dotted line, triangles) has been plotted against the proportion of protein in the film (%mol/mol).

4.2.4 STABILITY OF MONOLAYER COMPRESSED STATES

To evaluate the effect of SP-C proteins on phospholipid monolayer stability, we monitored the spontaneous relaxation of protein/lipid films compressed to high pressures (figure 31). Both DPPC and DPPC:DPPG films can be compressed to collapse pressures near or above 70mN/m at temperatures below gel to liquid phase transition of their bilayers, which is 41^0C for both lipids. This compressed state is metastable and the film relaxes slowly to the equilibrium pressure (48mN/m). Although DPPC should in principle form films able to sustain high pressures with slow relaxation rates, the formation of the metastable films depends on compression rate and the particular experimental conditions. The relatively fast relaxation observed for DPPC in our experiments is probably due to the fast compression and the geometry of compression imposed by the balance characteristics. The compressed film relaxed within 1-2 minutes to below 56-58 mN/m which was followed by a slower decay to the equilibrium values. Similar relaxation kinetics was observed for DPPC:DPPG (7:3,w:w) monolayers.

Lipid and protein/lipid films were compressed to 60 mN/m, a pressure above the exclusion pressure but still below the collapse pressure of the whole film in order to avoid uncontrolled differences in overcompression states. Overcompression generates associated three-dimensional structures with significant contributions to film stability.

Although SP-C is squeezed out from phospholipid films at pressures above equilibrium (48mN/m) it remains at least partially associated with compressed phases and exerts significant effects on the relaxation kinetics. The presence of small amounts of either native or recombinant proteins speed up the relaxation kinetics of the compressed films. In both tested lipid combinations the recombinant SP-Cs induced a faster drop to pressure values close to their equilibrium. Native SP-C induced a slower relaxation than recombinant proteins and, similarly to the spreading assay, approached equilibrium values that were below the equilibrium for films containing recombinant SP-C forms. This behaviour is opposite to that of SP-B, which stabilizes phospholipids films at high pressures (Cruz et al., 2000; Serrano et al., 2005). SP-B association with PL head groups could provide a structural support to compressed interfacial films. In contrast, SP-C which inserts deeper than SP-B into PL monolayers, can disturb close packing of disaturated acyl chains at high pressures favouring lipid expulsion and relaxation of compressed films. The stronger relaxation effect exerted by recombinant SP-Cs is consistent with their ability to induce compression-driven exclusion better than the native protein by pumping out more lipid molecules per molecule of protein.

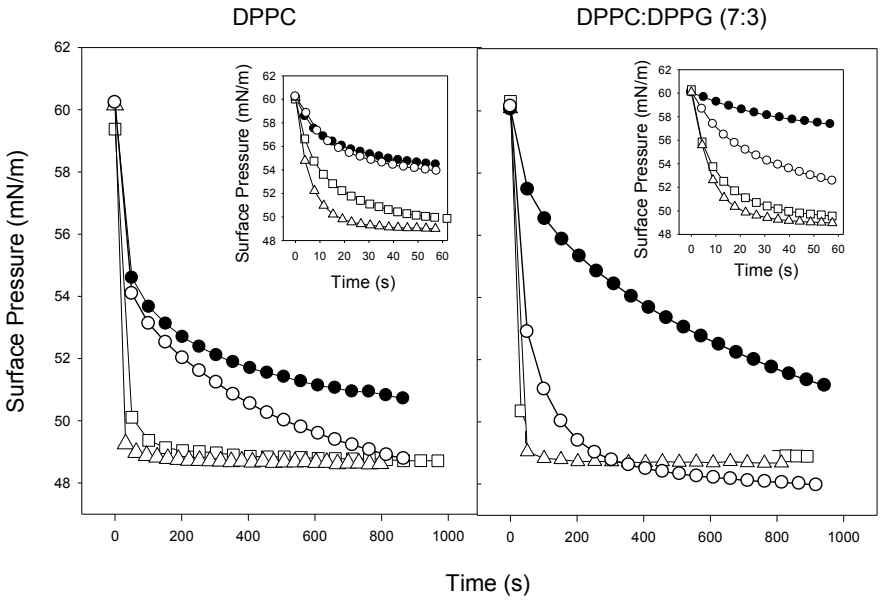

Figure 31. Stability of compressed lipid monolayers in the presence or absence of 2% native or recombinant SP-C. a. π-t relaxation kinetics of DPPC monolayer in the absence of protein (closed circles) or presence of 2%SP-C (open circles), rGP-SP-Cff (squares) or rSP-Cff (triangles). b. π-t kinetics of DPPC:DPPG (7:3) monolayer in the absence (closed circles), or presence of SP-C (open circles) , rGP-SP-Cff (squares) or rSP-Cff (triangles). The monolayers were prepared by spreading lipid or lipid/peptide organic solutions on top of the buffered hypophase and compressed to 60mN/m at 25^{0}C. Inset: re-scaling of the relaxation kinetics during the initial 60 seconds.

4.2.5 ORGANIZATION OF LIPID/PEPTIDE FILMS

The effect of native and recombinant SP-Cs on lipid packing in monolayers was analysed by epifluorescence microscopy. Monolayers formed by depositing lipid or lipid/protein mixtures dissolved in organic solvents (chloroform:methanol (2:1, v:v)) on a Langmuir-Wilhemy surface balance, were compressed and simultaneously transferred onto glass slides. The obtained immobilized films represent a visual record of the whole compression isotherm where each specific point along the slide represents lipid organization at a particular surface pressure. Lipid organization is monitored by including a trace of the fluorescent lipid probe 1-palmitoyl-2-{12-[(7-nitro-2,1,3-benzoxadiazol-4-yl)amino]dodecanoyl} phosphatidyl choline (NBD-PC), which associates with fluid liquid-expanded phases and is excluded from condensed regions. The recorded isotherms of DPPC film in the absence or presence of 5% (w/w) of native or recombinant proteins are shown in figure 32a. As seen previously, the presence of any protein expands the isotherm at low pressures, while at high pressures the lipid and lipid/protein isotherms converge at around 50mN/m indicating the exclusion of the protein together with lipids. The same figure includes epifluorescence images taken at different pressures along the compression isotherm of DPPC or DPPC/protein films doped with fluorescent dye. The light regions represent lipids in fluid phase while the dark ones represent condensed domains. Compression of pure DPPC films induces the appearance of LE-LC transition visualized as nucleation and growth of dark spots that occupy up to 80% of surface at pressures higher than 15mN/m. As compression progresses, the dark

domains grow in size and obtain a characteristic flower-like shape. The absence of kidney bean-shaped condensed domains such as those usually observed in DPPC films (Plasencia et al., 2005) is probably due to incomplete equilibration of the films transferred during continuous compression.

The presence of native or recombinant proteins induces a drastic reduction of condensed area, which is especially significant at pressures higher than 15mN/m. This effect is achieved by inhibiting growth of condensed domains creating therefore a larger number of domains with diminished area. A quantitative evaluation of protein effect on PL organization is represented in figure 32c. The most remarkable feature due to lipid-protein interaction is the visualization of potential protein-containing peripheral regions in LC domains, at 16mN/m, in the form of filamentous protrusions with reduced fluorescent contrast (see arrows in the pictures of figure 32b), likely due to partial penetration of the probe. Upon further compression the protrusions grow at the expense of the condensed and fluid phase. Similar protrusions were observed previously (Nag et al., 1996; Kruger et al., 2002; Kruger et al., 1999) although not at that extent. Quantification of these protein-promoted regions indicates that they cover an area equivalent to the decrease of condensed domains induced by the presence of protein (figure 32c, first panel, grey symbols). These results are consistent with previous studies on the effect of SP-C on DPPC condensation, where it was also observed that the protein inhibited the formation of condensed phase (Perez-Gil at al., 1992). The results presented here suggest that the proteins, native or recombinant, penetrate into the monolayer, perturb the packing of the lipid chains into LC domains and induce the dissolution of the domains preferentially at pressures around and beyond 16mN/m. Previous studies have shown that SP-C partitions preferentially to the liquid –expanded regions of PL films (Nag et al., 1996). Our epifluorescence experiments suggest that at least part of SP-C accumulates at the boundaries of the condensed lipid domains, perturbing their packing. Recent observations of preferential distribution of fluorescently labelled SP-C accumulating at the periphery of LC PL domains (Wustneck et al., 2005) is consistent with the lipid perturbation described here.

a.

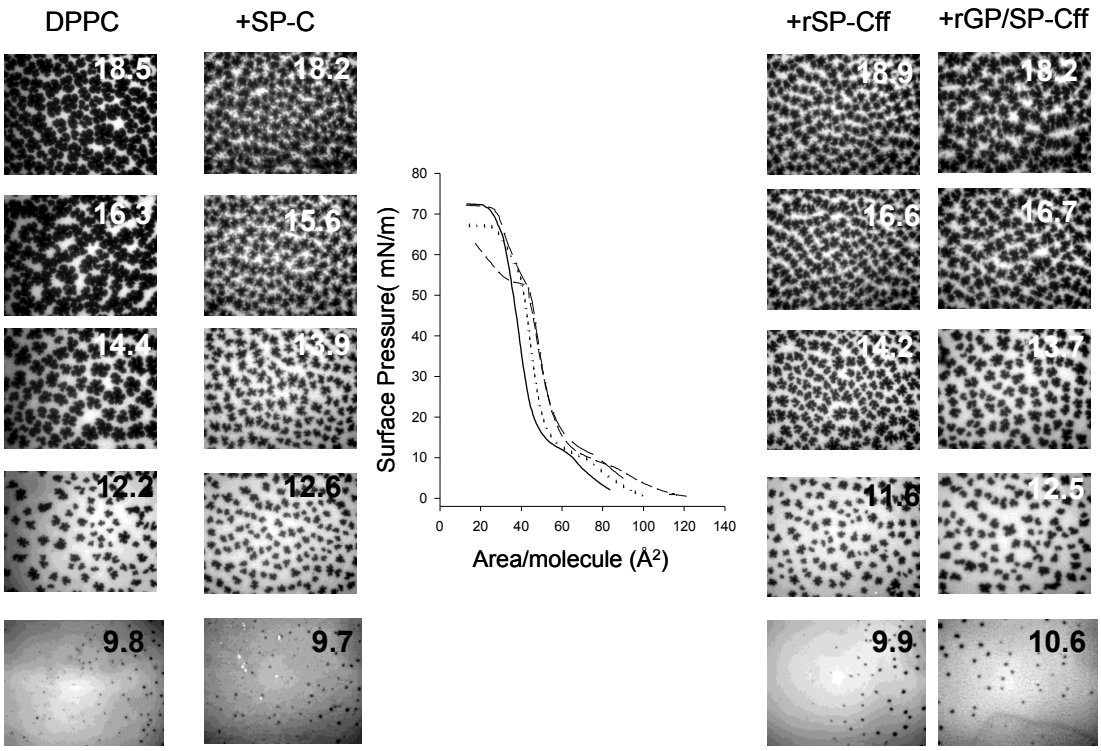
DPPC
+SP-C
+rSP-Cff
+rGP/SP-Cff
18.5
18.2
18.9
18.2
16.3
15.6
16.6
16.7
14.4
13.9
14.2
13.7
12.2
12.6
11.6
12.5
9.8
9.7
9.9
10.6
Surface Pressure(mN/m)
Area/molecule (Å²)

b.

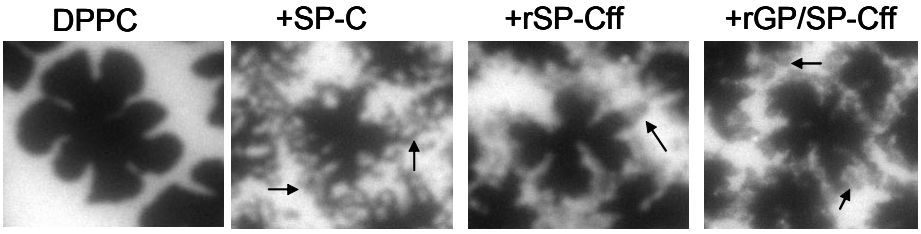
DPPC
+SP-C
+rSP-Cff
+rGP/SP-Cff

C.

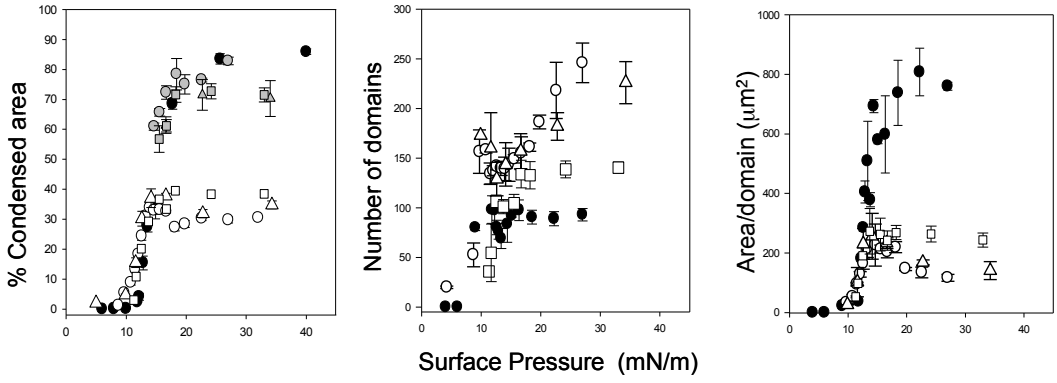
% Condensed area
Number of domains
Area/domain (µm²)
Surface Pressure (mN/m)

Figure 32. Effect of native and recombinant SP-Cs on the compression-driven condensation of DPPC monolayers.
a. π-A isotherm of compressed monolayers of DPPC in the absence (full line) and presence of 5% (w/w) native SP-C (long dashed line), rGP/SP-Cff (dotted line) or rSP-Cff (short dashed line). Images of epifluorescence microscopy have been taken from pure DPPC, DPPC/SP-C, DPPC/rGP/SP-Cff or DPPC/rSP-Cff monolayers compressed to the indicated pressures.
b. Epifluorescence images depicting the morphology of LC domains taken from films of the indicated composition, compressed to 16mN/m.
c. Quantitative analysis of the total fraction of condensed area (left panel), number of domains per frame (middle panel) and the average domain area (right panel) versus surface pressure. Data have been plotted for DPPC monolayers in the absence (closed circles) or in the presence of 5% SP-C (open circles), rGP/SP-Cff (squares) or rSP-Cff (triangles). Gray symbols indicate the proportion of condensed phase when the filamentous region, marked by arrows in pictures in b., is taken also into consideration. Data plotted represent means S.D. after averaging 5 images at each pressure.

Figure 33 illustrates the effect of native and recombinant SP-C forms on the microstructure of DPPC:DPPG (7:3) monolayers. There is a remarkable difference between the condensed domains observed in pure DPPC and those in DPPC:DPPG films. LC domains in DPPC:DPPG films are substantially smaller than those in DPPC monolayers at equivalent pressures. The negative charge of this film probably precludes nucleation of condensed domains at points where accumulation of negative charge might create destabilizing repulsive interactions. Inclusion of native SP-C reduces the size and increases the number of the condensed domains in these films, in a similar manner as in the condensation of DPPC monolayers. However, in the presence of the recombinant SP-C forms the condensed phase is nucleated in the form of larger domains, probably as a consequence of the extensive electrostatic interaction of the N-terminal segment of these recombinant SP-C proteins with the anionic PL, counteracting the repulsion between negatively–charged lipid molecules. Figure 33c provides quantitative analysis of the influence of the native and recombinant proteins on the condensation of DPPC/DPPG films. The condensation-inhibitory effect of all the proteins was less pronounced in these negatively-charged films than in DPPC monolayers. Here, native and recombinant proteins seem to achieve the condensation reduction effect through different mechanisms. Native SP-C does not alter the number of condensing domains but reduces their growth by introducing a marked perturbation of LC domains at the periphery and generating a new phase of apparently intermediate packing density, in the same manner as observed in DPPC films. Recombinant proteins in contrast reduce the number of nucleating domains at low pressures, which are larger in size and grow in a similar way to the pure DPPC/DPPG condensed domains up to the pressures of 15mN/m, when they start to dissolve at the edges to form a new phase of intermediate packing. This pressure threshold could be associated with the pressure-induced expulsion of at least part of the N-terminal segments out from the interface. At pressures lower than 15 mN/m, extensive interaction of the N-terminal segment of the SP-C variants with a large number of phospholipids would counteract the lipid negative charge favouring condensation. At pressures higher than 15 mN/m, the squeezed-out portion of the N-terminal segment could lead to conformations/dispositions more similar to those of the native protein perhaps facilitating interaction and subsequent perturbation of the condensed domains.

a.

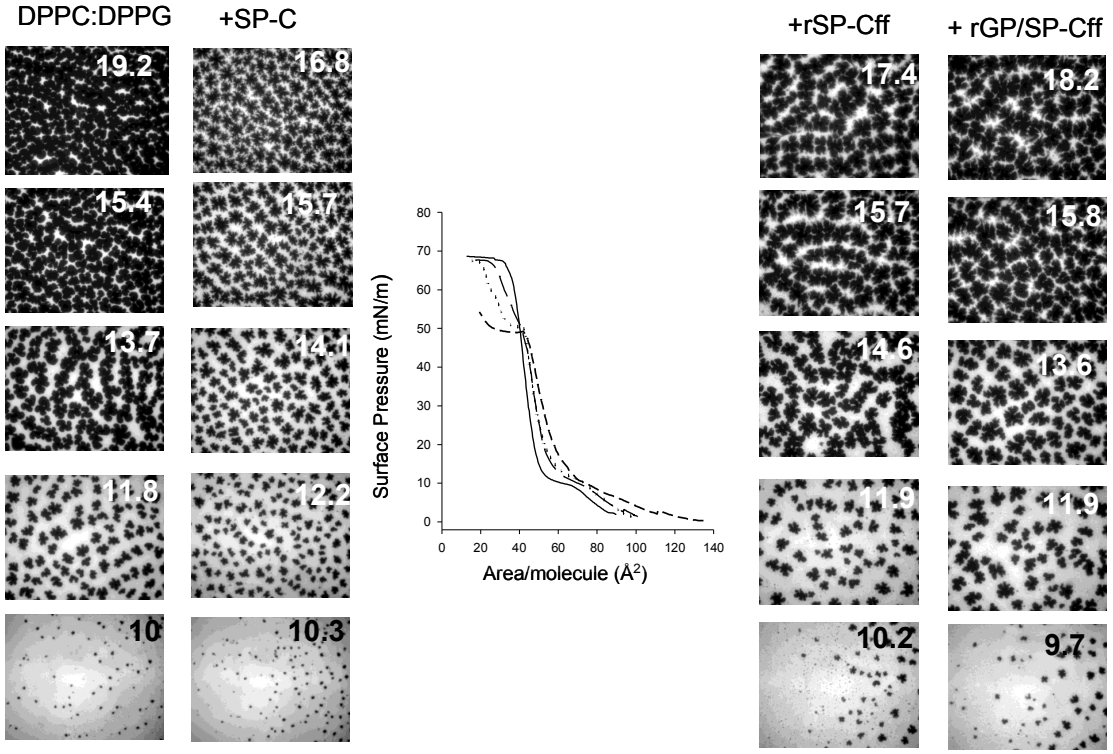
DPPC:DPPG
+SP-C
+rSP-Cff
+ rGP/SP-Cff
19.2
16.8
17.4
18.2
15.4
15.7
15.7
15.8
13.7
14.1
14.6
13.6
11.8
12.2
11.9
11.9
10
10.3
10.2
9.7
Surface Pressure (mN/m)
Area/molecule (Å²)

b.

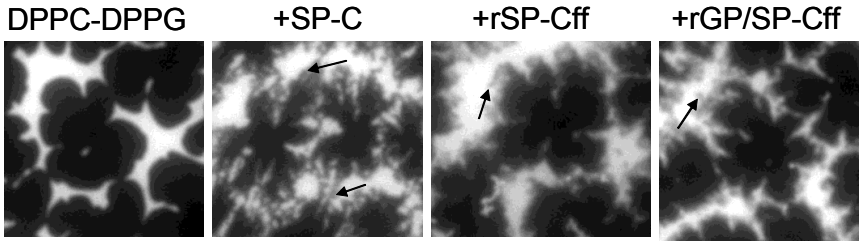
DPPC-DPPG
+SP-C
+rSP-Cff
+rGP/SP-Cff

c.

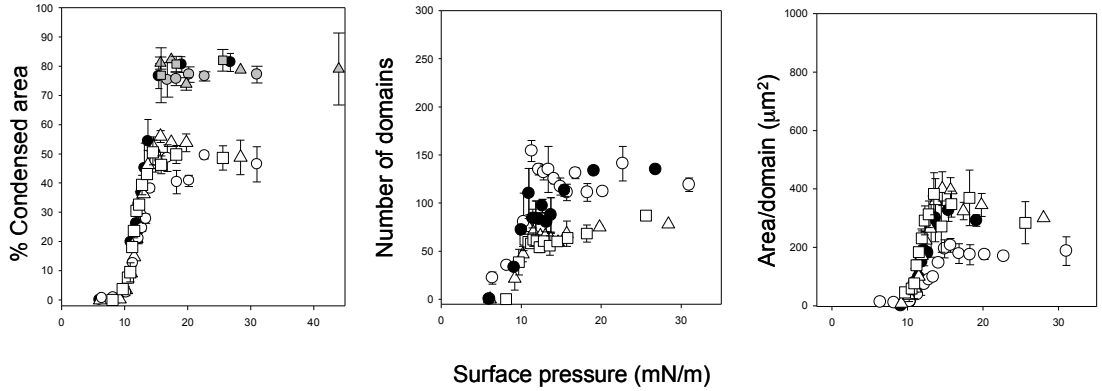
% Condensed area
Number of domains
Area/domain (µm²)
Surface pressure (mN/m)

Figure 33. Effect of native and recombinant SP-Cs on the compression-driven condensation of DPPC:DPPG monolayers.
a.π–A compression isotherm of DPPC:DPPG (7:3) monolayers in the absence (full line) or presence of 5% (w/w) native SP-C (long dashed line), rGP/SP-Cff (dotted line) or rSP-Cff (short dashed line). Images of epifluorescence microscopy have been taken from pure DPPC:DPPG, DPPC:DPPG/SP-C, DPPC:DPPG/rGP/SP-Cff or DPPC:DPPG/rSP-Cff monolayers compressed to the indicated pressures.
b. Epifluorescence images remarking the morphology of LC domains taken from films of the indicated composition, compressed to 16mN/m.
c. Quantitative analysis of the total fraction of condensed area (left panel), number of domains per frame (middle panel) and the average domain area (right panel) versus surface pressure. Data have been plotted for DPPC:DPPG (7:3) monolayers in the absence (dark closed circles) or in the presence of 5% SP-C (open circles), rGP/SP-Cff (squares) or rSP-Cff (triangles). Gray symbols indicate the proportion of condensed phase when the filamentous region, marked by arrows in pictures in b., is taken also into consideration. Data plotted represent means S.D. after averaging 5 images at each pressure.

4.2.6 SURFACE ACTIVITY IN CAPTIVE BUBBLE SURFACTOMETER

4.2.6.1 Interfacial adsorption

The ability of recombinant variants to promote phospholipid adsorption was assayed in more physiological conditions, at 37 ^{0}C and 100% humidity, in a captive bubble surfactometer. Native or recombinant protein was reconstituted in DPPC:POPG (68:31) at 2% (w/w) and injected into the chamber of a CBS before forming a 50-μL air-bubble. Surfactant absorption increased the surface pressure of the bubble which resulted in changes in bubble shape. The bubble was recorded by a video system during 5 minutes and the changes in surface tension calculated based on the bubble shape. Figure 34 shows that injection of pure lipid suspensions in the absence of protein induces a surface pressure increase only to ~25mN/m, while presence of either recombinant or native SP-C, at 2% (protein/lipid, w/w) leads to an almost instantaneous pressure increase up to an equilibrium pressure of ~47 mN/m.

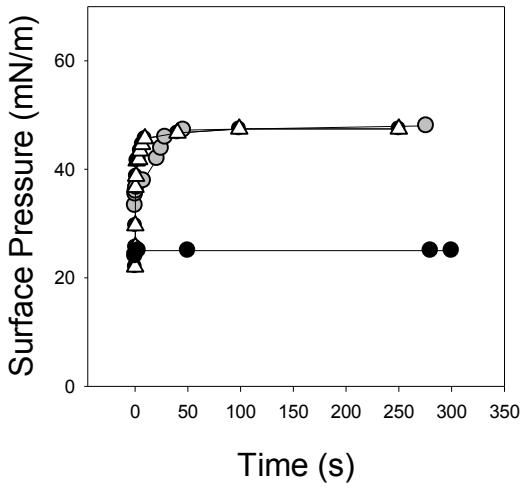

Figure 34. Interfacial adsorption isotherms in a captive bubble surfactometer. Interfacial adsorption isotherms of DPPC:POPG (68:31,w/w) suspensions in the absence (closed circles) or presence of 2% (protein/lipid, w/w) rGP/SP-Cff (open triangles), rSP-Cff (closed squares) or native SP-C (grey circles).

The influence of experimental conditions such as temperature, surfactant concentration and humidity on phospholipid adsorption is evident from comparison of this experiment to the surface adsorption measurements performed in the Wilhemy balance (figure 25), where the same percentage of protein in the bilayers was not sufficient to reach equilibrium pressures. On the other hand, the difference between recombinant and native protein activity is less evident in this experiment where both proteins reach the same equilibrium pressures. However, the adsorption kinetics was different in samples containing native versus recombinant protein: all proteins promoted a rapid pressure increase to ~38mN/m within the first few seconds, which in the case of samples containing the native protein was followed by a slower increase to equilibrium pressures compared to the recombinant proteins' performance. This observation suggests that the differences in equilibrium pressures reached by suspensions containing native vs. recombinant SP-C, as observed in Wilhemy balance, are rather due to slower native protein performance and not so much to an intrinsic feature of native protein to generate monolayers of different composition.

4.2.6.2 Quasi-static film compression and expansion cycles

After an initial adsorption period of 5 minutes, the bubble was compressed stepwise with 20s pause between compression steps. When further compression does not induce further reduction of bubble height, the bubble has reached maximal surface pressure and was expanded in the same stepwise manner to its original volume. This compression/expansion cycling was repeated 5 times and the pressure/area isotherms for the first, third and fifth cycles are shown in figure 35. The figure shows that all protein/lipid complexes reach maximal surface pressure in all five cycles meaning that the proteins, either native or recombinant, are able to promote repeated surface film compression/expansion without a loss of surface active material from the interface. The first compression step showed hysteretic behaviour with rapid pressure fall upon expansion which indicates a slow surface active material reincorporation, which was more pronounced in the suspensions bearing native protein. The following cycles did not demonstrate hysteretic behaviour suggesting that a stable surfactant reservoir was formed that facilitated reinsertion of compression-driven excluded material. Analyses of the degree of area compression required to reach the maximum surface pressure reveals that the suspension containing native SP-C required larger area reduction compared with those suspensions containing recombinant protein in order to reach similar surface pressures. DPPC:POPG/SP-C films had to be compressed to 40% of the initial surface to produce pressures of around 70mN/m in the first cycle. By the third and fifth compression, the maximal pressures were reached with ~30% compression. Both recombinant proteins reached first maximal pressure by ~29% area compression and only required 23% area reduction in the following cycles. This data confirm the previous observations in surface balance that recombinant proteins have higher potential in PL respreading.

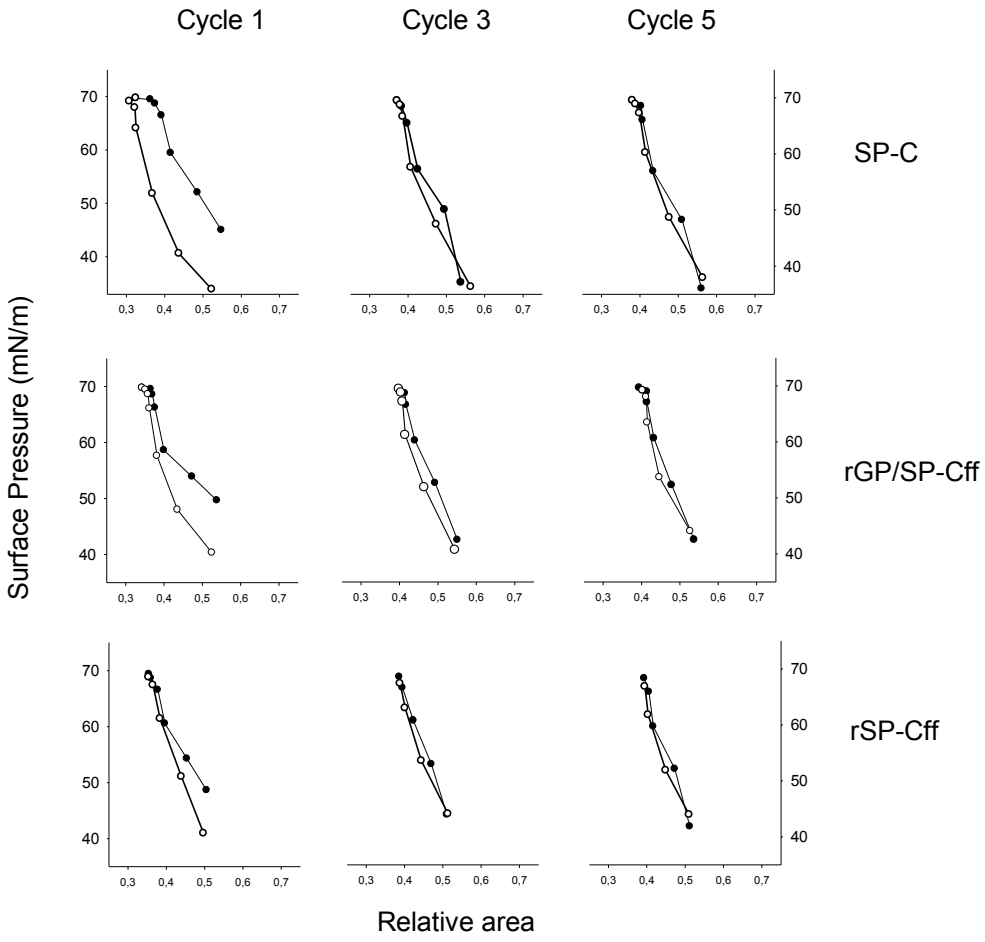

Figure 35. Effect of recombinant and native SP-C variants on the compression-expansion behaviour of lipid protein films under quasi-static conditions. Quasi-static compression (●) and expansion (○) isotherms of suspensions of DPPC:POPG (68:31, w/w) in the presence of 2%(w/w) rGP/SPCff, rSP-Cff or native SP-C. Representative isotherms for the first, third and fifth compression-expansion cycles of three different experiments are represented. The concentration of surfactant material was 10mg/ml (see Materials and Methods)

4.2.6.3 Dynamic film compression and expansion cycles

After the initial 5 minute adsorption and 5 quasi static compression/expansion cycles, in the presence of the same suspension as the ones used in previous experiments, the bubble was continuously compressed and expanded in the CBS at a rate of 20 cycles per minute during one minute. The bubble was recorded during cycling and the first, tenth and the twentieth cycle were analysed and compared. The figure 36 shows that all suspension preparations produced bubbles that could be repeatedly compressed and expanded for 20 cycles reaching the maximal surface pressures without any hysteresis.

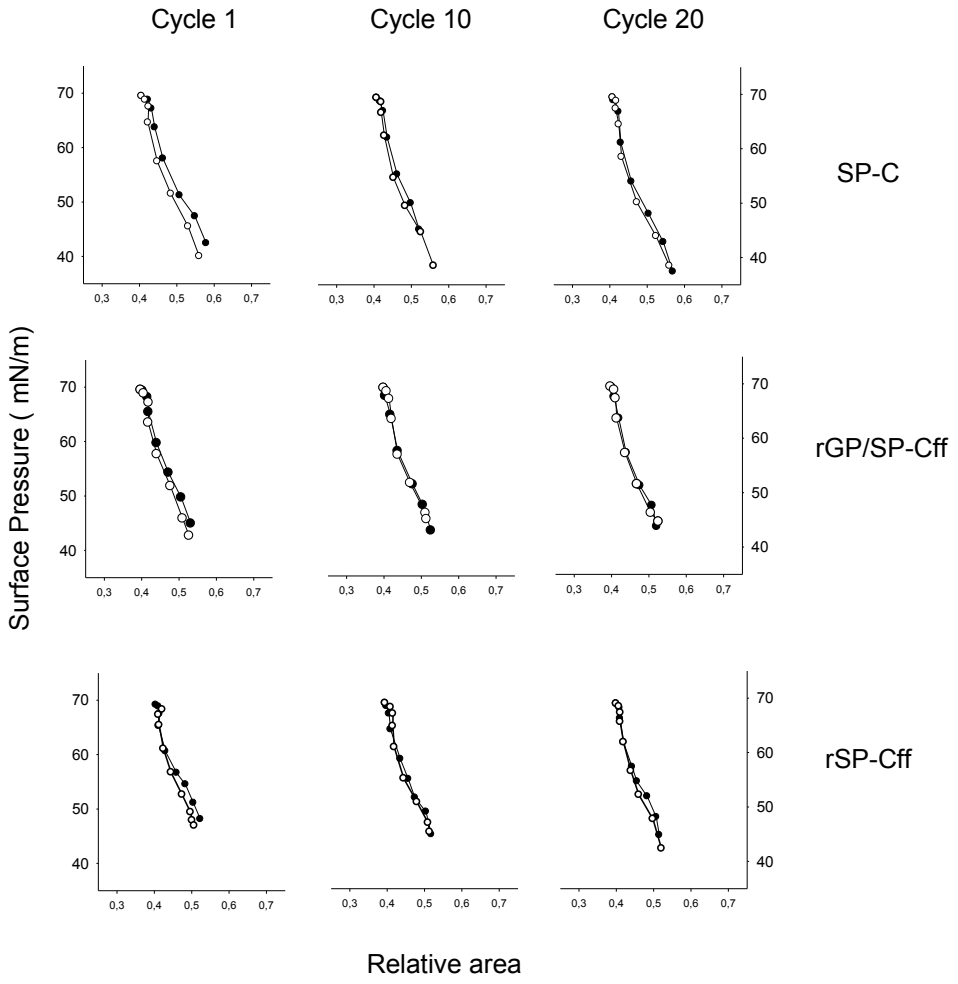

Figure 36. Effect of the native and recombinant SP-C variants on the compression-expansion behaviour of lipid protein films under dynamic conditions. Dynamic compression (●) and expansion (○) isotherms of DPPC:POPG (68:31, w/w) in the presence of 2%(w/w) rGP/SPCff, rSP-C or native SP-C. Representative isotherms for the first, tenth and twentieth compression-expansion cycles of three different experiments are represented. The concentration of surfactant material was 10mg/ml (see Materials and Methods).

Analysis of percent area required for reaching maximal surface pressure for recombinant and native protein (Table 5) does not reveal any discernible differences, except for the first cycle where a larger area reduction is required for suspensions containing native protein vs. recombinant ones to reach pressures of 70mN/m. The first compression requires 30% area reduction for native protein containing suspensions while ~23% is required for recombinant proteins. The following cycles demonstrated similar compression extent for native and recombinant proteins.

This observation reflects the fact that in the case of the native protein the stable surfactant reservoir is formed with a certain delay, but that once formed, the native protein has the capacity to promote PL reinsertion as efficiently as the recombinant proteins.

Table 3. Percent of area reduction necessary in order to reach minimum surface tension during compression-expansion cycles of a captive bubble formed in the presence of native or recombinant protein /lipid (DPPC:POPG, 68:31 w/w) films.

%AREA COMPRESSION REQUIRED TO REACH MAXIMUM SURFACE PRESSURE						
	Quasi Static			Dynamic		
Cycle	**1**	**3**	**5**	**1**	**10**	**20**
SP-C	40.7±1.5	30.9±2.3	32.14±2.8	29.9±1.6	21.8±2.5	25.3±2.1
rGP/SP-Cff	28.3±0.7	23.4±0	22±0	24±17	24±0.1	23.1±0.9
rSP-Cff	29.8	22.8±2.8	23.17±1.3	22.7±1.1	23.86±0	22.48± 0.8

4.2.7 DISCUSSION

In this chapter we describe the effect of the recombinant SP-C forms on the surface behaviour of PL films compared with films containing SP-C isolated form porcine lungs. Interfacial adsorption measurements suggest that, at least regarding promotion of bilayer to monolayer conversions, the SP-C versions produced in bacterial cultures have equivalent or superior properties to the native protein purified from animal lungs. This finding indicates that palmytoyl chains are either not required to promote monolayer formation or that Phe substitution is sufficient to overcome its deficiency. In order to test the hypothesis that the introduced phenylalanine residues could be important for the activity of the recombinant protein we have approached production and characterization of recombinant variants bearing tryptophanes or cysteines (next chapter). Anyhow, the results presented so far are confirming the potential utility of bacterial SP-C forms as part of clinical surfactant preparations. Also, the possibility to create site-directed variants to analyse in detail structure – function determinants, allowing targeted amino acid substitutions, represents a significant step toward elucidation of SP-C molecular mechanism.

The compression isotherms of phospholipid films containing increasing proportions of protein indicate that the recombinant versions of SP-C expel more phospholipid molecules from the interface than the native protein, when the lipid-peptide films are compressed beyond the collapse pressure of the protein. These results suggest that the aromatic residues included into the N-terminal region of the recombinant forms may either increase the affinity of the protein to associate with phospholipids or promote a more appropriate conformation of this region to accommodate a higher number of lipid molecules. Expulsion of higher number of PL molecules from the interface at high pressures and more efficient insertion of PL at low pressure could be two consequences of SP-C variants bearing an N-terminal tail with enhanced exposure and association to PL. On the other hand, our production procedure, which maintains the structural integrity of the recombinant SP-C forms, may preserve better its activity in quantitative terms, compared to the delipidation and purification procedure of native SP-C

from animal lungs. The role of SP-C *in vivo* has been mostly discussed in connection to the protein-mediated stability of the interfacial surface active film at end-expiration, and not much as promoting interfacial adsorption, an activity which seems to be better performed by SP-B (Wang et al. 1996; Perez-Gil, 2001). However, there are strong evidences suggesting that a Phe-containing rSP-C version has enough surface activity to be used as the only protein component of therapeutic surfactant preparations (Davis et al., 1998; Spraag et al., 1996). The N-terminal segment of SP-C has been revealed as a very dynamic structural motif (Plasencia et al., 2004) which is able to interact and perturb by itself the PL packing of phospholipid bilayers and monolayers (Plasencia et al., 2005). Acylation of this segment may be rather important to maintain association with the interface of the lipid/protein structures squeezed-out from the films compressed to the highest pressures (Bi et al., 2002), reached in the lungs at end-expiration. In native surfactant complexes, efficient bilayer-monolayer (during adsorption and re-extension upon expansion) and monolayer-bilayer (during compression) conversions are ensured by the presence of SP-B. A high affinity of the protein to associate with the interface has been recently shown to be a crucial determinant for the SP-B activity, this association being critically dependent on the presence of aromatic residues at the N-terminal segment of the protein (Serrano et al., 2006). It is thus reasonable to expect that in the absence of SP-B, SP-C variants with enhanced affinity for the interface may show enough activity to promote bilayer-monolayer transitions and serve as the only additive needed for efficient therapeutic surfactant formulations. Further biophysical studies of the surface behaviour of these and other variants are ongoing and will allow the establishment of their potential as SP-C (or SP-B) mimics, as well as the determination of critical structure-function motifs.

Fluorescence micrographs indicate that, similarly to the native protein, recombinant proteins promote perturbations of lipid packing at the condensed phase and formation of less ordered phase of intermediate packing, starting at surface pressures of ~ 16mN/m. As pressure increases further, this phase grows at the expense of the solid and expanded phase, maintaining a substantial proportion of condensed phase up to the highest pressures analysed. This disorder and packing perturbation introduced by the protein may facilitate surface film deformations and formation of 3-D structures at regions with intermediate compaction. Compression-driven formation of large three-dimensional structures associated to the interfacial films is particularly promoted by the presence of SP-C as observed by scattered light microscopy beyond 20mN/m (Kruger et al., 1999) and in fixed alveoli by electron microscopy (Schurch et al., 1998). These localized multilayered structures considered as a "surface-associated surfactant reservoir" are thought to contribute to attaining the highest surface pressures -lowest surface tensions- and to facilitate efficient reinsertion, without necessarily considering a supposed compositional refinement of the surface film, as proposed by the *squeeze-out* theory.

We have used here protein contents of 5% (protein to lipid by weight), which is above physiological protein levels, in order to better visualize the effect of proteins on lipid organization. Similar qualitative disordering of LC phase by physiological amounts of SP-C was observed previously by Kruger and colleagues (Kruger et al., 1999).

Finally we have shown that lipid /protein suspensions containing 2% (protein to lipid by weight) recombinant proteins absorb instantaneously into the air-water interface, forming films that are able to sustain repetitive compression-expansion cycling under physiological conditions of temperature and compression-expansion speeds, without apparent loss of surface lowering capacity. These experiments

under dynamic conditions confirm the observations found in studies with surface balances that the recombinant proteins are more efficient in promoting surface adsorption and reducing surface tension to the lowest values with lower degree of area compression.

4.3 EFFECT OF THE PRESENCE OF AROMATIC RESIDUES ON THE SURFACE BEHAVIOUR OF RECOMBINANT SP-C FORMS

In the previous chapter we have studied the activity of recombinant variants of SP-C compared with the native protein isolated from porcine lungs. The main structural difference between the protein expressed in bacteria and the native protein lies in position 5 and 6 of its amino acid sequence. We introduced a $C_5C_6 \rightarrow F_5F_6$ double mutation in the human SP-C sequence for several reasons. Knowing that bacteria are unable to perform postranslational palmitoylation we searched for a natural substitute to palmitoylated cysteines. We hypothesised that phenylalalnines that are present in canine SP-C at position 6, which is occupied by palmitoylated cysteine in most of the species could be its natural functional equivalent. Second, this amino acid has high affinity toward membrane interfaces, which could improve the surface activity of the protein. Finally, a recombinant protein with this particular substitution was produced before and shown evidence to possess sufficient surface activity (Davis et al., 1998). Although a very similar surface activity was observed when comparing recombinant and native proteins, our experiments demonstrated that recombinant variants interact slightly differently with PL than native sample. We propose that this distinct behaviour is attributed to the presence of phenylalanines. This amino acid, as well as the other two aromatic amino acids was found to promote high affinity toward membrane interfaces (White and Wimley, 1998). In this sense, we propose that the affinity for the membrane interface as a site of hydrophobic/hydrophilic biphasic environment is equivalent to that provided by the air-water interface such as the one present in lungs. It was observed previously (Ryan et al., 2005; Serrano et al., 2006) that tryptophane is crucial for the activity of the other hydrophobic surfactant protein, SP-B, at the interface since the substitution of tryptophane by alanine in a peptide that mimics SP-B biophysical properties leads to the loss of surface activity. We have tested here the hypothesis that phenylalanines are responsible for the slightly higher equilibrium pressures reached in spreading experiments and contribute to the greater efficiency of recombinant forms of SP-C to mobilize PL molecules between bilayers and monolayer and vice versa.

For this purpose we have produced two new variants of SP-C: a variant bearing tryptophanes in place of phenylalanines and a variant containing two cysteines at equivalent positions. Since tryptophanes have been shown to possess the highest affinity of all amino acids to associate with interfaces we expected that it would also confer the highest surface activity when present in the recombinant protein. On the contrary, the variant bearing cysteines was expected to show lower activity than the variants bearing aromatic groups in all assays.

4.3.1 Expression and purification of recombinant sp-c variants

Figure 37a shows the complete sequence of the new recombinant SP-C forms produced. Figure 37b shows an SDS gel loaded with the purified recombinants. All the proteins showed a main band in the gels consistent with a monomeric character, both under reducing and non-reducing conditions. The proteins also showed a minor band with mobility corresponding to the dimer, suggesting

that all the variants maintain the strong tendency of the native protein to oligomerize. CD measurements discarded however structural changes to β-sheet conformations due to protein aggregation. These results are in contrast with the work of Baatz and colleagues that found that native depalmotoylated SP-C formed dimers with predominantly β sheet structure (Baatz et al., 1992). The observed differences may be explained by different solvent environments through which the proteins were obtained. Figure 37c shows the far UV circular dicroism spectra of the new recombinant SP-C forms, reconstituted in lipid vesicles (DPPC:DPPG, 7:3 (w/w)) or in micelles of the lysophospholipid LPC. All the proteins showed CD spectra consistent with a mainly α-helical conformation. Table 4 summarizes the secondary structure proportions in the conformation of the three analyzed SP-C variants, estimated from their CD spectra.

a.

GPFGIP**FF**PVHLKRLLIVVVVVVLIVVVIVGALLMGL	rGP/SP-Cff
GPFGIP**CC**PVHLKRLLIVVVVVVLIVVVIVGALLMGL	rGP/SP-Ccc
GPFGIP**WW**PVHLKRLLIVVVVVVLIVVVIVGALLMGL	rGP/SP-Cww

b.

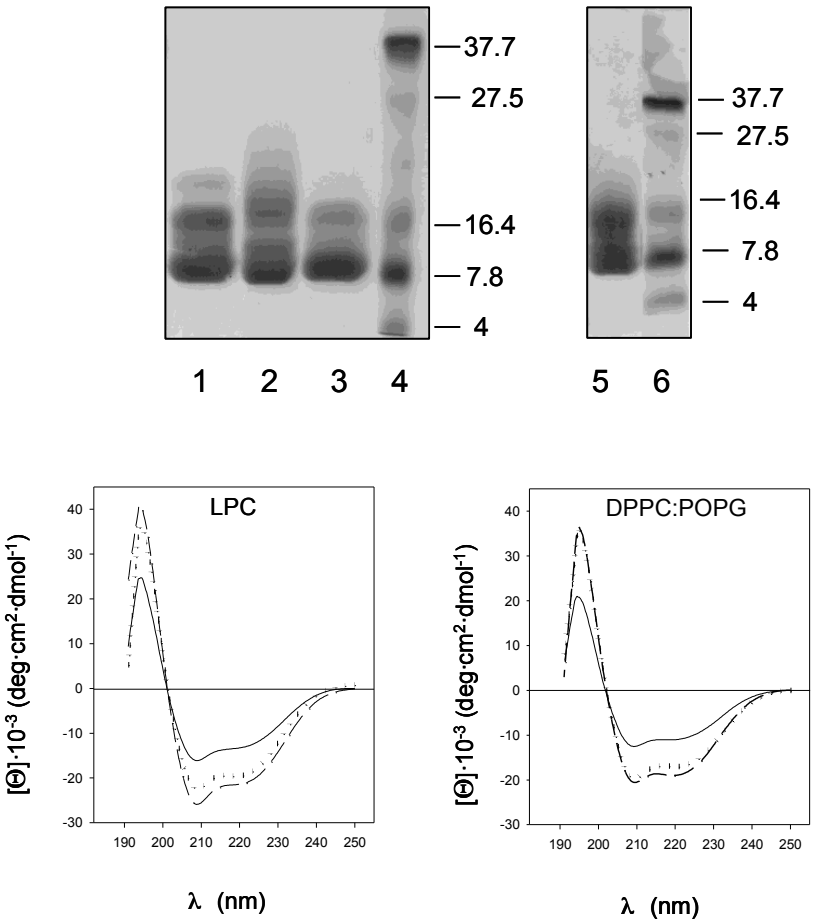

Figure 37. Sequence, electrophoretic behaviour and secondary structure of SP-C recombinant variants bearing or not aromatic residues.
A.The sequences of new recombinant forms of human SP-C bearing cysteines, phenylalanines or tryptophans at positions 5 and 6 of the original sequence. **B**. Coomassie blue stained SDS gels loaded with molecular weight markers (lanes 4 and 6), rGP/SP-Cff (lane 1), rGP/SP-Ccc (lane 2 and 5) and rGP/SP-Cww (lane 3). The gel on the left was run under reducing, and that on the right side, under non-reducing conditions. **C**. Far UV CD spectra of rGP/SP-Cff (full line), rGP/SP-Ccc (dotted line) and rGP/SP-Cww (dashed line) in LPC micelles (left) or lipid vesicles (DPPC:POPG, 7:3 (w/w)) (right).

Table 4. Secondary structure (%) of recombinant SP-C proteins after analysis of the CD spectra using the CDPro package (Sreerama et al., 2004; Sreerama et al., 2000).

	LPC				DPPC:POPG			
	H [a]	S [b]	t [c]	r [d]	H [a]	S [b]	t [c]	r [d]
rGP/SP-Cff	52	7	22	19	47	8	22	23
rGP/SP-Cww	78	6	8	8	73	9	8	10
rGP/SP-Ccc	70	8	11	11	67	6	14	13

[a] H: accumulated value for regular and distorted α-helix

[b] S: accumulated value for regular and distorted β-strand

[c] t: turn

[d] r: random

4.3.2 Interfacial spreading π-t isotherms

We monitored interfacial film formation induced by deposition of lipid suspensions bearing rGP/SP-Cff, rGP/SP-Cww or rGP/SP-Ccc on the liquid surface of a Wilhemy balance (as described in chapter 5, figure 25). The film formation was observed from bilayers of DPPC:POPG (figure 38, upper panels) or the mixture DPPC:POPC:POPG:Cholesterol (50:25:15:10, w:w:w:w) (lower panels), containing different proportions of the proteins. The maximum surface tension reached for all variants was similar and close to the values obtained previously for rGP/SP-Cff. The three proteins showed again better interfacial activity for the mixture containing cholesterol than for the binary DPPC:POPG system. There were no apparent differences between the three compared proteins in promoting adsorption from DPPC:POPG bilayers. Small differences between variants are observed in the case of small protein percentage (in case of 2% protein in DPPC:POPG (7:3) and 1% protein in DPPC:POPC:POPG:Cholesterol). In the mixture containing cholesterol, presence of limiting amounts of the proteins suggests that the order of surface activity is SP-Cff ≥ SP-Ccc ≥ SP-Cww. This result suggests that the slight difference in the equilibrium surface pressure produced by suspensions containing native and recombinant protein (figure 25) can not be attributed strictly to the presence of aromatic residues, since the rGP/SP-Ccc variant reached similar equilibrium pressures as rGP/SP-Cff and rGP/SP-Cww.

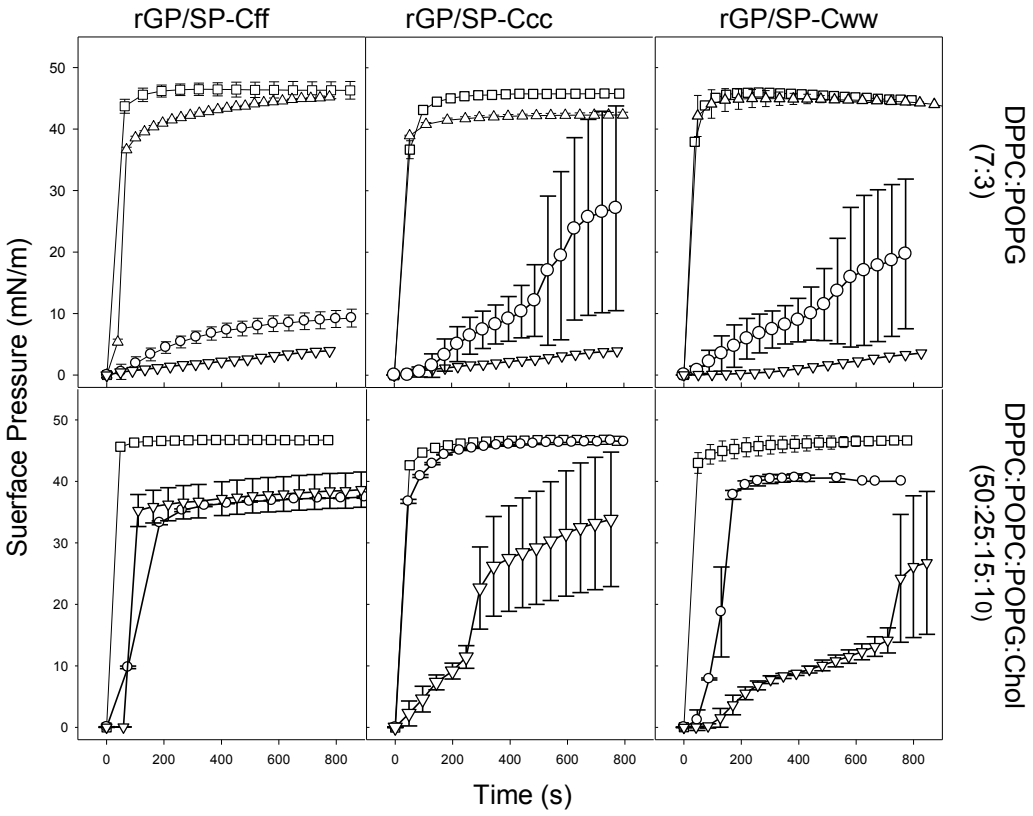

Figure 38. Interfacial adsorption activity of recombinant SP-C forms bearing or not aromatic residues. The panels show π-t adsorption isotherms for interfacial film formation after deposition of 10μl of 10mg /ml of a lipid suspension made of either DPPC:POPG (7:3, w:w) (upper panels) or DPPC:POPC:POPG:Cholesterol (50:25:15:10) in the presence of 1%(w/w) (triangles down), 2% (circles), 5% (triangles up) or 10% (squares) of the indicated protein forms (protein to lipid by weight).

The ability of recombinant variants to promote phospholipid adsorption was also assayed in more physiological conditions (37^{0}C and 100% humidity) in a captive bubble surfactometer. Suspensions of DPPC:POPG (68:31, w/w) bilayers containing 2% (w/w) recombinant proteins were placed in a CBS chamber where the air bubble was introduced. The bubble was recorded during 5 minutes and the changes in surface tension were calculated using the equation that relates bubble shape and surface tension. Figure 39 shows that the presence of 2% recombinant protein promotes increase in surface pressure to equilibrium values within several seconds. The effect of surfactant mixtures bearing either one of the three recombinant variants was similar to that of Curosurf®, a preparation used in clinical treatment. Pure lipid suspensions reached only pressures of ~24mN/m during the time of recording.

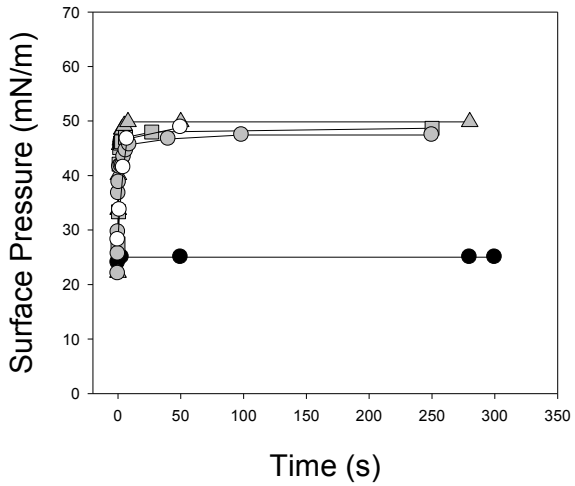

Figure 39. Interfacial adsorption isotherms of SP-C forms in a captive bubble surfactometer. Interfacial adsorption of DPPC:POPG (68:31,w/w) bilayers containing 2% (w/w) of rGP/SP-Cff (grey triangles), rGP/SP-Cww (grey circles) or rGP/SP-Ccc (grey squares), compared with Curosurf® (open circles) and with a pure lipid suspension (closed circles).

4.3.3 Protein compression isotherms

π-A compression isotherms of pure recombinant protein films were recorded as described before on a Wilhemy balance by depositing protein dissolved in organic solvent on top of the buffered subphase and compressing the resulting film until the collapse pressure was reached. The obtained isotherms of rGP/SP-Ccc and rGP/SP-Cww are shown in figure 40 and compared with those of rGP/SP-Cff, native SP-C and rSP-Cff. The isotherm of rGP/SP-Ccc was practically identical to that of rSP-Cff regarding the areas along the compression curve and the presence of the plateau at 6mN/m. However the isotherms of rGP/SP-Cww are shifted to larger areas per molecule all along the isotherm. The larger area per molecule of rGP/SP-Cww can be interpreted as due to the higher affinity of tryptophanes for air-water interface, which preclude the complete ejection of the N-terminal segment to the water subphase that occurs in other SP-C variants at around 6mN/m, maintaining thus the large molecular area during compression.

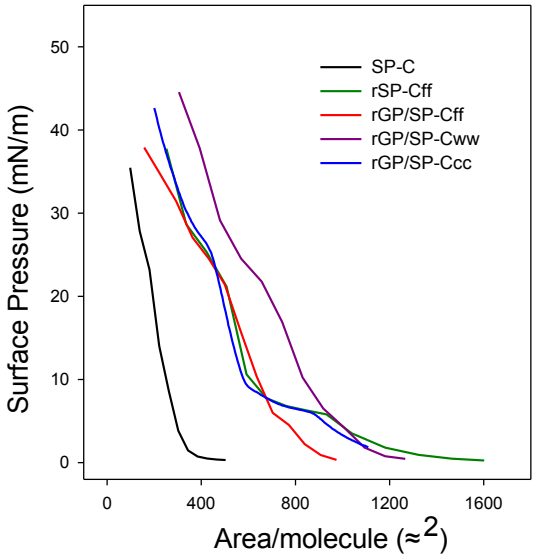

Figure 40. Pressure-area isotherms of films of SP-C, rGP/SP-Cff, rGP/SP-Ccc, rGP/SP-Cww and rSP-Cff.

Table 5. *Characteristics of pressure-area curves of native and recombinant SP-Cs*

	Extrapolated area in the isotherm (Å^2/molecule)*	Area at lift-off at π= 0mN/m (Å^2)
SP-C	200	350
rGP/SP-C	780	980
rGP/SP-Ccc	780	1200
rGP/SP-Cww	900	1300
rSP-C	680	1600

* Determined by extrapolation of linear parts of the surface pressure-area curves to π=0

4.3.4 Atomic force microscopy (AFM) of recombinant protein monolayers

To further analyze differences in protein disposition in the films made of different SP-C variants, recombinant protein monolayers were compressed to 30mN/m, transferred to mica supports and studied by AFM (figure 41). The major advantages of AFM are increased resolution, characterization of 3-dimensional structures and no necessity of probe inclusion in the film (Cruz et al., 2005).

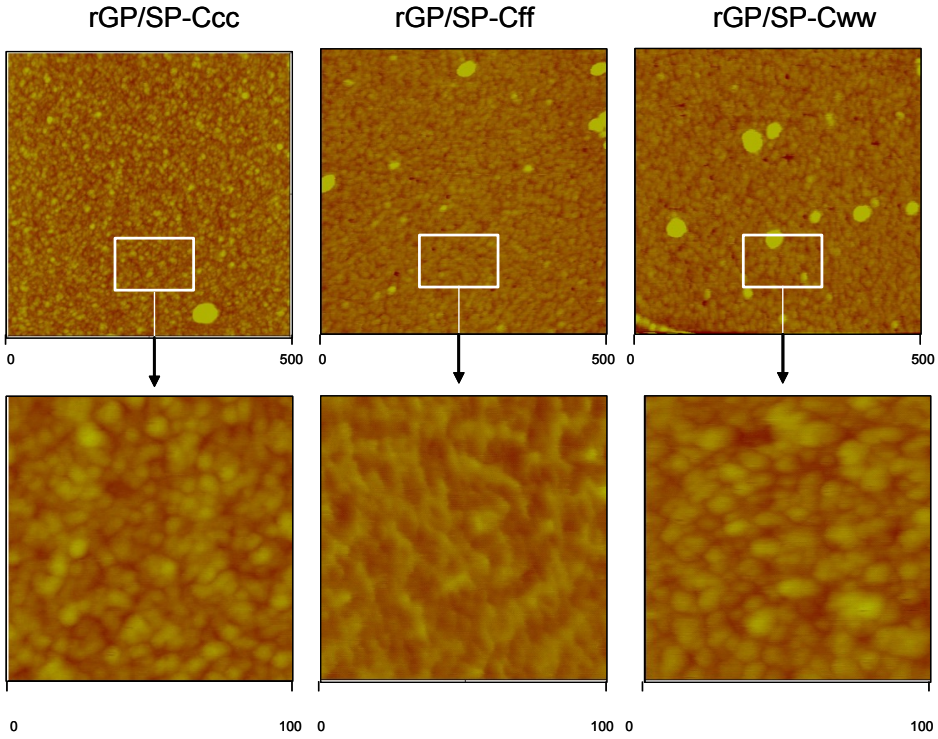

F**igure 41. AFM images from recombinant protein films compressed to 30mN/m and transferred to a freshly cleaved mica surface**. The width of the size (in nm) covered by each micrograph is indicated. Lower pictures were taken with larger magnification from the same films.

Figure 41 shows that in protein monolayers compressed to pressures close to the protein exclusion all three proteins are tightly packed as nanometer-sized particles with regular shapes. These particles having rounded shape probably represent individual or grouped helices orientated with their main axis perpendicular to the plane of mica and scanned by the AFM cantilever from the C-terminal side of the helical rods. Some aggregates of squeezed–out material forming stacked layers above the films are clearly visible in the three samples. In all three cases the surface of the round repetitive structures is around 1000Å^2. The area/molecule calculated from the isotherms (see figure 40) at 30 mN/m is around 400-500 Å². Therefore the observed particles could represent single helical molecules or small oligomers of perhaps 2 or 3 helices packed together. No large differences could be seen between the shapes and sizes of the different protein forms that could justify the difference in area/molecule seen in rSP-Cww compared with the other variants.

4.3.5 Protein/lipid compression isotherms

We have recorded π-A compression isotherms of DPPC or DPPC:DPPG films in the absence or presence of different proportions of the new recombinant SP-C variants (figure 42). The isotherms demonstrate area expansion at lower pressures as well as area reduction at pressures above 50mN/m

that are similar to those induced by rGP/SP-Cff or rSP-Cff. As with rGP/SP-Cff in monolayers of DPPC, the new variants show isotherm expansion beyond the area taken by the protein molecules themselves indicating that lipid/protein interactions introduce perturbations of lipid packing toward more disordered configurations occupying larger area/molecule. In monolayers made of DPPC:DPPG (7:3) the area occupied by the molecules was larger than the addition of areas taken by the pure lipid and protein monolayer molecules but again lower than the expansion observed in DPPC/protein films. These data confirm that electrostatic forces influence the organization of molecules in the monolayer.

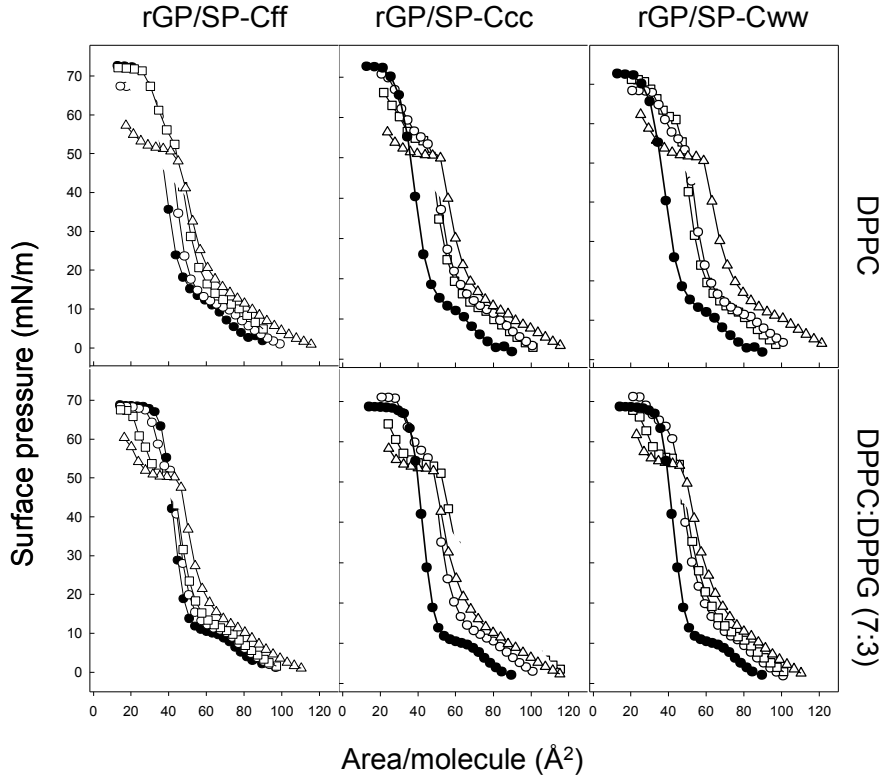

Figure 42. Compression π-A isotherms of lipid and lipid/protein films containing rGP/SP-Cff, rGP/SP-Ccc, or rGP/SP-Cww. Lipid films in the absence of protein (black circles) or in the presence of 2% (white circles) 5% (squares) or 10% (triangles) of rGP/SP-Cff (left panels), rGP/ SP-Ccc (middle panel) or rGP/SP-Cww (right panel) were spread on aqueous hypophases and compressed at 65cm^2/min at 25 ^{0}C.

Quantitative analysis of the lipid molecules ejected by the squeezing of the protein out of the interface is shown on figure 43. The regression curves demonstrate that the two new variants interact with PL at similar extent as the rGP/SP-Cff form. SP-C variants bearing cysteines or tryptophanes at the N-terminal segment were excluded from the interface accompanied by a similar number of PL molecules as calculated for phenylalanine–containing SP-C, which were also significantly larger than the molecules expelled with the native palmitoylated protein. This result indicates that palmitoylation is a major determinant of the configuration of the N-terminal segment of the protein which also defines the stoichiometry of the SP-C/lipid interaction. In this sense, palmitoylation seems much more determinant than the presence of aromatic residues, which affect only marginally lipid molecule mobilization from

and into the interface by SP-C.

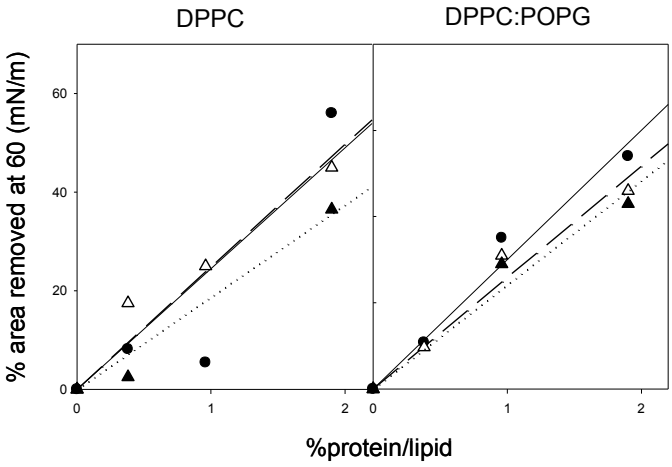

Figure 43. Effect of amino acids at position 5 and 6 on the removal of lipid/protein material from highly compressed interfacial films. Percent of lipid film area at 60 mN/m reduced by the presence of native rGP/SP-Cff (full line), rGP/SP-Ccc (dashed line) or rGP/SP-Cww (dotted line) plotted against the proportion of protein in the film (mol/mol).

4.3.5.1 Compression-expansion cyclic isotherms

In order to test the effect of the presence of the recombinant proteins on the behaviour of interfacial lipid/protein films subjected to dynamic compression, lipid monolayers were subjected to several cycles of compression and expansion in the absence or presence of 10% (w/w) native or recombinant (rGP/SP-Cff or rGP/SP-Cww) proteins (figure 44).

In the absence of protein, the lipid film reaches the maximum surface pressures in all the compression/expansion cycles, although the reduction in area during overcompression at 70 mN/m produced irreversible loss of material squeezed-out from the interface. In the presence of protein, either native or recombinant, the exclusion of proteins leads to the formation of a conspicuous exclusion plateau at around 50mN/m. The same exclusion plateau was observed before in compression isotherms (figure 28). Upon expansion, the surface pressure falls rapidly in protein-free films; however in the presence of protein the compression driven excluded material cooperatively reinserts generating small plateaus at pressures around 40mN/m (see arrows in isotherms of figure 44). The rate of protein –promoted material reinsertion was compared by plotting the % of reinserted area at pressures below 40mN/m versus the number of cycles. Figure 45 shows that the recombinant protein rGP-SP-Cww is more efficient in material resinsertion than other proteins, in the order rGP/SP-Cww > SP-C > rGPSP-Cff.

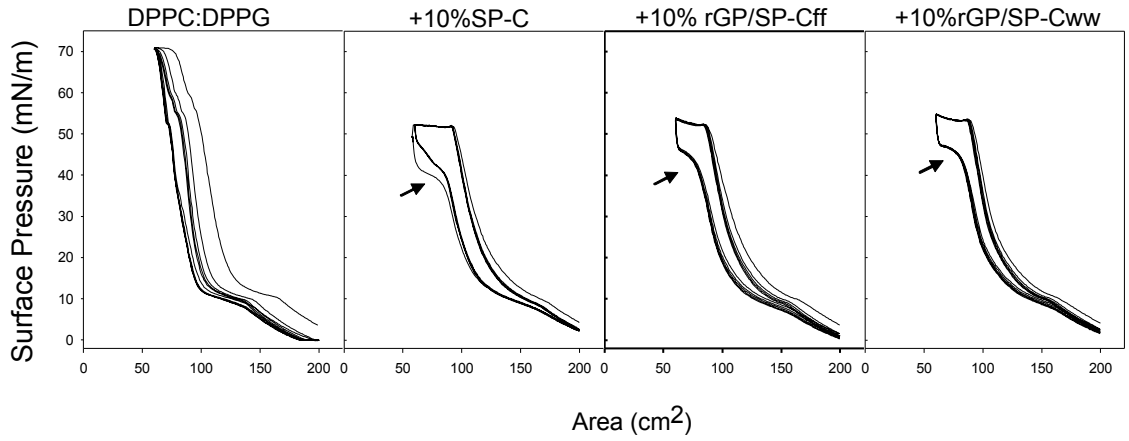

Figure 44. Effect of native and recombinant proteins on cyclic compression-expansion π-A isotherms of lipid and lipid/peptide films. Compression–expansion cyclic isotherms of DPPC:DPPG (7:3, w/w) monolayers were obtained in the absence or in the presence of 10% (w/w) of the indicated protein forms. Films were formed by spreading chloroform/methanol solutions of lipid or lipid/protein films on top of the buffered subphase (Tris 5mM, NaCl 150mM, pH 7). After 10-min equilibration, the monolayers were compressed and expanded up to 5 cycles at 25^0C, and the changes in surface pressure were registered versus area.

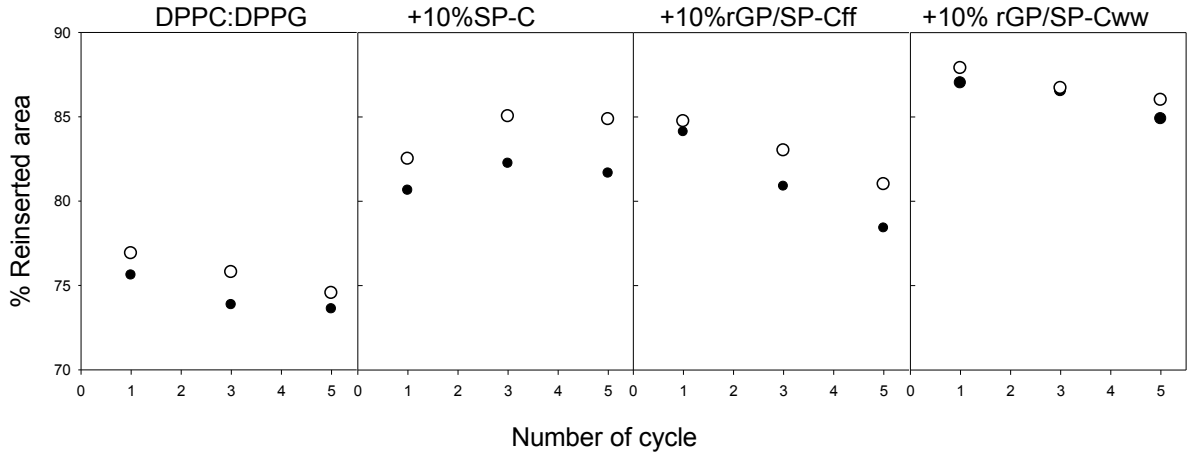

Figure 45. Percent of area recovered during expansion in compression/expansion cycling of lipid or lipid/protein monolayer at 15mN/m (black circles) and 30mN/m (white circles). % area is calculated with respect to the area occupied during the initial compression of the first cycle.

4.3.6 Protein activity in captive bubble surfactometer

We have finally compared the surface properties of the three different variants in a captive bubble surfactometer which allows evaluation of surface activity in more physiological conditions (37 ^{0}C, 100% humidity). As for the adsorption experiment the lipid protein suspensions were introduced into the CBS chamber and the bubble formed by injection of the proper volume of air with a syringe. After initial

adsorption, the activity of the recombinant proteins was tested in conditions of successive bubble compression-expansion, mimicking alveolar breathing. First the bubble was subjected to 5 quasi static cycles, which imply a slow compression and expansion that allows optimal packing of lipids and proteins at each new pressure, conditions similar to equilibrium adsorption. The performance of recombinant protein/lipid mixtures was compared to Curosurf® (Chiesi Farmaceutici, Parma, Italy) a native surfactant currently used in clinical therapy. Figure 46 shows π-A isotherms recorded in bubbles formed in the presence of the different suspensions and subjected to 5 quasi-static compression-expansion cycles. Figure 46 shows that all recombinant proteins are able to induce surface pressure increase to maximum values in all five cycles. The percentage of area reduction required to reach maximum surface pressures is shown in Table 6. The area reduction required to reach the highest pressure diminishes during cycling. In the first cycle area compressions of around 40% were necessary. During the first expansion the pressure drop was more abrupt leading to hysteresis. The fifth cycle required reduction of around 20 % for Curosurf® and suspensions containing rGP/SP-Cff, while a larger compression was necessary for samples containing mutants with tryptophanes or cysteines. In all cases hysteresis was particularly abolished in the second cycle. This reduction of area with cycling would be traditionally interpreted as a depuration of the interfacial films to produce layers highly enriched in DPPC. However current models would rather explain it as associated with the function of a surface reservoir or 3-dimensional structure, which allows more efficient respreading with each cycle.

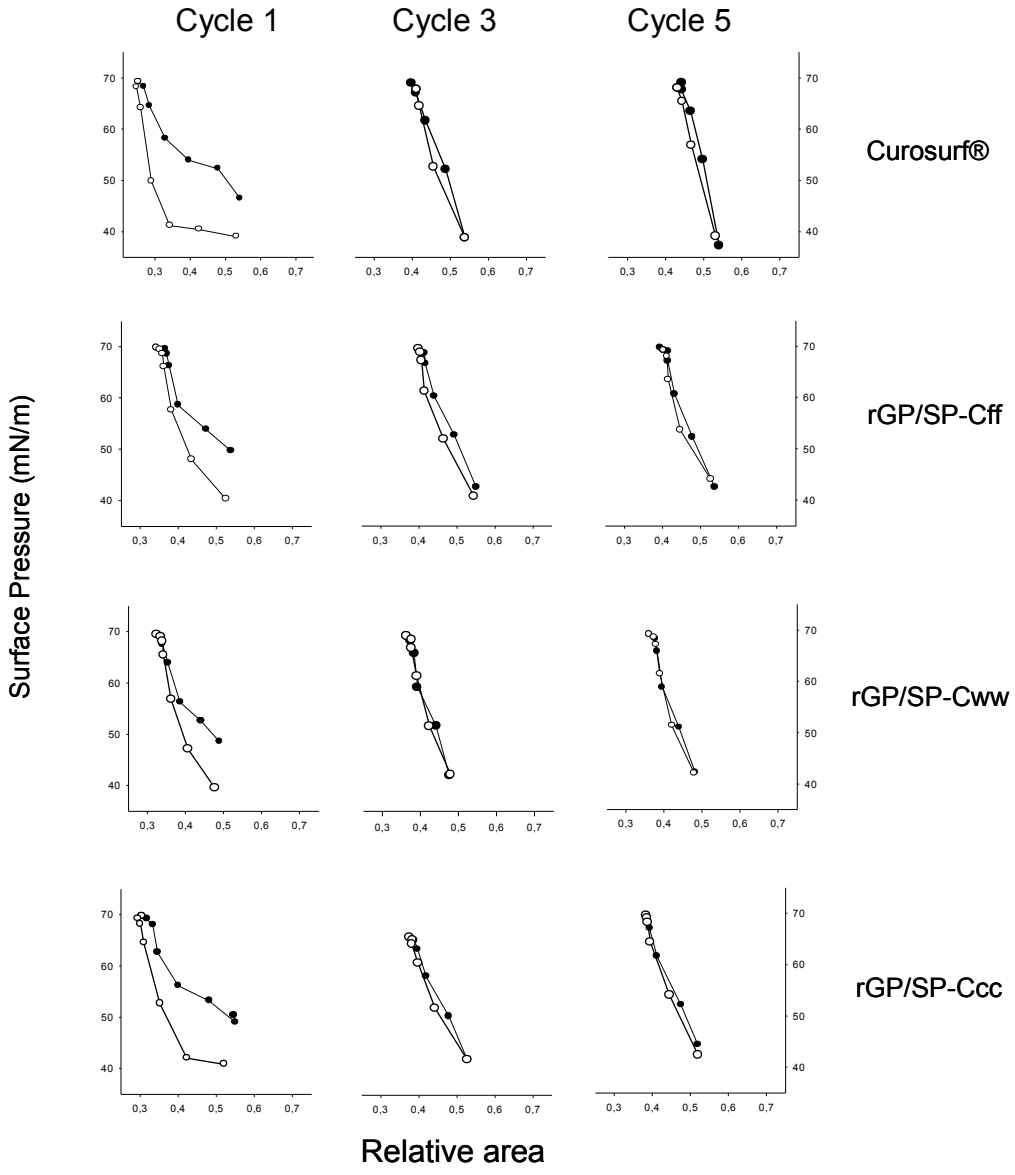

Figure 46. Effect of recombinant SP-C variants on the compression-expansion behaviour of lipid protein films under quasi-static conditions. Quasi-static compression (●) and expansion (○) isotherms of Curosurf ® and DPPC:POPG (68:31, w/w) suspensions containing 2%(w/w) rGP/SPCff, rGP/SP-Cww or rGP/SP-Ccc. Representative isotherms for the first , third and fifth compression-expansion cycles of three different experiments are presented. The concentration of surfactant material was 10mg/ml (see Materials and Methods).

The same samples were subsequently analysed under the more physiologically relevant conditions of dynamic cycling (20 cycles per minute) (figure 47). Films formed by either Curosurf® or recombinant protein/lipid suspensions could be repeatedly compressed for 20 cycles while maintaing the ability to reach maximum surface pressures. None of the samples showed hysteretic behaviour in the first cycle and the area reduction required to reach maximum pressure of around 70mN/m, were lower than during quasi-static cycling. 20% area reduction was required for Curosurf® while rGP/SP-Cff containing films required a little higher compression (24%). Area reduction of 25 and 27% was required for rGP/SP-Cww and rGP/SP-Ccc respectively. These values were almost equivalent to those of the twentieth cycle, meaning that the surface film had been previously refined or rearranged. There was no significant difference between the suspensions bearing the different recombinant variants in

terms of the level of required compression.

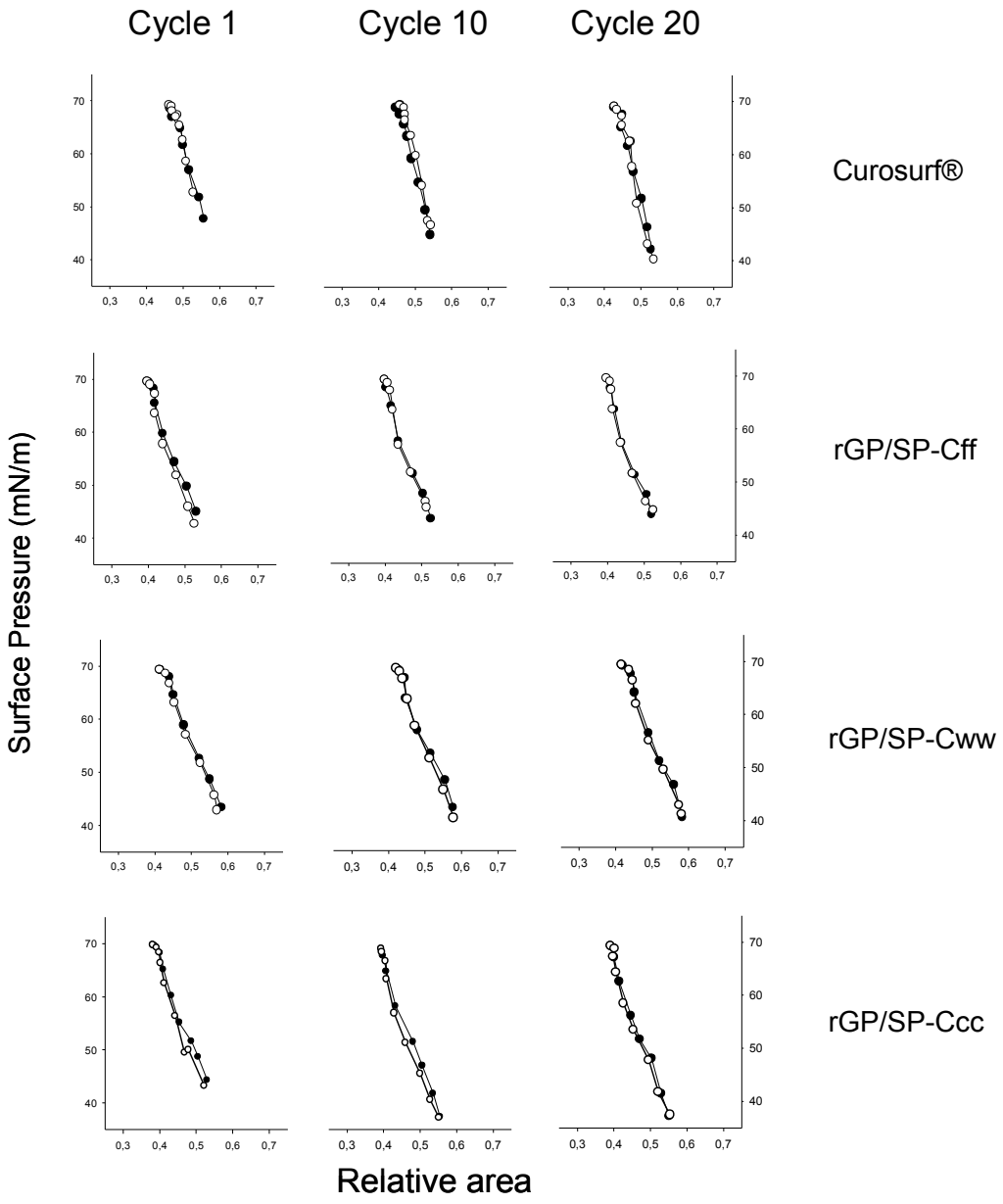

Figure 47. Effect of recombinant SP-C variants on the compression-expansion behaviour of lipid protein films under dynamic conditions. Dynamic compression (●) and expansion (○) isotherms of Curosurf ® and DPPC:POPG (68:31, w/w) suspensions containing 2%(w/w) rGP/SPCff, rGP/SP-Cww or rGP/SP-Ccc. Representative isotherms for the first , tenth and twentieth compression-expansion cycles of three different experiments are presented. The concentration of surfactant material was 10mg/ml (see Materials and Methods).

Table 6. %Area reduction necessary in order to reach minimum surface tension during compression-expansion cycles in a captive bubble formed in the presence of Curosurf® or recombinant protein /lipid (DPPC:POPG, 68:31 w/w) films.

%AREA COMPRESSION REQUIRED TO REACH MAXIMUM SURFACE PRESSURE						
	Quasi Static			Dynamic		
Cycle	**1**	**3**	**5**	**1**	**10**	**20**
Curosurf ®	45.2±11.5	24.6±1.9	20.3±3	17.5±5.1	16.9±3.1	19±3.8
rGP/SP-Cff	28.3±0.7	23.4±0	22±0	24±17	24±0.1	23.1±0.9
rGP/SP-Cww	36.1±3.3	26.3±3.8	27.7±3.8	25.8±4.7	25.2±2.4	27.2±2.2
rGP/SP-Ccc	44.9±1.1	31.2±3.5	28.1±3	27.8±0.8	26.4±3	28.5±0.8

4.3.7 Discussion

We have evaluated here the importance of aromatic residues at position 5 and 6 of the human sequence for surface activity of SP-C. In the previous chapter we have observed that Phe-bearing mutants exhibit a slightly faster adsorption into the air-water interface and have higher influence on PL interfacial organization than native SP-C. We hypothesised that this behaviour could be due to the presence of aromatic residues which might have a higher affinity toward the polar/non-polar interface. In order to test this possibility we produced new recombinant SP-C variants, one bearing tryptophane residues, with even higher affinity for membrane interfaces than phenylalanines, and another one bearing cysteines as the wild-type SP-C sequence.

We have successfully produced recombinant variants bearing tryptophanes or cysteines at positions 5 and 6 of the human sequence. Both proteins run as smeared bands on SDS gels like the variants having phenylalanines and like wild-type SP-C. CD spectra showed that all variants have predominantly helical structure with the rGP/SP-Cww and rGP/SP-Ccc having higher helical content than rGP/SP-Cff. The helical content of the new variants is similar to the helical content of rSP-Cff and higher than that of the wild-type protein. Previous studies have compared the structures of depalmitoylated and non-palmitoylated SP-C analogues to the palmitoylated protein with different outcomes. Non–palmitoylated synthetic peptides were shown to have lower helical content in a study by Johansson and colleagues (Johansson et al., 1995b). Crewels and colleagues showed that chemical palmitoylation of recombinant protein does not significantly alter the proportion of α helix (Crewels et al., 1993) while a higher helicity of recombinant proteins (bearing two cysteines) compared with the native protein was also reported (Shiffer et al., 1993). The lower helical content of the rGP/SP-Cff variant can

be attributed to a possible direct interaction of glycine or proline residues with phenylalanines at positions 5 and 6, which impedes stabilization of an additional helical turn as proposed by Luy and colleagues (Luy et al., 2004).

New variants are also able to form pure protein interfacial films on top of the aqueous subphase. Variant rGP/SP-Ccc produced similar compression-area isotherms as those obtained from previously studied recombinant SP-C forms. However, the rGP/SP-Cww variant showed an isotherm slightly shifted to larger areas, possibly due to stronger affinity of Trp for the interface leading to association/insertion of the N-terminal segment of the protein at pressures along the whole isotherm. The structure of pure protein films was analyzed at high resolution by AFM, at pressures close to maximal lateral packing, revealing organization of the protein as a homogeneous film containing closely packed shape-defined nano-sized structures of possible helical aggregates. Eventual differences found in film topography could be interpreted as the presence of structures with different heights, possibly as a result of different helical tilting or partial squeeze-out from the monolayer.

Comparison of interfacial activity of the new recombinant SP-C variants in the Wilhelmy balance as well as in the captive bubble surfactometer did not reveal differences in the surface behaviour of proteins bearing or not different aromatic groups, suggesting that the small differences previously observed when comparing native and recombinant proteins are not due to the presence of phenylalanines but to the intrinsically better activity of non-palmitoylated recombinant proteins or the more protective procedure of their production and purification compared to the isolation of native protein from animal lungs. The possibility that the protein preparations isolated from lung tissues could contain intrinsic surface activity inhibitors cannot be entirely discarded. We have compared the activity of samples containing rGP/SP-Cff, rGP/SP-Ccc or rGP/SP-Cww with the well-characterized clinical preparation Curosurf® under physiologically relevant conditions in a captive bubble surfactometer and all the three proteins conferred similarly good properties to DPPC:POPG (7:3) suspensions to produce efficient interfacial adsorption as well as surfactant respreading during successive compression/ expansion cycling.

4.4 LUNG FUNCTION IN PREMATURE RABBITS TREATED WITH RECOMBINANT HUMAN SP-C VARIANTS

After analysing the activity of recombinant sp-c variants *in vitro* we proceeded to studying their ability to restore lung function *in vivo*. As described in general introduction there are several animal models that are being used to test the effect of synthetic surfactants in vivo. Usually, synthetic preparations are tested first in small animal models (rabbits or rats) and posteriorly in bigger ones like lambs and baboons which allow monitorization of different physiological parameters for longer time. We tested the ability of lipid/protein preparations containing the recombinant proteins produced in this work to improve lung function in premature rabbit littermates and to assess the potential importance of specific amino acids at position 5 and 6 for *in vivo* performance of the protein. *In vitro* comparative studies only showed relatively small differences in the surface behaviour of SP-Cariants bearing Cys5Cys6, Phe5Phe6 or Trp5Trp6 (rGP/SP-Ccc, rGP/SP-Cff and rGP/SP-Cww). A lipid mixture of DPPC:POPG, 68:31 containing 2% (w/w) protein was used as a basis for all the *in vivo* experiments. This particular lipid mixture, similar to the canonical 7:3 mixture used throughout this thesis, was chosen because it was demonstrated as very effective in studies of SP-C 33 (sp-c synthetic analogue) based synthetic surfactant (Johansson et al., 2003). A protein/lipid ratio of 2% (w/w) was chosen based on the same study and previous studies treating premature rabbits with other recombinant sp-c versions (Davis et al., 1998). The lipid/protein mixture was suspended at a concentration of 80mg/ml (in 0.9% NaCl), which is the concentration of the natural surfactant used in clinical treatment of neonates.

This rabbit model is well established and faithfully mimics RDS ethiology in preterm babies. Preterm rabbit foetuses are obtained by hysterectomy at a gestational age of 27 days, with the term being 31 days. In each group of foetuses a negative control was used as tracheotomised but untreated foetus which actually confirmed the immaturity of the lungs in the whole group. Curosurf® (Chiesi Farmaceutici, Parma, Italy), a natural surfactant obtained by organic extraction of minced porcine lung tissue used in clinical therapy of preterm babies, was used as a positive control in each experiment. Lipids in the absence of proteins were not tested since it was demonstrated earlier that they have very low effect on restoration of breathing (Hawgood et al., 1996; Rider et al., 1993). Each group of foetuses consisted of 6-8 foetuses and were analysed simultaneously.

4.4.1 Tidal volumes and lung compliance

Hysterectomised foetuses received a dose of synthetic surfactant of 200mg/kg body weight and were subjected to ventilation during 35 minutes with different inflation pressure (see Materials and Methods). Tidal volume, which is the volume of gas inspired in the course of normal quiet breath was recorded at every 5 minutes intervals by means of pneumotachograph connected to the plethysmograph box where the foetuses were kept. At the same time points, compliance was calculated as the relationship between the volume change and the pressure applied to the lung to overcome elastic resistance. Lungs

with high elasticity have low compliance. Initially, the ventilation regime applied did not include positive end expiratory pressure (PEEP). Tidal volumes and compliance in lungs treated with the synthetic mixtures were similar to the ones treated with Curosurf® at inflation pressures of 25 and 20 cmH_2O. At 15 cmH_2O, however, the animals treated with the recombinant SP-C containing surfactants underwent collapse while the Curosurf®-treated ones stilled maintained low tidal volume. Littermates treated with recombinant proteins had lung gas volumes that were not different than the ones from untreated ones, and visually did not resemble to well aerated lungs as those treated with Curosurf®. This means that alveoli are unstable, expiring the total lung gas volume (tidal volume plus residual volume) and making the inspiration more difficult. Therefore these experiments were stopped and further on ventilation was applied including positive end expiratory pressure (PEEP).

PEEP imposes the maintenance of a pressure greater than atmospheric at the airway opening at the end of expiration during ventilation. The optimal value of PEEP was established previously in the laboratory where these experiments have been carried out and was set to 3 cmH_2O. After initial ventilatory pressure of 35 cmH_2O the inspiration pressure was lowered to 20 cmH_2O followed by 15, 10 and 7 cmH_2O. None of the animals treated with recombinant SP-C bearing surfactant underwent collapse even at the lowest pressures of 7 cmH_2O, and their tidal volumes were equivalent to those treated with natural surfactant (figure 48A). Figure 48B shows compliance values at the same time points. The fact that application of PEEP significantly improves the tidal volumes and gas volumes in littermates treated with synthetic surfactants is not a surprise since previous studies with either recombinant or synthetic protein analogues reported similar behaviour (Johansson et al., 2003; Hawgood et al., 1996; Davis et al., 1998).

A.

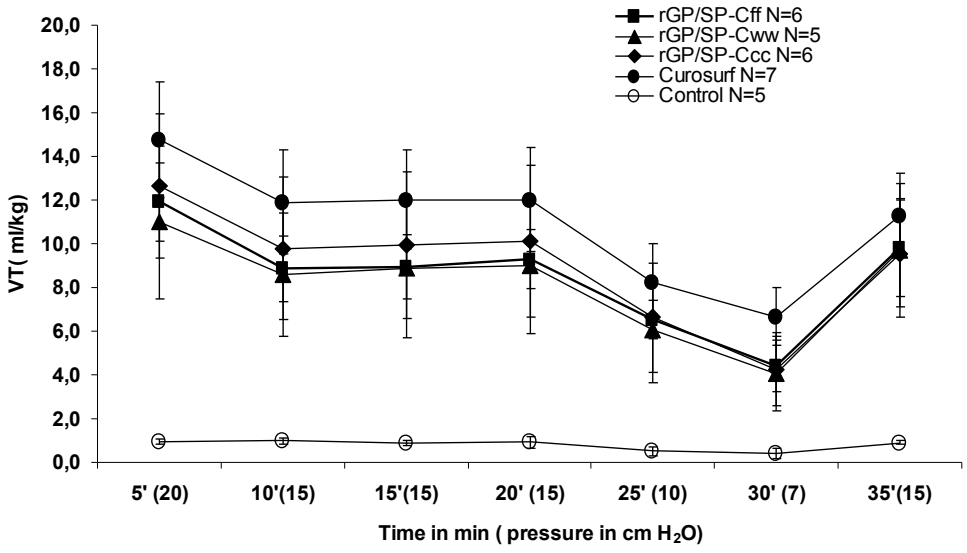

B.

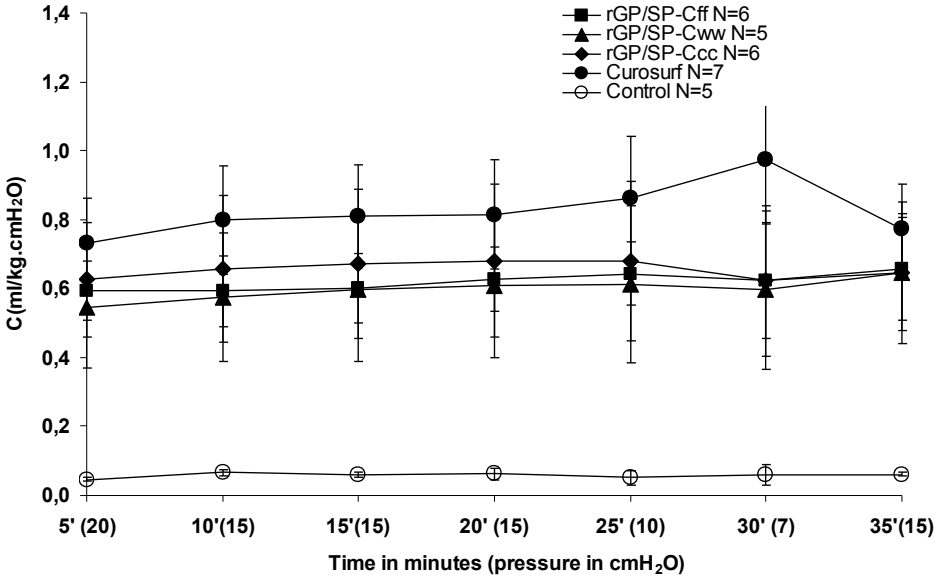

Figure 48. Effects of synthetic surfactants containing different recombinant SP-C versions on the respiratory parameters of preterm rabbits.
A.Tidal volumes (VT) during 35 min of ventilation in preterm newborn rabbits treated with lipid/protein suspensions containing 2% (w/w) rGP/SP-Cff (n=6), rGP/SP-Cww (n=5) or rGP/SP-Ccc (n=6) in DPPC:POPG (68:31) (all suspended in 0.9% NaCl at 80 mg/ml) or with Curosurf® (80 mg/ml, 2.5 ml/kg, *n* = 7), compared with nontreated littermates, (*n* = 5). Levels of statistical significance were calculated for final recordings: $^{**}P < 0.01$ vs. control; there was no significant difference between treatment with recombinant proteins and Curosurf. B. Compliance, calculated as tidal volume divided by inflation pressure.

Figure 48 shows that littermates treated with recombinant protein containing surfactant exhibit slightly lower tidal volume than the ones treated with Curosurf®, however the statistical analysis of this difference did not reveal any significance. The same figure shows that all recombinant variants exhibit virtually the same efficacy *in vivo*.

4.4.2 Lung gas volumes

After the 35 minutes ventilation, the lungs were ventilated for additional 5 minutes with N_2 in order to fill them with a non absorbing gas, the tracheas were then ligated and the lungs were excised and weighted (see Materials and Methods). Lungs obtained from littermates treated with recombinant SP-C bearing surfactant had gas volumes that were significantly higher than nontreated ones. Nontreated littermates had very low gas volumes (figure 49). There was no significant difference between the gas volumes generated by three recombinant proteins. Comparing to the Curosurf®, the suspensions bearing recombinant proteins rGP/SP-Ccc and rGP/SP-Cff had lower lung gas volumes (*P<0.05) and the ones with rGP-SP-Cww were lower with the significance *P<0.01. This finding suggests that recombinant proteins improve lung gas volumes in premature rabbits although not to the level of the natural preparation used in clinical therapy. The differences between natural and synthetic

preparations` effect were not exhibited at the morphological level. Aerated lungs are recognizable by their larger volume and white colour, while the non aerated ones stay reduced in size and red (figure 50).

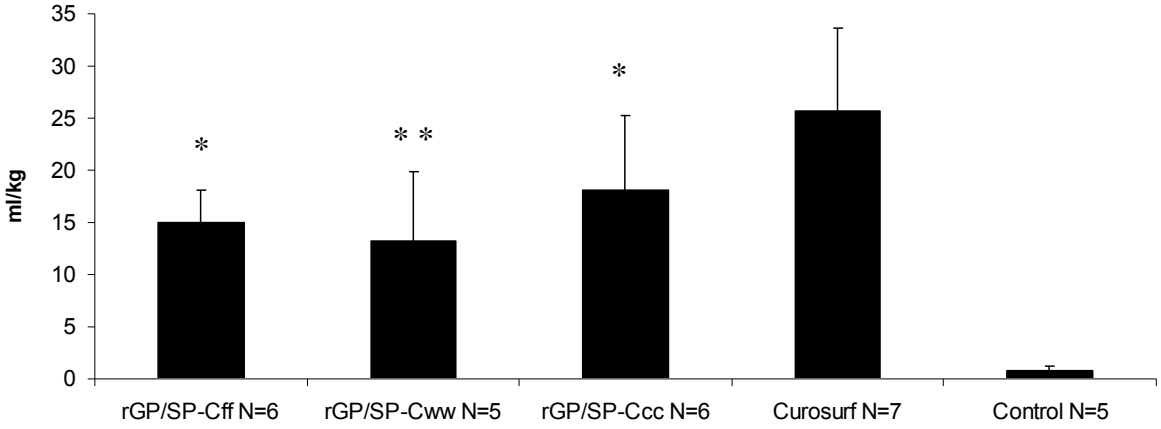

Figure 49. **Lung gas volumes**. Lung gas volumes measured upon 30 minutes ventilation after treatment with synthetic surfactant containing recombinant SP-Cs (rGP/SP-Ccc, rGP/SP-Cff or rGP/SP-Cww) or Curosurf compared with nontreated controls. All samples were significantly higher than control $^{**}P < 0.01$ vs. control. Levels of statistical significance between lungs treated with recombinant protein vs. Curosurf are indicated. rGP/SP-Cff and rGP/SP-Ccc $^{*}P < 0.05$ vs.Curosurf , rGP/SP-Cww $^{**}P <$ 0.01vs.Curosurf. There was no statistical difference between gas volumes in littermates treated with recombinant proteins.

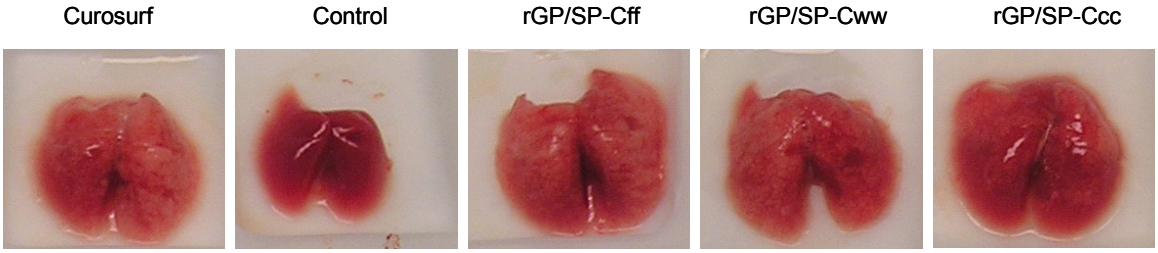

Figure 50. **Lung aeration**. Morphology of lungs treated with synthetic surfactants containing recombinant SP-Cs (rGP/SP-Ccc, rGP/SP-Cff or rGP/SP-Cww) or Curosurf® and compared with nontreated control lungs.

4.4.3 Discussion

The present work demonstrates that recombinant human SP-C analogues produced in bacteria combined with the simple lipid mixture DPPC:POPG (68:31) restore lung function in a rabbit premature

model comparably to the natural preparations currently used in clinical therapy of RDS. All three recombinant peptides exhibit similar performance *in vivo* independently of the amino acids present at position 5 and 6 of their sequence. These results are consistent with other previous studies. Takei and colleagues tested the activity of SP-C synthetic peptides of various lengths in the same rabbit preterm model and discovered that only 27 residues starting at position 6 of the wild type sequence and comprising the helical part of SP-C are essential for their activity (Takei et al., 1996a). In addition, the change of Cys by Ser at position 6 in such minimized peptide did not influence its performance. Even the complete substitution of the first ten amino acids with unrelated ones did not affect the in vivo performance of the synthetic SP-C analogue (Hawgood et al., 1996). Our recombinant protein/lipid mixtures could be suspended readily in solution at 80mg/ml, unlike some synthetic peptides that were difficult to suspend at concentrations higher that 20mg/ml (Nilsson et al., 1998). The initial experiment without the application of PEEP showed large tidal volumes combined with low lung gas volumes in animals receiving synthetic surfactant based on recombinant SP-C, indicating alveolar instability, which can be compensated by the application of PEEP. This is actually the main difference between the performance of all synthetic preparations produced so far and the natural ones (Hawgood et al., 1996; Davis et al., 1998). However PEEP is used routinely in clinical practice and therefore can compensate the difference in activity between synthetic and natural preparations.

The components of synthetic surfactant probably become recognized by endogenous surfactant recycling machinery and that could explain the observed prolonged effect of single surfactant treatment in clinical practice. The fate of the recombinant SP-C variants is unknown, although it is likely that it follows the fate of the native protein.

As discussed in general introduction, synthetic surfactants have to be simple mixtures of lipids and surfactant proteins SP-C and SP-B. Whether the presence of both proteins is required to achieve the best effect has not been resolved yet. The relative importance of SP-C versus SP-B and the existence of any synergistic activity of these two proteins were evaluated in several studies (Oosterlaken-Dijksterhuis et al., 1992; Wang et al., 1996b). In vitro studies of SP-B and SP-C suspended in various lipid components demonstrate a consistently more pronounced activity to promote interfacial adsorption by SP-B versus SP-C. A similar result was found under dynamic conditions in oscillating bubble surfactometer. No synergistic behaviour was observed in any of the assays, meaning that the addition of SP-C to SP-B containing mixtures did not improve the surface activity of preparations containing SP-B alone. The interpretation is that both hydrophobic proteins, although interacting extensively with phospholipids, act independently in the surfactant system. SP-B containing surfactants improved compliance better than the ones containing SP-C in studies *in vivo* (Rider et al., 1993). A conclusion may be drawn that single SP-B protein containing surfactants may be more effective than the ones containing only SP-C. This effect can however result from native SP-C instability and its tendency to aggregate under certain conditions. Therefore, inappropriate handling and storage conditions can lead to lower activity. In contrast to these comparative studies with native proteins, synthetic surfactants containing SP-C analogues have shown similar lung volumes and compliance responses to natural surfactant (Johansson et al., 2003; Hawgood et al., 1996; Davis et al., 1998). In addition, SP-B in its native form (79 amino acid dimeric protein) is not yet available for synthetic surfactant formulations, since it is too big to be synthesised chemically and structurally complex to be

obtained by a recombinant strategy. Therefore the most feasible possibility is to generate a peptide analogue which may not necessarily have superior activity to SP-C in synthetic surfactants.

Regarding the role of palmitoyl chains, two studies with SP-C based synthetic surfactants tested the contribution of palmitic acids to the protein performance *in vivo*. Hawgood and colleagues paltmitoylated chemically recombinant SP-C and compared its ability to restore lung function in preterm rabbits with the recombinant non-palmitoylated protein. No difference in activity was apparently detected (Hawgood et al., 1996). A study by Takei and colleagues compared the native palmitoylated protein with synthetic non palmitoylated analogues in synthetic surfactant mixtures and reached a similar conclusion (Takei et al., 1996a).

The drawbacks of the animal model used in the present study are the inability to measure gas exchange during the experiment and the short term nature of the protocol. These parameters could however be analysed in more detail in larger animals like lambs or baboons. The current models propose that SP-C has a major contribution in the long term stabilization of the respiratory surface, which by no means has been evaluated with reference to the potentials of the SP-C variants created here.

The dose of surfactant of 200mg/kg body weight presents a protein dose of 4mg/ kg for RDS. The current yield of recombinant SP-C optimized here, not higher than 0.5mg/l of culture, is not satisfactory for large scale production. However, with further optimization of expression and purification conditions and use of large fermentators the protein yield can be improved. We have already further optimized the thrombin cleavage conditions in order to reduce the amount of protease necessary.

In conclusion, this study demonstrates that the recombinant proteins produced can effectively fold into active molecules with the ability to facilitate respiration *in vivo*. The results presented here are encouraging for the development of new synthetic surfactant preparations based on recombinant SP-C forms. These experiments however have not shown particular advantages of synthetic preparations over the natural one. Further activities, such as resistance to inactivation by serum proteins (Seeger et al., 1992) or antibacterial defence activity have still to be evaluated as well as their potential utility to treat other respiratory pathologies or as complement with other proteins and lipids in other surfactants.

Finally, the production of new functional SP-C variants opens new perspectives for the analysis of structure-function determinants of SP-C, including the application of specialized biophysical techniques which require properly tailored (site-directed labelled with isotopes, spin or fluorescent probes, tags, etc) versions of the protein.

5 CONCLUSIONS

We have described a new procedure for production of recombinant human Surfactant Protein C from bacterial cultures, combining a common methodology for transmembrane protein expression and purification and SP-C extraction from pulmonary lavages.

We have expressed and purified recombinant non-acylated SP-C variants bearing phenylalanines, cysteines or tryptophanes at positions 5 and 6 of the protein sequence. All these variants exhibited high α helical content, a requisite for proteins activity. We have compared the surface behaviour of native and recombinant forms of SP-C under equilibrium and dynamic conditions. The surface spreading experiments demonstrate that all recombinant variants, independently of residues at positions 5 and 6, promote very rapid lipid film formation to reach equilibrium surface pressures at rates that were comparable or slightly higher than that promoted by native SP-C. Recombinant proteins arrange at the air-water interface occupying larger molecular area than native protein and exhibiting a plateau during protein film compression possibly reflecting a structural transition affecting the N-terminal segment of the protein. Pressure-area compression isotherms show that recombinant proteins interact with a higher number of lipid molecules than the native protein. Dynamical studies in a captive bubble surfactometer, under quasi-physiological compression-expansion regimes, demonstrate that recombinant proteins are able to stably maintain surface tension lowering during successive compression–expansion cycling. In the presence of recombinant proteins, a smaller area reduction is required to reach surface tensions close to zero than required for samples containing native SP-C. The three recombinant variants exhibited similar surface behaviour under dynamic cycling, sugesting that the surface activity of the protein was not particularly dependent on the interfacial affinity towards polar/non-polar interfaces with regard to the residues in positions 5 and 6. The better surface behaviour of bacterially produced SP-C compared to the native protein suggests that the expression and purification procedure could preserve at higher extent the active conformation of recombinant proteins compared with the SP-C activity extractable from lung tissue.

Finally, all recombinant SP-C variants restored lung function in preterm rabbits to a similar extent to Curosurf®, a clinical surfactant preparation from animal origin used today in clinical treatment to prevent and reverse neonatal RDS. However, recombinant SP-C-containing lipid/protein suspensions, but not Curosurf®, required application of positive end expiratory pressure (PEEP) during mechanical ventilation for optimal performance. However, this fact should not be considered as a disadvantage since PEEP is routinely used in clinical practice.

Taken together these results show that the described procedure to obtain recombinant SP-C is effective for production of SP-C variants with strong potential to be used as components of synthetic clinical formulations used to treat several respiratory pathologies, as well as a tool to obtain recombinant variants aimed for structure-function studies.

6 RESUMEN EN CASTELLANO

6.1 INTRODUCCION

El surfactante pulmonar es una mezcla de lípidos y proteínas imprescindible para la respiración en los animales pulmonados (Perez-Gil, 2002). Esta mezcla lípido-proteica está sintetizada por los neumocitos tipo II, células que junto con los neumocitos tipo I forman el epitelio alveolar. La superficie de este epitelio se encuentra humedecida, recubierta por una capa capilar de agua denominada *hipofase*. De esta manera en el alveolo existe una interfase aire–agua en la cual las moléculas que se disponen en la interfase generan un efecto físico denominado *tensión superficial*. Las moléculas que se localizan en la interfase, a diferencia de las moléculas en el interior del líquido, no están atraídas igualmente en todas las direcciones puesto que las moléculas de gas, en un estado mucho más diluido, ejercen comparativamente menor atracción que las moléculas de la subphase líquida. Esta atracción anisotrópica tiene como resultado una componente neta de fuerzas que tiende a reducir al mínimo el área que ocupa una superficie liquida, o en otras palabras, hace que la superficie sea resistente a su expansión de modo que se hace necesario aplicar una fuerza para ampliar dicha superficie. La razón de que la tensión superficial del líquido que reviste interiormente los alvéolos sea relativamente baja es la presencia de un sistema surfactante. Este complejo de lípidos y proteínas tiene como función principal reducir la tensión en los alvéolos facilitando el trabajo pulmonar y previniendo el colapso alveolar durante la espiración. La tensión superficial se describe a menudo en términos de presión superficial. La relación entre estos dos términos esta definida por la ecuación:

$$\pi=\gamma^{0}-\gamma$$

Donde γ^{0} es la tensión superficial del líquido puro mientras γ es la tensión en presencia de la película de surfactante en la superficie del líquido. La tensión, como la presión, viene expresada en unidades de mN/m.

Según la ley de Laplace la diferencia de presión entre el interior y el exterior de una burbuja es proporcional a la tensión superficial en la superficie de la burbuja e inversamente proporcional al radio de la misma. Así, si dos burbujas tienen una tensión superficial similar pero son de diferente tamaño, la presión en la burbuja pequeña será mayor que en la grande. Como resultado, si ambas burbujas están interconectadas, la burbuja pequeña se vaciará en la grande. La estructura de los alvéolos es análoga a una serie de burbujas conectadas entre si. Si la tensión superficial fuera similar en la superficie de los alvéolos de diferente tamaño, los pequeños tenderían a colapsarse vaciándose en los mayores. Normalmente eso no ocurre en el pulmón gracias a la presencia del surfactante, que disminuye la tensión superficial y la modifica en función del radio alveolar.

Las moléculas tensioactivas del surfactante pulmonar, como otras moléculas surfactantes, presentan una preferencia energética a localizarse en interfases debido a la presencia de regiones polares y no polares. Así, moléculas surfactantes son por ejemplo los detergentes o los fosfolipidos (PL). Las moléculas surfactantes tienden a organizarse en una monocapa o película monomolecular orientada en la interfase aire-agua. Esta película de surfactante siempre disminuye la tensión superficial de la interfase si se compara con la tensión que se genera en su ausencia. Así puede reducirse la tensión superficial hasta la tensión de equilibrio cuando toda la superficie está recubierta

por moléculas surfactante, mientras que la disminución por debajo de la tensión de equilibro solamente se consigue si se aplica una compresión lateral.

6.1.1 Composición del surfactante

La fracción lipídica del surfactante da cuenta de alrededor del 90% del peso de este complejo (Hawgood, 1997). El resto corresponde a la fracción proteica. El componente más abundante del surfactante pulmonar es la dipalmitilfosfatidilcolina (DPPC), que constituye alrededor del 40% del peso total. Además de las fosfatidilcolinas (PC) saturadas (entre las que se encuentra la DPPC) e insaturadas, que constituyen cerca del 80% de los PL del surfactante, están presentes en cantidades menores otros lípidos como el fosfatidilglicerol (PG), el fosfatidilinositol (PI), la fosfatidilserina (PS), la fosfatidiletanolamina (PE), la esfingomielima (SM) y el colesterol. Ninguno de estos lípidos por sí solo tiene capacidad para realizar la función del surfactante en los espacios alveolares del pulmón. Así, la DPPC se caracteriza especialmente por su capacidad para reducir al mínimo la tensión superficial de una interfase aire-líquido sometida a compresión, hasta valores cercanos a 0mN/m. Sin embargo, la DPPC tiene poca capacidad de adsorción interfacial lo que impide la eficiente formación de la película tensioactiva y además provocaría una marcada *histéresis* (pérdida importante de material desde la interfase después de cada compresión). Por el contrario, las películas de PL insaturados tienen una buena capacidad de adsorción lo que tiene como resultado una reextensión o reinserción de los lípidos expulsados de la interfase durante la compresión, pero no pueden producir los valores mínimos de tensión superficial que se requieren para estabilizar el pulmón.

La parte proteica del surfactante está constituida por cuatro proteínas denominadas SP-A, SP-B, SP-C y SP-D. Las proteínas SP-A y SP-D pertenecen a la familia de proteínas denominada colectinas que tienen un papel importante en la respuesta inmunológica innata. Las colectinas comparten una estructura común que incluye un dominio colagenoso en la parte N-terminal y un Dominio de Reconocimiento de Carbohidratos (CRD) en la parte C-terminal, y posee carácter oligomérico (figura 4). Estas proteínas participan en la defensa inmune mediante varios mecanismos: opsonización de los patógenos, lo que provoca una mejora en su fagocitosis de parte de células inmunogénicas; agregación de patógenos, lo que ayuda a su interacción con células inmunológicas; o estimulando la expresión de los receptores involucrados en el reconocimiento de patógenos. Por otro lado, las proteínas hidrofóbicas SP-B y SP-C son claves para desarrollar la función tensioactiva anteriormente descrita del surfactante pulmonar.

La SP-B, proteína altamente hidrofóbica de 8.7 kDa, se encuentra en forma de dímero. Su secuencia permite relacionarla con la familia de las saposinas (Munford et al., 1995). Se ha sugerido que la SP-B podría presentar también una estructura tridimensional similar a las saposinas, caracterizada por la presencia de 4 hélices anfipáticas (figura 6). Cuando la proteína interacciona con bicapas lipídicas estas hélices parecen orientarse de forma paralela al plano de la bicapa (Vandenbussche et al., 1992), de tal forma que los residuos polares interaccionan con las cabezas polares de fosfolípidos aniónicos. La SP-B induce la mezcla de PL entre vesículas y la pérdida de sus contenidos (Poulain et al., 1992). Además, la SP-B promueve muy eficientemente la adsorción de PL desde la subfase a la interfase aire-líquido (Oosterlaken-Dijksterhuis et al., 1992). Los estudios más

recientes indican que la SP-B favorece la formación de un reservorio asociado a la monocapa interfacial que facilita su reextensión durante la espiración (Taneva and Keough 1994b; Cruz et al., 2000).

La SP-C es una proteína extremadamente hidrofóbica de 35 aminoácidos (3.7kDa) con una secuencia muy conservada entre las diferentes especies. Su elevada hidrofobicidad se hace patente en el hecho de que se aísla junto con los lípidos durante la extracción orgánica de los lavados pulmonares a partir de los cuales se obtiene el surfactante. Estructuralmente se compone de una α hélice transmembranal en el extremo C-terminal, rica en residuos de valina, y un segmento N-terminal más hidrofílico sin una estructura secundaria definida (figura 9). Las posiciones 5 y 6 de la secuencia están ocupadas, en la mayoría de especies, por dos residuos de cisteína que se encuentran palmitoiladas. En la secuencia de la SP-C de algunos animales pulmonados como el perro y el visón sólo existe una cisteína en la posición 5, también palmitoilada, mientras que la posición 6 esta ocupada por un residuo de fenilalanina (figura 8). Aunque en menor medida que la SP-B, la SP-C también es capaz de promover la adsorción de PL para formar una película interfacial (Oosterlaken-Dijksterhuis et al, 1991). En este sentido, Taneva y colaboradores demostraron que la SP-C favorece la reextensión de los lípidos colapsados durante la compresión (espiración) (Taneva and Keough, 1994c). También se ha demostrado que la SP-C promueve la formación de las estructuras tridimensionales asociadas a la superficie en las altas presiones, lo que posteriormente, durante la expansión, ayuda a la reincorporación del material que fue previamente expulsado durante la compresión (es decir, durante la espiración) (Von Nahmen et al., 1997). Aparte de su elevada hidrofobicidad, la manipulación y caracterización estructural y biofísica de esta proteína se han visto dificultados por su tendencia a agregar de forma irreversible formando finalmente fibras amiloides. Esta inestabilidad estructural se debe probablemente a la abundancia de residuos de valina en el extremo C-terminal de la proteína, puesto que las valinas (al igual que otros residuos β-ramificados) presentan una elevada plasticidad estructural, favoreciendo la formación de láminas β en ambientes acuosos mientras que en entornos lipídicos tienen tendencia a la formación de α hélices.

6.1.2 Patologías asociadas con la disfunción del surfactante y su tratamiento

Las deficiencias en surfactante contribuyen a varias patologías respiratorias. La más común es el Síndrome del Distrés Respiratorio (RDS) de los neonatos prematuros originado en una deficiencia congénita del surfactante. Una vez conocida la causa de RDS, los experimentos en animales fueron cruciales para el establecimiento de un adecuado tratamiento con surfactante exógeno. Estudios realizados con modelos animales, como conejos prematuros o pulmones de ratas maduras a los que se elimina el surfactante mediante lavados pulmonares, demostraron que las proteínas SP-B y SP-C, junto con los lípidos, son críticas en el reestablecimiento del funcionamiento pulmonar. En los años 80 Fujiwara y colaboradores (Fujiwara et al., 1980) probaron las primeras terapias con surfactante exógeno en el tratamiento de niños con RDS En años posteriores se han patentado varios preparados para el tratamiento de SDR basados en surfactantes obtenidos de lavados o tejidos pulmonares porcinos o bovinos. bLES®, Curosurf®, Infasurf® , Surfactant TA® y Survanta®, son las marcas patentadas de surfactante que se están aplicando clínicamente para el tratamiento de los problemas

respiratorios de los niños prematuros. Aunque muy eficiente, el tratamiento con surfactantes naturales conlleva serios defectos susceptibles de mejora. Por un lado, los surfactantes animales varían en su composición y origen (lavado o tejido), lo que provoca diferencias en su actividad *in vitro* e *in vivo*. Además, su producción es costosa y las fuentes son limitadas. Y probablemente, el riesgo intrínseco de transmisión de patógenos es la principal razón para la búsqueda de nuevas formulaciones basadas en surfactantes sintéticos. Con este objetivo, diversas empresas farmacéuticas están trabajando en las últimas décadas en el desarrollo de una fórmula sintética que permita la utilización de surfactantes más controlados. Tanto en experimentos *in vivo* como *in vitro* se ha demostrado que además de lípidos las proteínas SP-B y SP-C deben estar presentes en los surfactantes sintéticos para desarrollar eficientemente su actividad tensioactiva. Sin embargo, la obtención de esas proteínas de forma sintética o recombinante no ha sido fácil. La SP-B es demasiado grande para su producción química y su plegamiento demasiado complejo para poderse producir de forma recombinante. Se han diseñado varios péptidos que mimetizan su papel y algunos están en fase de ensayos clínicos (Cochrane and Revak, 1991; Veldhuizen et al., 2000). Por lo que respecta a la SP-C se han realizado diversos esfuerzos para obtener análogos sintéticos de la proteína. Uno de los primeros ha sido su síntesis química, aunque en estas primeras aproximaciones la presencia de valinas dificultaba su plegamiento en α hélice (Johansson et al., 1995a), plegamiento que por otro lado resulta indispensable para su función tensioactiva. En trabajos posteriores, las valinas han sido reemplazadas por leucinas que favorecían la formación de α hélice (Nilsson et al., 1998; Johansson et al., 2003). Cabe mencionar que la SP-C también ha sido producida de forma recombinante y hoy en día forma parte de uno de los preparados farmacológicos, el denominado Venticute®. Esta molécula recombinante tiene, a diferencia de la proteína nativa, dos fenilalaninas en las posiciones 5 y 6. Los surfactantes basados en esta SP-C recombinante como único componente proteico demuestran una actividad parecida al surfactante autólogo *in vivo* (Hawgood et al., 1996). También favorece la respiración en modelos animales de síndrome de distrés respiratorio agudo (Hafner et al., 1998).

6.2 OBJETIVOS

El objetivo principal de esta Tesis ha sido la puesta a punto de un nuevo método de producción de la proteína SP-C mediante tecnología recombinante que podría servir como base para la obtención de nuevos surfactantes sintéticos, así como una herramienta inmejorable en la caracterización de determinantes estructura-función con el objetivo último de intentar mejorar las propiedades tensioactivas de la proteína.

Estos objetivos se han abordado en los siguientes apartados:

1. Diseño y optimización de la sobreexpresión recombinante y la estrategia de purificación de la secuencia de SP-C humana
   - I. Optimización de las condiciones de expresión en bacterias
   - II. Optimización del proceso de purificación

III. Confirmación de la identidad del péptido purificado y del mantenimiento de su estructura secundaria

2. Estudio de la actividad interfacial comparada con la proteína nativa aislada de lavados alveolares de pulmones de cerdo

I. Estudio comparativo de la adsorción interfacial de las proteínas recombinantes y la proteína nativa

II. Caracterización del comportamiento interfacial de las proteínas recombinantes en presencia y en ausencia de lípidos

3. Estudio de la importancia de los residuos que ocupan las posiciones 5 y 6 en la actividad de la proteína

I. Expresión y purificación de variantes recombinantes que contienen triptofanos o cisteinas en las posiciones 5 y 6

II. Estudio comparativo de la actividad interfacial de las nuevas variantes y de la proteína recombinante que presenta fenilalaninas en las posiciones 5 y 6

4. Estudios *in vivo* de la capacidad para restaurar la función respiratoria de las variantes recombinantes utilizadas como único componente proteico en preparaciones de surfactante sintético, utilizando un modelo de RDS en conejos prematuros.

6.3 MATERIALES Y METODOS

6.3.1 Expresión recombinante, purificación de la proteína SP-C y verificación de su estructura secundaria

Las construcciones generadas para la expresión en *E.coli*, mostradas en la figura 15, se introdujeron en la cepa BL21(DE3)pLys de *E.coli*. Los cultivos bacterianos crecieron en medio LB, hasta una OD=0.6 cuando se indujo la expresión con IPTG. La expresión se mantuvo durante 3 horas y después las células se centrifugaron y se procesaron según el esquema en la figura 16. La proteína de fusión se purificó mediante un equipo de FPLC ÄKTA (GE Healthcare) en presencia del detergente lauroylsarcosine. Después de eliminar el imidazol (necesario para la elución de las proteínas de la columna cargada con Ni^{2+}, a la que se une la proteína de fusión a través de la presencia de una cola de 6 residuos de histidina) mediante diálisis, se procedió a cortar la proteína de fusión para liberar la secuencia de SP-C (figura 20). El corte con trombina se hizo durante 16h a 21^0C en el tampón recomendado por la casa comercial, con agitación a 550rpm. Posteriormente se realizó una extracción orgánica según el protocolo de Bligh and Dyer (Bligh and Dyer, 1959). El extracto orgánico obtenido se aplicó a una columna cromatográfica de Sephadex LH-20 equilibrada con cloroformo/ metanol (2:1, v:v), se recogieron las fracciones y se midió su absorbancia a 240 y 280nm para detectar la presencia de la proteína. La presencia de la proteína en las fracciones del primer pico se confirmó mediante electroforesis en geles de SDS-PAGE al 16% y su tinción con Coomassi.

Los espectros de dicroísmo circular en el ultravioleta lejano (190-250nm) de la proteína purificada se obtuvieron en un espectropolarimetro Jasco J-810 utilizando una cubeta de cuarzo de 1mm de paso

óptico. Las proteínas se prepararon en forma de suspensiones micelares de LPC o suspensiones multilamelares de DPPC:POPG (7:3) en una proporción 1:5 (proteína/lípido, w:w).

6.3.2 Interacción con monocapas: actividad tensioactiva

El instrumento que permite medir la tensión o presión superficial de un líquido en función del área que ocupa su superficie se llama balanza de superficies.
La obtención de las suspensiones multilamelares que se requieren se llevó a cabo por el método de evaporación–rehidratación. Después de mezclar las soluciones orgánicas de lípido y proteína en un tubo de ensayo, se secó la mezcla bajo N_2 y en desecador durante 2h para eliminar las trazas de disolvente orgánico. La película de lípido y proteína se resuspendió posteriormente en tampón Tris 5mM, 150mM NaCl, pH 7, con agitación cada 10 minutos de 2min/14000rpm.

Para los experimentos de reextensión superficial se usó una balanza de tipo Wilhemy (Nima, Coventry, UK) con una minicubeta (15cm^2 superficie y 5ml de volumen de subfase) y usando como bandera papel Whatman $N^0$1 para medir la presión superficial. El material en forma de suspensiones multilamelares se deposita sobre la superficie del líquido y los cambios de presión superficial se monitorizan durante 15 minutos.

6.3.3 Isotermas presión-área

Las monocapas de lípidos en presencia o ausencia de las proteínas se sometieron a compresión dinámica registrándose los cambios de presión superficial.

Se partió de una solución madre de lípido 1 mg/ml en cloroformo/metanol (2:1, v/v) y de soluciones de proteína en la misma mezcla de disolventes. Para preparar las monocapas se llenó la cubeta de la balanza Wilhemy con 150ml de tampón Tris 5mM, 150mMNaCl pH 7, preparado con agua bidestilada y se depositó muy lentamente en la superficie entre 20 y 30 μl de muestra en disolventes orgánicos. Tras equilibrar la monocapa durante 10 minutos para permitir la evaporación del disolvente orgánico, se procedió a comprimir la superficie a 65cm^2/min (área máxima =200cm^2, área mínima =40cm^2) y registrar los cambios de presión superficial. En todos los casos la temperatura se mantuvo a 24 ±0.3 ^{0}C.

6.3.4 Microscopia de epifluorescencia

Para observar la organización de los lípidos en las películas interfaciales, se ha incluido una traza de la sonda fluorescente 1-palmitoil,2-nitrobenzoxadiol amino-dodecanoil (NBD)-fosfatidilcolina. La sonda se distribuye preferentemente en la fase expandida, de forma que cuando empiezan a formarse durante la compresión los dominios condensados de fosfolípido, que son estructuras altamente ordenadas en el plano de la interfase, el fluoróforo es excluido y los dominios condensados aparecen como manchas oscuras en un fondo luminoso constituido por la fase liquido-expandida. Las monocapas preparadas de esa manera se comprimieron a lo largo de la isoterma presión-área y mientras eran simultáneamente

transferidas a soportes de vidrio para formar películas de tipo Langmuir-Blodgett (LB). Los LB´s se secaron al aire y se observaron al microscopio, analizando las imágenes obtenidas con el programa SigmaScan Pro 5.

6.3.5 Surfactometro de burbuja cautiva

Este equipo permite obtener medidas de tensión superficial en la interfase de una burbuja encerrada en el interior de una suspensión de material surfactante. Las medidas de presión superficial se obtienen a partir del análisis de parámetros relacionados con la forma de la burbuja y la tensión superficial. La burbuja, bajo un soporte de agar, está sometida a compresión y expansión por variación de la presión externa y sus cambios de forma se monitorizan mediante una cámara de video. La cámara se llenó con la solución conteniendo 10% sacarosa y NaCl 150 mM, y a continuación se inyectó en la cámara 2μl de suspensión lípido/proteína (10 mg/ml, 2% proteína (w/w)). La temperatura se mantenía constante a 37^0C. Posteriormente la burbuja de aire se inyecto con una jeringa y se monitorizaron los cambios en la forma de la burbuja debidos a la adsorción del material a la interfase aire-líquido. Tras la adsorción de la muestra la cámara fue sellada y sometida a varios ciclos de compresión-expansión en condiciones quasi-estáticas y dinámicas. Las imágenes recogidas de cada experimento fueron analizadas en lo que se refiere a la forma y área de la burbuja para la obtención de los valores de presión superficial.

6.3.6 Experimentos *in vivo*

Las diferentes muestras de surfactante han sido ensayadas en 29 conejos prematuros, obtenidos por histerecotomía a los 27 días de gestación. Los animales fueron traqueotomizados y recibieron una dosis de 200mg/ml de surfactante sintético o comercial (Curosurf®), se pusieron en cámaras mantenidas a 37^0C y se sometieron a ventilación durante 35 minutos. La presión aplicada inicialmente fue de 35 cmH_2O durante un minuto para facilitar la distribución del surfactante. Luego la presión se bajó a 20 cmH_2O durante 5 minutos, a 15 cmH_2O durante 5 minutos, 5 minutos a 10 cmH_2O, 5 minutos a 7 cmH_2O y luego se subió a 15 cmH_2O. Los volúmenes ventilatorios residuales se registraron cada 5 minutos. Posteriormente los animales se ventilaron con N_2 y se calculó el volumen de gas en los pulmones como diferencia entre el volumen de pulmón (en mL) y el peso (en g), asumiendo que la densidad de tejido es la misma que la del agua.

6.4 EXPRESION Y PURIFICACION DE LA PROTEINA RECOMBINANTE SP-C

Como se ha mencionado anteriormente, las principales limitaciones para la sobreexpresión de SP-C recombinante en procariotas han sido su elevada hidrofobicidad, la palmitoilación de los residuos Cys-5 y Cys-6, y su tendencia a la formación de agregados amiloides en ausencia de lípidos. En el presente trabajo la primera de estas tres limitaciones se ha superado sobreexpresando la SP-C como una proteína quimérica fusionada a la nucleasa A de *Staphylococcus aureus* (SN) (Laage and Langosch,

2001) (figura 15). La SN es una proteína que previamente se había utilizado con éxito para la sobreexpresión de otros péptidos transmembranales debido a su elevada hidrofilia, probablemente asociada a la abundancia de residuos básicos en su superficie, lo que impide la agregación de la proteína. Considerando que en los sistemas procarióticos no se puede conseguir la palmitoilación de los residuos de cisteína, las cisteínas de la secuencia nativa han sido reemplazadas por fenilalaninas. Este cambio se ha realizado por varias razones: i) para prevenir la posible oligomerización a través de las cisteínas libres, ii) se eligió la fenilalanina para la sustitución porque está presente en lugar de la cisteína palmitoilada de la posición 6 en algunas especies (perro y el visón), lo que indica que este aminoácido puede ser un sustituto adecuado utilizado en algunas variantes naturales de la proteína, iii) una forma recombinante de SP-C con los cambios $C_5C_6 \rightarrow F_5F_6$ ya ha mostrado ser eficaz en ensayos *in vivo*. Finalmente, la tendencia de la proteína a la agregación en medios acuosos ha sido superada manteniendo la proteína en medios lípido-miméticos durante todo el proceso de purificación, para lo cual se ha realizado la extracción y la digestión de la proteína quimérica en presencia del detergente lauril-sarcosine y posteriormente se han realizado las purificaciones de las distintas variantes de la proteína mediante técnicas cromatográficas en presencia de disolventes orgánicos y, eventualmente, de fosfolípidos.

6.4.1 Sobreexpresión y purificación de la SP-C

La secuencia que codifica la proteína de fusión SN/SP-C contiene una extensión de 6 histidinas (para facilitar su aislamiento por cromatografía de afinidad) en el extremo N-terminal y una diana de digestión para la proteasa trombina con objeto de eliminar el módulo SN. Esta construcción ha sido clonada en el vector pET11 y sobreexpresada en células BL21(DE3)pLys mediante la inducción con IPTG durante 3 horas. Las células se han recogido mediante centrifugación, sometido a 3 rondas de congelación y descongelación y se han disuelto en 1% lauroil-sarcosine en TBS (figura 16). De esa manera la proteína de fusión se solubiliza y puede enriquecerse mediante cromatografía de afinidad utilizando columnas HiTrap® con resina cargada con Ni^{2+} en un cromatógrafo FPLC ÄKTA (GE Healthcare). En la figura 17a se muestra a modo de ejemplo un gel típico SDS-PAGE cargado con alícuotas tomadas en cada paso de este proceso inicial de purificación, mientras en la figura 17b se muestra la relación entre la proteína de fusión soluble y la fracción en cuerpos de inclusión. El perfil de elución de la cromatografía de afinidad de la proteína quimérica se muestra en la figura 18.

6.4.2 Digestión con trombina

Para separar la SN de la SP-C se ha procedido al corte de la proteína de fusión mediante tratamiento con trombina. En la figura 20 se presenta un gel SDS-PAGE cargado con la proteína quimérica antes y después de la digestión. Como puede observarse en esta figura la variante rSP-C presenta una menor susceptibilidad al corte con la proteasa por lo que en sus digestiones se utiliza una mayor cantidad de trombina.

6.4.3 Extracción orgánica

Una vez digerida la proteína quimérica, para separar la SP-C del resto de los componentes de la reacción de digestión con trombina se ha hecho uso de la naturaleza altamente hidrofóbica de la proteína. Así, al añadir cloroformo/metanol al producto de la reacción de digestión con trombina, la SP-C recombinante particiona a la fase orgánica mientras que el resto de las proteínas (trombina, SN y demás componentes que se hayan podido copurificar en la cromatografía de afinidad) permanecen en la fase acuosa. Como puede observarse en la figura 21, las alícuotas de extractos orgánicos cargadas en el gel SDS-PAGE evidencian la presencia mayoritaria de la proteína SP-C, dado que la única banda que puede observarse en una tinción con Coomassie presenta una movilidad electroforética indistinguible de la que muestra la proteína nativa aislada de pulmones de cerdo.

6.4.4 Cromatografía de exclusión molecular e identificación mediante espectrometría de masas de las proteínas purificadas

El último paso de purificación utilizado en el presente protocolo es una cromatografía de exclusión molecular para eliminar los contaminantes que se hayan podido copurificar junto con la SP-C durante la extracción orgánica. Para ello se usó la resina Sephadex LH 20 (GE Healthcare), resistente a disolventes orgánicos. Puesto que la extracción orgánica genera grandes volúmenes de la muestra, la proteína disuelta en disolventes orgánicos debió ser concentrada unas 100 veces para poder ser aplicada en la cromatografía de exclusión. La concentración de las muestras se realizó en presencia de lípidos (PC de yema de huevo) para evitar su posible agregación debida a la presencia de trazas de agua en los disolventes orgánicos. El perfil de elución de esta cromatografía se muestra en la figura 22a. Para identificar los picos se procedió a cargar pequeñas alícuotas de los dos picos en un gel SDS-PAGE (figura 22b).

Para comprobar su identidad las proteínas recombinantes purificadas fueron analizadas mediante espectrometría de masas. La figura 23 muestra los espectrogramas de masas de rGP/SP-Cff y rSP-Cff, que presentan un único pico de masa molecular coincidente con la masa molecular esperada en ambos casos.

6.4.5 Determinación de la estructura secundaria

Como paso inicial para verificar que la estructura nativa de las proteínas recombinantes había sido preservada al finalizar el proceso de purificación, se caracterizó la estructura secundaria de las proteínas mediante espectroscopía de dicroísmo circular. Los espectros de dicroismo circular en el ultravioleta lejano de la SP-C nativa y las dos variantes recombinantes, en micelas de LPC o en vesículas de DPPC:POPG (7:3, w/w), se presentan en la figura 24. Como puede observarse los espectros de ambas variantes recombinantes presentan al igual que la proteína nativa, dos mínimos de

elipticidad aproximadamente a 208 y 222nm, característicos de proteínas con estructura secundaria mayoritariamente en α hélice. Para obtener un análisis detallado de los espectros, los espectros se analizaron usando el algoritmo CDPro (Sreerama et al., 2000; Sreerama et al., 2004). Usando como referencia varias proteínas de membrana se calculó la contribución de los diferentes elementos de estructura secundaria en las proteínas recombinantes (tabla 1).

6.4.6 Discusión

La alta hidrofobicidad y la tendencia de la proteína SP-C a formar agregados dificulta su manipulación y obtención tanto de forma recombinante como mediante síntesis química.
En este primer capitulo se describe un protocolo de obtención de la proteína SP-C recombinante que está basado en una estrategia de obtención de proteínas transmembrana en bacterias y en las extracciones orgánicas empleadas en el aislamiento de la SP-C nativa de los lavados pulmonares. Este método resultó altamente eficaz en la preservación de la estructura helicoidal de la proteína, la principal característica de su actividad. Comparando el procedimiento aquí descrito con el procedimiento de Hawgood y colaboradores (Hawgood et al., 1996), que emplean cloranfenicolacetiltransferasa (CAT) como proteína de fusión, la estrategia que utiliza la fusión a la SN combinada con la presencia de detergentes evita la acumulación de la proteína en cuerpos de inclusión, es más rápida y probablemente mantiene de forma más eficaz la estructura secundaria de la proteína. Además, el protocolo de purificación desarrollado en el presente trabajo se podría aplicar para la purificación de otras proteínas altamente hidrofóbicas.

6.5 COMPORTAMIENTO INTERFACIAL DE LAS FORMAS RECOMBINANTES DE LA SP-C

6.5.1 Isotermas π-t de esparcimiento interfacial

Como ya se ha descrito previamente (Oosterlaken-Dijksterhuis et al., 1991) la SP-C tiene la capacidad de facilitar la transferencia de PL desde la fase acuosa a la interfase aire-liquido. En este capitulo se ha ensayado la capacidad de las dos variantes recombinantes, rSP-Cff y rGP/SP-Cff, de promover la formación de películas interfaciales desde suspensiones multilamelares (MLV). Esa capacidad se ensayó con proporciones de proteína crecientes (2%, 5% y 10%, proteína/lípido peso/peso) y en presencia de distintas mezclas lipídicas. La figura 25 demuestra que tanto las proteínas recombinantes como la proteína nativa tienen la capacidad de promover un aumento muy rápido de la presión superficial. Se puede observar que tanto la SP-C nativa como las variantes recombinante tienen mayor actividad en las combinaciones lipidicas que se parecen más a la composición del surfactante pulmonar. La diferencia entre la SP-C nativa y las variantes recombinantes está en la presión máxima que alcanzan suspensiones lipídicas conteniendo 5 o 10% de la proteína. Esas diferencias pueden tener origen en el distinto grado de purificación de las dos proteínas, o en la presencia de varias

isoformas de la proteína (Gustafsson et al., 1997).

6.5.2 Isotermas de compresión de películas de proteína pura

Como ya se ha descrito en estudios previos, la SP-C, siendo anfipática, tiene la capacidad de disponerse en la interfase y formar por sí misma una monocapa. Sabiendo el número de moléculas de proteína que se depositan en la superficie acuosa de la balanza Wilhemy, es posible calcular el área que ocupa cada molécula de proteína a cada valor concreto de presión superficial. Las isotermas de SP-C nativa y de las proteínas recombinates están representadas en la figura 26. Hay dos diferencias claras entre la proteína nativa y las dos formas recombinates. Primero, las proteínas recombinantes ocupan una mayor área en todas las presiones superficiales, y segundo, las dos proteínas dan lugar a un plateau en la isoterma cuando la presión alcanza 6mN/m, mientras la rSP-Cff también muestra uno a 9mN/m. El aumento del área se pude explicar a partir de una contaminación de las proteínas recombinantes o de una distinta disposición de las proteínas recombinantes y de la proteína nativa con respecto al plano de la interfase. Hasta el momento no se ha identificado ninguna molécula contaminante en las preparaciones de proteínas recombinantes (como por ejemplo el lípido PC, LPS o el detergente lauroilsarcosine). La diferencia en la disposición en la interfase podría ser provocada por la ausencia de las cadenas de palmítico en las proteínas recombinantes, las cuales podrían ser responsables de inducir una posición de la proteína nativa más perpendicular a la interfase (por ejemplo por su interacción con la hélice), mientras el segmento N-terminal libre de palmitoilación en las proteínas recombinantes ocuparía una mayor área en la interfase. La presencia de los plateaus o mesetas en las isotermas se podrían explicar como consecuencia de una transición progresiva en la inclinación de la hélice mientras el área que ocupa el segmento N terminal se mantiene constante.

6.5.3 Isotermas de compresión de películas proteína/lípido

Las isotermas de compresión reflejan la existencia de diferentes estados físicos o fases bidimensionales en las que se pueden encontrar las películas interfaciales. Para comprobar el efecto que la SP-C y las formas recombinantes tienen en la organización de los lípidos en la interfase se obtuvieron las isotermas de compresión de monocapas de lípidos en presencia y en ausencia de las proteínas. La figura 28 demuestra que la presencia de cantidades crecientes de las proteínas en la monocapa interfacial da lugar a una progresiva expansión de la isoterma de compresión. Este aumento del área aparente ocupada por el fosfolipido indica que la proteína ocupa también parte de la superficie interfacial. Cuando la monocapa se comprime hasta una determinada presión superficial, las isotermas de lípido y lípido/proteína tienden a converger, lo que se interpreta como una progresiva exclusión de la proteína. El efecto de las proteínas se ha observado en monocapas de distintas composiciones lipídicas y en todas las proteínas recombinantes tienen un efecto potenciado comparando con la proteína nativa. Las formas rSP-Cff y rGP/SP-Cff incrementan más el área a presiones por debajo de la presión de exclusión de las proteínas (lo que es de esperar puesto que las proteínas recombinantes ocupan una mayor área). A las presiones por encima de la presión de expulsión de las proteínas solas,

las proteínas recombinantes provocan una mayor pérdida de área indicando que la expulsión de las proteínas recombinantes está acompañada por un mayor número de moléculas lipídicas. La figura 30 presenta el análisis cuantitativo del efecto de las proteínas en las monocapas lipoproteicas sometidas a compresión. La mayor capacidad de las proteínas recombinantes para promover la expulsión de los lípidos podría estar relacionada con la mayor afinidad de su segmento N-terminal para interaccionar con PL.

6.5.4 Efecto de las proteínas en la estabilidad de monocapas comprimidas

Las monocapas de DPPC o DPPC:DPPG, en ausencia o presencia de 2% de la proteína SP-C nativa o de las formas recombinantes fueron comprimidas hasta altas presiones. Llegado este punto se monitorizó durante 15 minutos el descenso espontáneo de la presión superficial que se produce hacia la presión de equilibrio. La figura 31 muestra como la SP-C nativa acelera el proceso de relajación, lo que supone un efecto desestabilizador de las monocapas comprimidas. El efecto es algo mayor en el caso de monocapas DPPC:DPPG, lo que se podría explicar con una mayor interacción lípido/proteína, posiblemente con la contribución de interacciones electrostáticas.

Las proteínas recombinantes mostraron un comportamiento parecido e incluso más pronunciado, relajando la monocapa con una mayor velocidad. Este mayor efecto de las proteínas recombinantes es consistente con su mayor capacidad para expulsar lípidos de la interfase a partir de los estados comprimidos de las monocapas lípido/proteína.

6.5.5 Organización de las películas lípido/proteína

Los efectos de las proteínas en el empaquetamiento y orden de las moléculas lipídicas en las películas interfaciales pueden observarse directamente mediante microscopía de epifluorescencia. Para ello se prepararon monocapas de DPPC o DPPC:DPPG conteniendo 1% (mol/mol) de la sonda fluorescente NDB-PC. Este fosfolípido permite observar la distribución de fases condensadas y expandidas en monocapas sometidas a compresión dinámica y analizar el efecto de las proteínas en su distribución.
En la figura 32 se presentan imágenes de epifluorescencia de monocapas de DPPC tomadas a distintas presiones en ausencia y en presencia de 5% de la proteína SP-C, nativa o recombinante. La presencia de todas las proteínas causa una reducción importante del tamaño de los dominios condensados.

6.5.6 Actividad de las proteínas recombinantes en el surfactómetro de burbuja cautiva

El efecto de las proteínas recombinantes sobre isotermas π-A de películas lipoproteicas ha sido analizado también en un surfactómetro de burbuja cautiva (CBS), lo que permite el análisis del comportamiento tensioactivo de las proteínas en condiciones más próximas a las fisiológicas (37^0C, 100% humedad y velocidades de compresión y expansión comparables a las fisiológicas). Las figuras 35 y 36 muestran las isotermas π-A obtenidas a partir de burbujas formadas en presencia de

suspensiones de 2% proteína en DPPC:POPG (68:31, p/p). La presencia de solo un 2% (w/w) de la proteína en la mezcla lipídica permite alcanzar una presión superficial cercana a 70mN/m con una compresión del área de ~23% en el último ciclo de compresiones cuasi-estáticas (compresión muy lenta que permite el empaquetamiento óptimo de las moléculas en la interfase para cada nueva presión, y da por tanto información acerca de la interacción lípido/proteína en condiciones muy próximas al equilibrio) y en compresiones dinámicas.

6.5.7 Discusión

Este capítulo describe el efecto de las proteínas recombinantes sobre el comportamiento de las películas interfaciales sometidas a compresión-expansión, comparado con el efecto de la proteína nativa. La adsorción interfacial, las isotermas de compresión y relajación, y la actividad en el modelo de burbuja cautiva sugieren que las proteínas recombinantes tienen una actividad superficial equivalente o superior a la de la proteína nativa. Esta observación lleva a concluir que las cadenas de palmítico acopladas covalentemente a la proteína nativa no son indispensables para la función de la proteína *in vitro* o bien que las fenilalaninas sustituyen su función. En cualquier caso los resultados presentados indican que las proteínas recombinantes se podrían usar como análogos de la SP-C nativa en la producción de preparaciones de surfactante sintético de potencial utilidad terapéutica.

6.6 EFECTO DE LA PRESENCIA DE RESIDUOS AROMÁTICOS EN EL COMPORTAMIENTO INTERFACIAL DE LA SP-C

6.6.1 Expresión de nuevas proteínas recombinantes

Para comprobar la importancia de las fenilalaninas en las posiciones 5 y 6 de la SP-C recombinante, se produjeron nuevas variantes de la proteína SP-C (figura 37), que poseen C_5C_6 (rGP/SP-Ccc) o W_5W_6 (rGP/SP-Cww). El objetivo era comprobar hasta qué punto una mayor actividad de la proteína podía estar definida por una mayor afinidad del segmento N-terminal hacia las interfases. Según esta hipótesis la variante con dos triptófanos podría tener una actividad aún mayor que la forma de SP-C que posee fenilalaninas, mientras que la que posee dos cisteínas podría mostrar una actividad inferior (Wimley and White, 1996). La dos nuevas variantes se expresaron y purificaron de manera análoga a las dos primeras variantes (rSP-Cff y rGP/SP-Cff) y resultaban poseer igualmente una conformación mayoritaria en α hélice (Figura 37c, Tabla 4).

6.6.2 Isotermas π-t de esparcimiento interfacial

Las cinéticas de adsorción interfacial se registraron en la balanza Wilhemy mediante depósito de

suspensiones lípido/ proteína conteniendo cantidades crecientes de las proteínas recombinantes rGP/SP-Cff, rGP/SP-Ccc, o rGP/SP-Cww en bicapas de DPPC:POPG(7:3) o DPPC:POPC:POPG:Colesterol (5:2.5:1.5:1, w/w/w/w) (figura 38). Se observó que en presencia de las nuevas variantes recombinantes la presión de equilibrio se alcanzaba con una cinética similar a la observada anteriormente para la forma rGP/SP-Cff y que las presiones alcanzadas en presencia de las tres proteínas eran similares. La adsorción se midió también en un surfactómetro de burbuja cautiva (CBS) que permite condiciones más parecidas a las fisiológicas (37^0C y 100% de humedad). La presión superficial de la burbuja se registró durante 5 minutos y está representada en la figura 39. En el CBS la formación de la película interfacial ocurría prácticamente en un par de segundos en presencia de las proteínas recombinates, al igual que en presencia del Curosurf®.

6.6.3 Isotermas de compresión de las proteínas

Se ensayó la capacidad de las nuevas variantes recombinantes para modular el comportamiento de películas lipoproteicas interfaciales en la interfase de la balanza Wilhemy, comparando las isotermas de compresión obtenidas en presencia de la proteína nativa y con las obtenidas en películas conteniendo las variantes rSP-Cff, rGP/SP-Cww o rGP/SP-Cff. Estas isotermas se muestran en la figura 40. La isoterma en presencia de rGP/SP-Ccc se parecía a la isoterma con rSP-Cff en cuanto al área a lo largo de toda la isoterma y a la presencia del plateau a alrededor de 6mN/m. Las películas en presencia de rGP/SP-Cww muestran un área mayor comparada con las de todas las demás proteínas a lo largo de toda la isoterma y además no presenta la existencia del plateau. La posible explicación de esa diferencia es que los triptófanos proporcionan una mayor afinidad hacia la interfase y a diferencia de lo que ocurre con las demás proteínas, mantienen el segmento N-terminal asociado con la superficie a presiones superficiales que inducen la exclusión del segmento N-terminal de las demás formas recombinantes.

6.6.4 Isotermas de compresión proteína/lípido

En la figura 42 se presentan isotermas de compresión de películas lipídicas o lipoproteicas en presencia de cantidades crecientes de las proteínas recombinantes rGP/SP-Cff, rGP/SP-Ccc, o rGP/SP-Cww, representando el área aparente ocupada por las moléculas de fosfolipido frente a la presión superficial. La presencia de proporciones crecientes de las proteínas da lugar a una progresiva expansión de la isoterma, una prueba de que la proteína ocupa también parte de la superficie interfacial. Como ya se ha visto antes con rSP-Cff y rGP/SP-Cff (figura 28, capitulo 5), cuando la monocapa se comprime hasta una determinada presión superficial, las isotermas de lípido y las de lípido/proteína tienden a converger lo que se interpreta como una progresiva exclusión de la proteína. El análisis cuantitativo del área excluida como consecuencia de la expulsión de la proteína indica que no hay diferencias significativas entre las tres variantes recombinantes en cuanto a los lípidos que se asocian y resultan expulsados de la interfase acompañando a las proteínas (figura 43).

6.6.5 Actividad de las proteínas en condiciones dinámicas

El efecto de las proteínas recombinantes rGP/SP-Cff, rGP/SP-Ccc, y rGP/SP-Cww sobre isotermas π-A se ha analizado también en el CBS. La figura 46 presenta las isotermas π-A obtenidas a partir de burbujas formadas en suspensiones de DPPC:POPG (68:31) conteniendo las diferentes proteínas y sometidas a ciclos de compresión–expansión cuasi–estática. Estas condiciones implican una compresión lenta permitiendo el empaquetamiento óptimo de las moléculas en la interfase en cada nueva presión. La figura demuestra que durante los 5 ciclos se alcanzaba la presión máxima, con una progresiva reducción del ara necesaria para alcanzar la máxima presión (Tabla 6), lo que se explica por una reorganización de la interfase formando las estructuras 3-dimensionales que promueven la reinserción del material excluido durante la compresión.

A continuación la burbuja de aire se sometió a ciclos dinámicos (20 ciclos de compresión-expansión por minuto), fisiológicamente mas relevantes. Los surfactantes conteniendo las proteínas recombinantes, al igual que la preparación clínica Curosurf®, alcanzaban la máxima presión durante 20 ciclos con una reducción del área de alrededor de 20 % en todos los ciclos.

6.7 FUNCIONALIDAD RESPIRATORIA EN CONEJOS PREMATUROS TRATADOS CON LAS VARIANTES RECOMBINANTES DE LA SP-C

El objetivo en este capítulo ha sido ensayar la capacidad de las preparaciones lípido/proteína que contienen las proteínas recombinantes producidas en ese trabajo, para mejorar el funcionamiento pulmonar en conejos prematuros, naturalmente deficientes en surfactante. La composición de lípidos que se ha usado ha sido DPPC:POPG, 68:31, una mezcla previamente demostrada como muy eficiente en el tratamiento de modelos animales con SP-C 33, un análogo sintético de la SP-C (Johansson et al., 2003). La proporción de las proteínas recombinantes usada ha sido de 2%, basado en el mismo estudio y en otros estudios con las proteínas recombinantes (Davis et al., 1998). Después de obtener los fetos prematuros mediante histerectomía, se hizo una traqueotomía para depositar el material surfactante. Los fetos traqueotomizados pero sin ningún tratamiento fueron considerados como control negativo. Los fetos tratados con Curosurf®, el surfactante comercial que se está aplicando de manera habitual en tratamientos clínicos, se utilizaron como control positivo. Los fetos tratados con una dosis de 200 mg/ml de surfactante fueron sido sometidos a 35 minutos de ventilación con distintas presiones. Cada 5 minutos se registró el volumen residual, que es el volumen de gas inspirado durante la respiración normal. Como se puede ver en la figura 48 este volumen era, en los animales tratados con las preparaciones que contenían proteínas recombinantes, ligeramente menor que en los tratados con Curosurf® (aunque la diferencia no tenía significación estadística) y era significamente mayor que en los animales control no tratadas. Es importante destacar que aun bajo la mínima presión de 7cm H_20, los pulmones tratados con proteínas recombinantes no colapsan.

6.7.1 Volumen de gas en los pulmones

Después de 35 minutos de ventilación los pulmones se llenaron con N_2, se extirparon y se midió el volumen de gas en cada pulmón. La figura 49 demuestra que todos los pulmones tratados con surfactante sintético o clínico mostraban un volumen significativamente más grande que el control no tratado. Entre los pulmones tratados con rGP/SP-Cff, rGP/SP-Ccc la diferencia era de $P<0.05$ vs. Curosurf mientras la diferencia entre rGP/SP-Cww y Curosurf® era de $P<0.01$. No había diferencias significativas entre surfactantes que llevaban distintas variantes recombinantes. La figura 50 muestra la morfología de los diferentes pulmones después de un régimen de ventilación de 35 minutos. El color claro de los pulmones tratados con Curosurf o con surfactantes sintéticos indica una mayor aireación comparado con los pulmones oscuros y de menor tamaño como es el de control negativo no tratado.

6.7.2 Discusión

El presente capitulo demuestra que los análogos recombinantes de la SP-C producidos en bacterias combinados con la mezcla lipidica DPPC:POPG (68:31) restauran el funcionamiento pulmonar en los fetos prematuros de conejos de forma parecida a como lo hace un surfactante de amplia aplicación actualmente en clínica. Las tres proteínas recombinantes mostraron un comportamiento similar independientemente de los amino ácidos presentes en la posición 5 y 6 de su secuencia.

6.8 CONCLUSIONES

Hemos descrito un nuevo método de obtención de la proteína SP-C recombinante de cultivos bacterianos, para su posible uso en preparaciones de surfactante sintético usadas para el tratamiento de patologías pulmonares, así como su utilización como herramienta poderosa para generar variantes en estudios estructura-función de la proteína.

Las variantes de SP-C recombinante obtenidas poseen una estructura altamente helicoidal, indispensable para su actividad biológica. Hemos demostrado que estas variantes poseen *in vitro* una actividad tensioactiva igual o superior a la de la proteína nativa aislada de pulmones porcinos. Además, se ha demostrado que esta importante actividad tensioactiva no se debe únicamente a la presencia de residuos aromáticos en las posiciones 5 y 6 de la secuencia de la proteína.

Finalmente, las variantes recombinantes ensayadas fueron eficaces *in vivo* en un modelo animal de tratamiento de RDS, en concreto en la restauración del funcionamiento pulmonar de conejos prematuros. Mostrando una capacidad comparable a Curosurf®, uno de los surfactantes más utilizados actualmente para el tratamiento de los partos prematuros. Requiriéndose la aplicación de PEEP

durante la ventilación mecánica, para su óptima actividad.

7 REFERENCES

Aguzzi A, Weissmann C. Prion research: the next frontiers. Nature. 1997;389(6653):795-8.

Andersson M, Curstedt T, Jornvall H, Johansson J An amphipathic helical motif common to tumourolytic polypeptide NK-lysin and pulmonary surfactant polypeptide SP-B. FEBS Lett. 1995;362(3):328-32.

Amirkhanian JD, Bruni R, Waring AJ, Navar C, Taeusch HWFull length synthetic surfactant proteins, SP-B and SP-C, reduce surfactant inactivation by serum. Biochim Biophys Acta. 1993;1168(3):315-20

Amrein M, von Nahmen A, Sieber M. A scanning force- and fluorescence light microscopy study of the structure and function of a model pulmonary surfactant. Eur Biophys J. 1997;26(5):349-57

Augusto LA, Li J, Synguelakis M, Johansson J, Chaby R. Structural basis for interactions between lung surfactant protein C and bacterial lipopolysaccharide. J Biol Chem. 2002;277(26):23484-92.

Augusto LA, Synguelakis M, Johansson J, Pedron T, Girard R, Chaby R. Interaction of pulmonary surfactant protein C with CD14 and lipopolysaccharide. Infect Immun. 2003;71(1):61-7.

Baatz JE, Smyth KL, Whitsett JA, Baxter C, Absolom DR. Structure and functions of a dimeric form of surfactant protein SP-C: a Fourier transform infrared and surfactometry study.Chem Phys Lipids. 1992;63(1-2):91-104.

Baudouin SV. Exogenous surfactant replacement in ARDS--one day, someday, or never?
N Engl J Med. 2004;351(9):853-5.

Beers MF, Mulugeta S. Surfactant protein C biosynthesis and its emerging role in conformational lung disease. Annu Rev Physiol. 2005;67:663-96.

Beharka AA, Gaynor CD, Kang BK, Voelker DR, McCormack FX, Schlesinger LS.Pulmonary surfactant protein A up-regulates activity of the mannose receptor, a pattern recognition receptor expressed on human macrophages. J Immunol. 2002;169(7):3565-73.

Bi X, Flach CR, Perez-Gil J, Plasencia I, Andreu D, Oliveira E, Mendelsohn R.Secondary structure and lipid interactions of the N-terminal segment of pulmonary surfactant SP-C in Langmuir films: IR reflection-absorption spectroscopy and surface pressure studies. Biochemistry. 2002;41(26):8385-95.

Bligh EG, Dyer WJ. A rapid method of total lipid extraction and purification.Can J Biochem Physiol. 1959;37(8):911-7

Botas C, Poulain F, Akiyama J, Brown C, Allen L, Goerke J, Clements J, Carlson E, Gillespie AM, Epstein C, Hawgood S.Altered surfactant homeostasis and alveolar type II cell morphology in mice lacking surfactant protein D. Proc Natl Acad Sci U S A. 1998;95(20):11869-74.

Brasch F, Ten Brinke A, Johnen G, Ochs M, Kapp N, Muller KM, Beers MF, Fehrenbach H, Richter J, Batenburg JJ, Buhling F. Involvement of cathepsin H in the processing of the hydrophobic surfactant-associated protein C in type II pneumocytes. Am J Respir Cell Mol Biol. 2002;26(6):659-70.

Cajal Y, Dodia C, Fisher AB, Jain MK.Calcium-triggered selective intermembrane exchange of phospholipids by the lung surfactant protein SP-A. Biochemistry. 1998;37(35):12178-88.

Casals C, Herrera L, Miguel E, Garcia-Barreno P, Municio AM. Comparison between intra- and extracellular surfactant in respiratory distress induced by oleic acid. Biochim Biophys Acta. 1989;1003(2):201-3.

Clark JC, Wert SE, Bachurski CJ, Stahlman MT, Stripp BR, Weaver TE, Whitsett JA.Targeted disruption of the surfactant protein B gene disrupts surfactant homeostasis, causing respiratory failure in newborn mice.Proc Natl Acad Sci U S A. 1995;92(17):7794-8

Cockshutt AM, Weitz J, Possmayer F.Pulmonary surfactant-associated protein A enhances the surface activity of lipid extract surfactant and reverses inhibition by blood proteins in vitro. Biochemistry. 1990;29(36):8424-9.

Cochrane CG, Revak SD. Pulmonary surfactant protein B (SP-B): structure-function relationships. Science. 1991;254(5031):566-8.

Cochrane CG, Revak SD, Merritt TA, Heldt GP, Hallman M, Cunningham MD, Easa D, Pramanik A, Edwards DK, Alberts MS.The efficacy and safety of KL4-surfactant in preterm infants with respiratory distress syndrome. Am J Respir Crit Care Med. 1996;153(1):404-10.

Creuwels LA, Demel RA, van Golde LM, Benson BJ, Haagsman HP. Effect of acylation on structure and function of surfactant protein C at the air-liquid interface.J Biol Chem. 1993;268(35):26752-8.

Creuwels LA, Boer EH, Demel RA, van Golde LM, Haagsman HP.Neutralization of the positive charges of surfactant protein C. Effects on structure and function. J Biol Chem. 1995;270(27):16225-9.

Crouch E, Wright JR. Surfactant proteins a and d and pulmonary host defence. Annu Rev Physiol. 2001;63:521-54.

Cruz A, Casals C, Perez-Gil J. Conformational flexibility of pulmonary surfactant proteins SP-B and SP-C, studied in aqueous organic solvents. Biochim Biophys Acta. 1995;1255(1):68-76.

Cruz A, Worthman LA, Serrano AG, Casals C, Keough KM, Perez-Gil J.Microstructure and dynamic surface properties of surfactant protein SP-B/dipalmitoylphosphatidylcholine interfacial films spread from lipid-protein bilayers. Eur Biophys J. 2000;29(3):204-13.

Cruz A, Vazquez L, Velez M, Perez-Gil J. Influence of a fluorescent probe on the nanostructure of phospholipid membranes: dipalmitoylphosphatidylcholine interfacial monolayers.Langmuir. 2005;21(12):5349-55.

Crouch E, Wright JR.Surfactant proteins a and d and pulmonary host defense. Annu Rev Physiol. 2001;63:521-54.

Curstedt T, Jornvall H, Robertson B, Bergman T, Berggren P. Two hydrophobic low-molecular-mass protein fractions of pulmonary surfactant. Characterization and biophysical activity. Eur J Biochem. 1987;168(2):255-62.

Davis AJ, Jobe AH, Hafner D, Ikegami M. Lung function in premature lambs and rabbits treated with a recombinant SP-C surfactant.Am J Respir Crit Care Med. 1998;157(2):553-9.

Dietl P, Haller T, Mair N, Frick M. Mechanisms of surfactant exocytosis in alveolar type II cells in vitro and in vivo.News Physiol Sci. 2001;16:239-43.

Ding J, Takamoto DY, von Nahmen A, Lipp MM, Lee KY, Waring AJ, Zasadzinski JA.Effects of lung surfactant proteins, SP-B and SP-C, and palmitic acid on monolayer stability. Biophys J. 2001;80(5):2262-72.

Eijking EP, Gommers D, So KL, de Maat MP, Mouton JW, Lachmann B. Prevention of respiratory failure after hydrochloric acid aspiration by intratracheal surfactant instillation in rats. Anesth Analg. 1993;76(3):472-7

Enhorning G, Robertson B. Lung expansion in the premature rabbit fetus after tracheal deposition of surfactant.Pediatrics. 1972;50(1):58-66.

Enhorning G, Grossmann G, Robertson B. Pharyngeal deposition of surfactant in the premature rabbit fetus. Biol Neonate. 1973;22(1):126-32.

Friedrich W, Schmalisch G, Stevens PA, Wauer RR.Surfactant protein SP-B counteracts inhibition of pulmonary surfactant by serum proteins. Eur J Med Res. 2000;5(7):277-82.

Fujiwara T, Maeta H, Chida S, Morita T, Watabe Y, Abe T.Artificial surfactant therapy in hyaline-membrane disease. Lancet. 1980;1(8159):55-9.

Gericke A, Flach CR, Mendelsohn R. Structure and orientation of lung surfactant SP-C and L-alpha-dipalmitoylphosphatidylcholine in aqueous monolayers.Biophys J. 1997;73(1):492-9.

Glasser SW, Burhans MS, Korfhagen TR, Na CL, Sly PD, Ross GF, Ikegami M, Whitsett JA. Altered stability of pulmonary surfactant in SP-C-deficient mice.Proc Natl Acad Sci U S A. 2001;98(11):6366-71

Glasser SW, Detmer EA, Ikegami M, Na CL, Stahlman MT, Whitsett JA. Pneumonitis and emphysema in sp-C gene targeted mice. J Biol Chem. 2003;278(16):14291-8.

Goerke J. Pulmonary surfactant: functions and molecular composition. Biochim Biophys Acta. 1998;1408(2-3):79-89.

Gustafsson M, Curstedt T, Jornvall H, Johansson J. Reverse-phase HPLC of the hydrophobic pulmonary surfactant proteins: detection of a surfactant protein C isoform containing Nepsilon-palmitoyl-lysine. Biochem J. 1997;326 (Pt 3):799-806.

Gustafsson M, Thyberg J, Naslund J, Eliasson E, Johansson J. Amyloid fibril formation by pulmonary surfactant protein C. FEBS Lett. 1999;464(3):138-42.

Gustafsson M, Griffiths WJ, Furusjo E, Johansson J. The palmitoyl groups of lung surfactant protein C reduce unfolding into a fibrillogenic intermediate.J Mol Biol. 2001;310(4):937-50

Hakes DJ, Dixon JE. New vectors for high level expression of recombinant proteins in bacteria.
Anal Biochem. 1992;202(2):293-8.

Hafner D, Germann PG, Hauschke D. Effects of lung surfactant factor (LSF) treatment on gas exchange and histopathological changes in an animal model of adult respiratory distress syndrome (ARDS): comparison of recombinant LSF with bovine LSF. Pulm Pharmacol. 1994;7(5):319-32

Hafner D, Beume R, Kilian U, Krasznai G, Lachmann B. Dose-response comparisons of five lung surfactant factor (LSF) preparations in an animal model of adult respiratory distress syndrome (ARDS).Br J Pharmacol. 1995;115(3):451-8.

Hafner D, Germann PG, Hauschke D. Effects of rSP-C surfactant on oxygenation and histology in a rat-lung-lavage model of acute lung injury. Am J Respir Crit Care Med. 1998;158(1):270-8.

Hafner D, Germann PG, Hauschke D, Kilian U. Effects of early treatment with rSP-C surfactant on oxygenation and histology in rats with acute lung injury. Pulm Pharmacol Ther. 1999;12(3):193-201.

Hallman M, Glumoff V, Ramet M. Surfactant in respiratory distress syndrome and lung injury.
Comp Biochem Physiol A Mol Integr Physiol. 2001;129(1):287-94.

Hawgood S, Ogawa A, Yukitake K, Schlueter M, Brown C, White T, Buckley D, Lesikar D, Benson B. Lung function in premature rabbits treated with recombinant human surfactant protein-C.
Am J Respir Crit Care Med. 1996;154(2 Pt 1):484-90

Hawgood, S. Surfactant: composition, structure and metabolism. The lung Scientific Foundations.W.J.Crysal RG, Weibel ER, Barnes PJ. Lippincott-Raven.Philadelphia, 1997; 701-734.

Horowitz AD, Moussavian B, Whitsett JA Roles of SP-A, SP-B, and SP-C in modulation of lipid uptake by pulmonary epithelial cells in vitro. Am J Physiol. 1996;270(1 Pt 1):L69-79.

Hynes TR, Fox RO. The crystal structure of staphylococcal nuclease refined at 1.7 A resolution. Proteins. 1991;10: 92-105.

Ito Y, Goffin J, Veldhuizen R, Joseph M, Bjarneson D, McCaig L, Yao LJ, Marcou J, Lewis J. Timing of exogenous surfactant administration in a rabbit model of acute lung injury. J Appl Physiol. 1996;80(4):1357-64.

Johansson J, Szyperski T, Curstedt T, Wuthrich K. The NMR structure of the pulmonary surfactant-associated polypeptide SP-C in an apolar solvent contains a valyl-rich alpha-helix.
Biochemistry. 1994;33(19):6015-23.

Johansson J, Szyperski T, Wuthrich K. Pulmonary surfactant-associated polypeptide SP-C in lipid micelles: CD studies of intact SP-C and NMR secondary structure determination of depalmitoyl-SP-C(1-

17). FEBS Lett. 1995a;362(3):261-5.

Johansson J, Nilsson G, Stromberg R, Robertson B, Jornvall H, Curstedt T. Secondary structure and biophysical activity of synthetic analogues of the pulmonary surfactant polypeptide SP-C. Biochem J. 1995b;307 (Pt 2):535-41.

Johansson J, Some M, Linderholm BM, Almlen A, Curstedt T, Robertson B. A synthetic surfactant based on a poly-Leu SP-C analog and phospholipids: effects on tidal volumes and lung gas volumes in ventilated immature newborn rabbits. J Appl Physiol. 2003;95(5):2055-63.

Johansson J, Weaver TE, Tjernberg LO. Proteolytic generation and aggregation of peptides from transmembrane regions: lung surfactant protein C and amyloid beta-peptide.Cell Mol Life Sci. 2004;61(3):326-35.

Johansson J, Curstedt T. Molecular structures and interactions of pulmonary surfactant components. Eur J Biochem. 1997;244(3):675-93.

Kelly JW. Alternative conformations of amyloidogenic proteins govern their behavior. Curr Opin Struct Biol. 1996;6(1):11-7.

Kiefer H. In vitro folding of alpha-helical membrane proteins. Biochim Biophys Acta. 2003 Feb 17;1610(1):57-62.

Korimilli A, Gonzales LW, Guttentag SH.Intracellular localization of processing events in human surfactant protein B biosynthesis. J Biol Chem. 2000;275(12):8672-9.

Korfhagen TR, LeVine AM, Whitsett JA. Surfactant protein A (SP-A) gene targeted mice. Biochim Biophys Acta. 1998;1408(2-3):296-302.

Krol S, Ross M, Sieber M, Kunneke S, Galla HJ, Janshoff A. Formation of three-dimensional protein-lipid aggregates in monolayer films induced by surfactant protein B. Biophys J. 2000;79(2):904-18.

Kruger P, Schalke M, Wang Z, Notter RH, Dluhy RA, Losche M. Effect of hydrophobic surfactant peptides SP-B and SP-C on binary phospholipid monolayers. I. Fluorescence and dark-field microscopy. Biophys J. 1999;77(2):903-14.

Kruger P, Baatz JE, Dluhy RA, Losche M. Effect of hydrophobic surfactant protein SP-C on binary phospholipid monolayers. Molecular machinery at the air/water interface. Biophys Chem. 2002 ;99(3):209-28

Kuronuma K, Sano H, Kato K, Kudo K, Hyakushima N, Yokota S, Takahashi H, Fujii N, Suzuki H, Kodama T, Abe S, Kuroki Y.Pulmonary surfactant protein A augments the phagocytosis of Streptococcus pneumoniae by alveolar macrophages through a casein kinase 2-dependent increase of cell surface localization of scavenger receptor A. J Biol Chem. 2004;279(20):21421-30.

Laage L and Langosch D. Strategies for prokaryotic expression of eukaryotic membrane proteins, Traffic 2 (2001) 99-104.

LeVine AM, Bruno MD, Huelsman KM, Ross GF, Whitsett JA, Korfhagen TRSurfactant protein A-deficient mice are susceptible to group B streptococcal infection. J Immunol. 1997;158(9):4336-40.

LeVine AM, Whitsett JA Pulmonary collectins and innate host defense of the lung.Microbes Infect. 2001;3(2):161-6

Lewis J, McCaig L, Hafner D, Spragg R, Veldhuizen R, Kerr C. Dosing and delivery of a recombinant surfactant in lung-injured adult sheep.Am J Respir Crit Care Med. 1999;159(3):741-7.

Lewis JF, Veldhuizen R. The role of exogenous surfactant in the treatment of acute lung injury. Annu Rev Physiol. 2003;65:613-42.

Li SC, Deber CM. A measure of helical propensity for amino acids in membrane environments. Nat Struct Biol. 1994;1(8):558.

Li J, Liepinsh E, Almlen A, Thyberg J, Curstedt T, Jornvall H, Johansson J. Structure and influence on stability and activity of the N-terminal propeptide part of lung surfactant protein C. FEBS J. 2006;273(5):926-35.

Liepinsh E, Andersson M, Ruysschaert JM, Otting G. Saposin fold revealed by the NMR structure of NK-lysin. Nat Struct Biol. 1997;4(10):793-5.

Luy B, Diener A, Hummel RP, Sturm E, Ulrich WR, Griesinger C. Structure and potential C-terminal dimerization of a recombinant mutant of surfactant-associated protein C in chloroform/methanol. Eur J Biochem. 2000;271(11):2076-85.

Mackenzie KR. Folding and stability of alpha-helical integral membrane proteins. Chem Rev. 2006;106(5):1931-77.

Mathialagan N, Possmayer F. Low-molecular-weight hydrophobic proteins from bovine pulmonary surfactant. Biochim Biophys Acta. 1990;1045(2):121-7.

McCormack FX, Whitsett JA. The pulmonary collectins, SP-A and SP-D, orchestrate innate immunity in the lung.J Clin Invest. 2002;109(6):707-12.

McLean LR, Krstenansky JL, Jackson RL, Hagaman KA, Olsen KA, Lewis JE. Mixtures of synthetic peptides and dipalmitoylphosphatidylcholine as lung surfactants. Am J Physiol. 1992;262(3 Pt 1):L292-300.

Miles PR, Bowman L, Rao KM, Baatz JE, Huffman L Pulmonary surfactant inhibits LPS-induced nitric oxide production by alveolar macrophages.Am J Physiol. 1999;276(1 Pt 1):L186-96

Mingarro I, Whitley P, Lemmon MA, von Heijne G. Ala-insertion scanning mutagenesis of the glycophorin A transmembrane helix: a rapid way to map helix-helix interactions in integral membrane proteins. Protein Sci. 1996;5(7):1339-41.

Munford RS, Sheppard PO, O'Hara PJ. Saposin-like proteins (SAPLIP) carry out diverse functions on a common backbone structure.J Lipid Res. 1995;36(8):1653-63

Nag K, Perez-Gil J, Cruz A, Keough KM. Fluorescently labeled pulmonary surfactant protein C in spread phospholipid monolayers.Biophys J. 1996;71(1):246-56.

Nag K, Taneva SG, Perez-Gil J, Cruz A, Keough KM Combinations of fluorescently labeled pulmonary surfactant proteins SP-B and SP-C in phospholipid films. Biophys J. 1997;72(6):2638-50.

Nag K, Munro JG, Inchley K, Schurch S, Petersen NO, Possmayer F.SP-B refining of pulmonary surfactant phospholipid films. Am J Physiol. 1999;277(6 Pt 1):L1179-89.

Nicholas TE, Power JH, Barr HA. Surfactant homeostasis in the rat lung during swimming exercise. J Appl Physiol. 1982;53(6):1521-8.

Nilsson G, Gustafsson M, Vandenbussche G, Veldhuizen E, Griffiths WJ, Sjovall J, Haagsman HP, Ruysschaert JM, Robertson B, Curstedt T, Johansson Synthetic peptide-containing surfactants--evaluation of transmembrane versus amphipathic helices and surfactant protein C poly-valyl to poly-leucyl substitution. Eur J Biochem. 1998;255(1):116-24.

Nogee LM, Wert SE, Proffit SA, Hull WM, Whitsett JA Allelic heterogeneity in hereditary surfactant protein B (SP-B) deficiency.Am J Respir Crit Care Med. 2000;161(3 Pt 1):973-81

Notter R., Lung Surfactants: Basic Science and Clinical Applications, 2000.

Oosterlaken-Dijksterhuis MA, Haagsman HP, van Golde LM, Demel RA Characterization of lipid insertion into monomolecular layers mediated by lung surfactant proteins SP-B and SP-C. Biochemistry. 1991;30(45):10965-71.

Oosterlaken-Dijksterhuis MA, van Eijk M, van Golde LM, Haagsman HP.Lipid mixing is mediated by the

hydrophobic surfactant protein SP-B but not by SP-C. Biochim Biophys Acta. 1992;1110(1):45-50.

Orzaez M, Perez-Paya E, Mingarro Influence of the C-terminus of the glycophorin A transmembrane fragment on the dimerization process. Protein Sci. 2000;9(6):1246-53.

Palmblad M, Johansson J, Robertson B, Curstedt T. Biophysical activity of an artificial surfactant containing an analogue of surfactant protein (SP)-C and native SP-B. Biochem J. 1999;339 (Pt 2):381-6.

Perez-Gil J, Nag K, Taneva S, Keough KM. Pulmonary surfactant protein SP-C causes packing rearrangements of dipalmitoylphosphatidylcholine in spread monolayers. Biophys J. 1992;63(1):197-204.

Perez-Gil J, Cruz A, Casals C. Solubility of hydrophobic surfactant proteins in organic solvent/water mixtures. Structural studies on SP-B and SP-C in aqueous organic solvents and lipids. Biochim Biophys Acta. 1993;1168(3):261-70.

Perez-Gil J, Casals C, Marsh D. Interactions of hydrophobic lung surfactant proteins SP-B and SP-C with dipalmitoylphosphatidylcholine and dipalmitoylphosphatidylglycerol bilayers studied by electron spin resonance spectroscopy. Biochemistry. 1995;34(12):3964-71.

Perez-Gil J. Lipid-protein interactions of hydrophobic proteins SP-B and SP-C in lung surfactant assembly and dynamics. Pediatr Pathol Mol Med. 2001;20(6):445-69

Perez-Gil J. Molecular interactions in pulmonary surfactant films. Biol Neonate. 2002;81 Suppl 1:6-15.

Piknova B, Schram V, Hall SB. Pulmonary surfactant: phase behavior and function. Curr Opin Struct Biol. 2002;12(4):487-94.

Plasencia I, Rivas L, Keough KM, Marsh D, Perez-Gil J. The N-terminal segment of pulmonary surfactant lipopeptide SP-C has intrinsic propensity to interact with and perturb phospholipid bilayers. Biochem J. 2004;377(Pt 1):183-93.

Plasencia I, Keough KM, Perez-Gil J. Interaction of the N-terminal segment of pulmonary surfactant protein SP-C with interfacial phospholipid films. Biochim Biophys Acta. 2005;1713(2):118-28.

Poulain FR, Nir S, Hawgood S.Kinetics of phospholipid membrane fusion induced by surfactant apoproteins A and B. Biochim Biophys Acta. 1996 Jan 31;1278(2):169-75.

Poulain FR, Allen L, Williams MC, Hamilton RL, Hawgood S.Effects of surfactant apolipoproteins on liposome structure: implications for tubular myelin formation. Am J Physiol. 1992;262(6 Pt 1):L730-9.

Possmayer F, Nag K, Rodriguez K, Qanbar R, Schurch S.Surface activity in vitro: role of surfactant proteins. Comp Biochem Physiol A Mol Integr Physiol. 2001;129(1):209-20.

Rider ED, Ikegami M, Whitsett JA, Hull W, Absolom D, Jobe AH. Treatment responses to surfactants containing natural surfactant proteins in preterm rabbits. Am Rev Respir Dis. 1993;147(3):669-76.

Robertson B, Halliday HL. Principles of surfactant replacement. Biochim Biophys Acta. 1998;1408(2-3):346-61.

Rooney SA. Regulation of surfactant secretion.Comp Biochem Physiol A Mol Integr Physiol. 2001;129(1):233-43.

Rodriguez RJ. Management of respiratory distress syndrome: an update. Respir Care. 2003;48(3):279-86; discussion 286-7.

Rodriguez-Capote K, Nag K, Schurch S, Possmayer F. Surfactant protein interactions with neutral and acidic phospholipid films. Am J Physiol Lung Cell Mol Physiol. 2001;281(1):L231-42.

Rouser G., Siakotos A.N. and Fleischer A.S. Quantitative analysis of phospholipids by thin layer chromatography and phosphorus analysis of spots. Lipids. 1996,1:85-86.

Ryan MA, Qi X, Serrano AG, Ikegami M, Perez-Gil J, Johansson J, Weaver TE. Mapping and analysis of the lytic and fusogenic domains of surfactant protein B. Biochemistry. 2005;44(3):861-72.

Sane AC, Young SL.The stimulation of cellular phospholipid uptake by surfactant apoproteins. Biochim Biophys Acta. 1994;1213(1):107-12.

Sano H, Sohma H, Muta T, Nomura S, Voelker DR, Kuroki Y.Pulmonary surfactant protein A modulates the cellular response to smooth and rough lipopolysaccharides by interaction with CD14. J Immunol. 1999;163(1):387-95.

Sano H, Kuroki Y. The lung collectins, SP-A and SP-D, modulate pulmonary innate immunity. Mol Immunol. 2005;42(3):279-87.

Scherle W. A simple method for volumetry of organs in quantitative stereology. Mikroskopie. 1970 ;26(1):57-60.

Schurch S, Possmayer F, Cheng S, Cockshutt AM.Pulmonary SP-A enhances adsorption and appears to induce surface sorting of lipid extract surfactant. Am J Physiol. 1992;263(2 Pt 1):L210-8.

Schurch S, Qanbar R, Bachofen H, Possmayer F The surface-associated surfactant reservoir in the alveolar lining. Biol Neonate. 1995;67 Suppl 1:61-76.

Schurch S, Green FH, Bachofen H. Formation and structure of surface films: captive bubble surfactometry.Biochim Biophys Acta. 1998;1408(2-3):180-202.

Seeger W, Gunther, A Thede C. Differential sensitivity to fibrinogen inhibition of SP-C- vs. SP-B-based surfactants. Am J Physiol. 1992;262(3 Pt 1):L286-91

Seymour JF, Presneill JJ. Pulmonary alveolar proteinosis: progress in the first 44 years. Am J Respir Crit Care Med. 2002;166(2):215-35.

Serrano AG, Cruz A, Rodriguez-Capote K, Possmayer F, Perez-Gil J. Intrinsic structural and functional determinants within the amino acid sequence of mature pulmonary surfactant protein SP-B.Biochemistry. 2005;44(1):417-30.

Serrano AG, Ryan M, Weaver TE, Perez-Gil J Critical structure-function determinants within the N-terminal region of pulmonary surfactant protein SP-B. Biophys J. 2006;90(1):238-49.

Seurynck SL, Patch JA, Barron AE Simple, helical peptoid analogs of lung surfactant protein B. Chem Biol. 2005;12(1):77-88.

Shiffer K, Hawgood S, Haagsman HP, Benson B, Clements JA, Goerke J. Lung surfactant proteins, SP-B and SP-C, alter the thermodynamic properties of phospholipid membranes: a differential calorimetry study. Biochemistry. 1993 Jan 19;32(2):590

Spragg RG, Lewis JF, Wurst W, Hafner D, Baughman RP, Wewers MD, Marsh JJ. Treatment of acute respiratory distress syndrome with recombinant surfactant protein C surfactant. Am J Respir Crit Care Med. 2003;167(11):1562-6.

Spragg RG, Lewis JF, Walmrath HD, Johannigman J, Bellingan G, Laterre PF, Witte MC, Richards GA, Rippin G, Rathgeb F, Hafner D, Taut FJ, Seeger W.Effect of recombinant surfactant protein C-based surfactant on the acute respiratory distress syndrome. N Engl J Med. 2004;351(9):884-92.

Sreerama N, Woody RW. Estimation of protein secondary structure from circular dichroism spectra: comparison of CONTIN, SELCON, and CDSSTR methods with an expanded reference set. Anal Biochem. 2000;287(2):252-60.

Sreerama N, Woody RW. On the analysis of membrane protein circular dichroism spectra. Protein Sci. 2004;13(1):100-12.

Stevens PA, Wissel H, Sieger D, Meienreis-Sudau V, Rustow B Identification of a new surfactant

protein A binding protein at the cell membrane of rat type II pneumocytes. Biochem J. 1995,15;308 (1):77-81.

Strayer DS, Pinder R, Chander A.Receptor-mediated regulation of pulmonary surfactant secretion. Exp Cell Res. 1996,10;226(1):90-7.

Stults JT, Griffin PR, Lesikar DD, Naidu A, Moffat B, Benson BJ.Lung surfactant protein SP-C from human, bovine, and canine sources contains palmityl cysteine thioester linkages: Am J Physiol. 1991;261(2 Pt 1):L118-25.

Sun B, Kobayashi T, Curstedt, Grossman G, and Robertson B. Application of ventilator-multy-plethysmograph system for testing efficacy of surfactant replacement in newborn rab bits. Eur Respir J.1991; 4: 364-370.

Szyperski T, Vandenbussche G, Curstedt T, Ruysschaert JM, Wuthrich K, Johansson J. Pulmonary surfactant-associated polypeptide C in a mixed organic solvent transforms from a monomeric alpha-helical state into insoluble beta-sheet aggregates.Protein Sci. 1998;7(12):2533-40.

Takahashi A, Fujiwara T.Proteolipid in bovine lung surfactant: its role in surfactant function. Biochem Biophys Res Commun. 1986;135(2):527-32.

Takei T, Hashimoto Y, Aiba T, Sakai K, Fujiwara T. The surface properties of chemically synthesized peptides analogous to human pulmonary surfactant protein SP-C. Biol Pharm Bull. 1996a;19(10):1247-53.

Takei T, Hashimoto Y, Ohtsubo E, Sakai K, Ohkawa H. Characterization of poly-leucine substituted analogues of the human surfactant protein SP-C. Biol Pharm Bull. 1996b;19(12):1550-5.

Taneva SG, Keough KM. Dynamic surface properties of pulmonary surfactant proteins SP-B and SP-C and their mixtures with dipalmitoylphosphatidylcholine. Biochemistry. 1994a;33(49):14660-70.

Taneva S, Keough KM. Pulmonary surfactant proteins SP-B and SP-C in spread monolayers at the air-water interface: I. Monolayers of pulmonary surfactant protein SP-B and phospholipids. Biophys J. 1994b;66(4):1137-48.

Taneva S, Keough KM. Pulmonary surfactant proteins SP-B and SP-C in spread monolayers at the air-water interface: II. Monolayers of pulmonary surfactant protein SP-C and phospholipids.Biophys J. 1994c;66(4):1149-57

Taneva SG, Stewart J, Taylor L, Keough KM. Method of purification affects some interfacial properties of pulmonary surfactant proteins B and C and their mixtures with dipalmitoylphosphatidylcholine. Biochim Biophys Acta. 1998;1370(1):138-50.

Therien AG, Glibowicka M, Deber CM. Expression and purification of two hydrophobic double-spanning membrane proteins derived from the cystic fibrosis transmembrane conductance regulator. Protein Expr Purif. 2002;25(1):81-6.

Tschumperlin DJ, Margulies SS. Alveolar epithelial surface area-volume relationship in isolated rat lungs. J Appl Physiol. 1999;86(6):2026-33.

Vandenbussche G, Clercx A, Clercx M, Curstedt T, Johansson J, Jornvall H, Ruysschaert JMSecondary structure and orientation of the surfactant protein SP-B in a lipid environment. A Fourier transform infrared spectroscopy study. Biochemistry. 1992a;31(38):9169-76.

Vandenbussche G, Clercx A, Curstedt T, Johansson J, Jornvall H, Ruysschaert JM. Structure and orientation of the surfactant-associated protein C in a lipid bilayer. Eur J Biochem. 1992b;203(1-2):201-9.

Veldhuizen EJ, Batenburg JJ, Vandenbussche G, Putz G, van Golde LM, Haagsman HP. Production of surfactant protein C in the baculovirus expression system: the information required for correct folding and palmitoylation of SP-C is contained within the mature sequence.Biochim Biophys Acta. 1999;1416(1-2):295-308.

Veldhuizen EJ, Waring AJ, Walther FJ, Batenburg JJ, van Golde LM, Haagsman HP.Dimeric N-terminal segment of human surfactant protein B (dSP-B(1-25)) has enhanced surface properties compared to monomeric SP-B(1-25). Biophys J. 2000;79(1):377-84.

Veldhuizen EJ, Haagsman HP. Role of pulmonary surfactant components in surface film formation and dynamics.Biochim Biophys Acta. 2000 Aug 25;1467(2):255-70.

Von Nahmen A, Schenk M, Sieber M, Amrein M. The structure of a model pulmonary surfactant as revealed by scanning force microscopy. Biophys J. 1997;72(1):463-9.

Vorbroker DK, Profitt SA, Nogee LM, Whitsett JA. Aberrant processing of surfactant protein C in hereditary SP-B deficiency. Am J Physiol. 1995;268(4 Pt 1):L647-56.

Wang Z, Gurel O, Baatz JE, Notter RH. Acylation of pulmonary surfactant protein-C is required for its optimal surface active interactions with phospholipids.J Biol Chem. 1996a;271(32):19104-9.

Wang Z, Gurel O, Baatz JE, Notter RH. Differential activity and lack of synergy of lung surfactant proteins SP-B and SP-C in interactions with phospholipids.J Lipid Res. 1996b;37(8):1749-60

Walther FJ, Hernandez-Juviel JM, Mercado PE, Gordon LM, Waring AJ Surfactant with SP-B and SP-C analogues improves lung function in surfactant-deficient rats. Biol Neonate. 2002;82(3):181-7

Weaver TE.Synthesis, processing and secretion of surfactant proteins B and C. Biochim Biophys Acta. 1998;1408(2-3):173-9.

Weaver TE, Conkright JJ. Function of surfactant proteins B and C. Annu Rev Physiol. 2001;63:555-78

Weaver TE, Na CL, Stahlman M. Biogenesis of lamellar bodies, lysosome-related organelles involved in storage and secretion of pulmonary surfactant.Semin Cell Dev Biol. 2002;13(4):263-70.

Wert SE, Yoshida M, LeVine AM, Ikegami M, Jones T, Ross GF, Fisher JH, Korfhagen TR, Whitsett JA. Increased metalloproteinase activity, oxidant production, and emphysema in surfactant protein D gene-inactivated mice.Proc Natl Acad Sci U S A. 2000;97(11):5972-7.

Whitsett JA, Nogee LM, Weaver TE, Horowitz AD. Human surfactant protein B: structure, function, regulation, and genetic disease.Physiol Rev. 1995;75(4):749-57.

Williams MC, Hawgood S, Hamilton RL. Changes in lipid structure produced by surfactant proteins SP-A, SP-B, and SP-C.Am J Respir Cell Mol Biol. 1991;5(1):41-50.

Wimley WC, White SH. Experimentally determined hydrophobicity scale for proteins at membrane interfaces, Nature Struct Biology. 1996; (3) 842-848.

White SH, Wimley WC. Hydrophobic interactions of peptides with membrane interfaces.Biochim Biophys Acta. 1998;1376(3):339-52.

Wirtz HR, Dobbs LG Calcium mobilization and exocytosis after one mechanical stretch of lung epithelial cells. Science. 1990;250(4985):1266-9.

Wu CW, Seurynck SL, Lee KY, Barron AE. Helical peptoid mimics of lung surfactant protein C.Chem Biol. 2003;10(11):1057-63.

Wustneck R, Perez-Gil J, Wustneck N, Cruz A, Fainerman VB, Pison U. Interfacial properties of pulmonary surfactant layers. Adv Colloid Interface Sci. 2005;117(1-3):33-58.

Zaltash S, Palmblad M, Curstedt T, Johansson J, Persson B. Pulmonary surfactant protein B: a structural model and a functional analogue.Biochim Biophys Acta. 2000;1466(1-2):179-86.